WOOD AND FIBER SCIENCE

The Sustainable Natural Materials Journal

Volume 58, Number 2, 2026 (ISSN 0735-6161)

Open Access

JOURNAL OF THE

SWST – International Society of Wood Science and Technology

EDITORIAL AND PUBLICATION POLICY

Wood and Fiber Science as the official publication of the Society of Wood Science and Technology publishes open access papers with both professional and technical content. Original papers of professional concern, or based on research of international interest dealing with the science, processing, and manufacture of wood and composite products of wood or wood fiber origin will be considered.

All manuscripts are to be written in US English, the text should be proofread by a native speaker of English prior to submission. Any manuscript submitted must be unpublished work not being offered for publication elsewhere.

Papers will be reviewed by referees selected by the editor and will be published in approximately the order in which the final version is received. Research papers will be judged on the basis of their contribution of original data, rigor of analysis, and interpretations of results; in the case of reviews, on their relevancy and completeness.

Color photos/graphics will be offered at no additional cost to authors. The Open Access fee will be $1800/article for SWST members and $2000/article for nonmembers. Reduced rates are available for authors based in developing countries.

Technical Notes

Authors are invited to submit Technical Notes to the Journal. A Technical Note is a concise description of a new research finding, development, procedure, or device. The length should be **no more than two printed pages in WFS**, which would be five pages or less of double-spaced text (TNR12) with normal margins on 8.5 x 11 paper, including space for figures and tables. In order to meet the limitation on space, figures and tables should be minimized, as should be the introduction, literature review and references. The Journal will attempt to expedite the review and publication process. As with research papers, Technical Notes must be original and go through a similar double-blind, peer review process.

On-line Access to *Wood and Fiber Science* Back Issues

SWST is providing readers with a means of searching all articles in *Wood and Fiber Science* from 1968 to present.

Visit the SWST website at https://www.swst.org and go to Wood & Fiber Science Online. Click on either SWST Member Publication access (SWST members) or Subscriber Publication access (Institution Access). All must login with their email and password on the https://www.swst.org site or use their ip authentication if they have a site license.

As an added benefit to our current subscribers, you can now access the electronic version of every printed article along with exciting enhancements that include:

- IP authentication for institutions (only with site license)
- Enhanced search capabilities
- Email alerting of new issues
- Custom links to your favorite titles

(ISSN 0735-6161)

WOOD AND FIBER SCIENCE

JOURNAL OF THE SOCIETY OF WOOD SCIENCE AND TECHNOLOGY

VOLUME 58 APRIL 2026 NUMBER 2

CONTENTS

Articles

On site moisture protection: An unnoticed but essential basis for sustainable timber construction

Kai Schubert†*
University of Rostock / Germany
Email: kai.schubert@uni-rostock.de

Claudia von Laar
Professor Dr. rer. nat. / Wismar University of Applied Sciences
Department of Civil Engineering / Germany
Email: claudia.von_laar@hs-wismar.de

Henning Bombeck
Professor Dr. / University of Rostock
Faculty of Agriculture, Civil and Environmental Engineering / Germany
Email: henning.bombeck@uni-rostock.de

(Received 1 December 2025)

Abstract: Timber construction is gaining popularity in Germany due to its sustainability, versatility, and aesthetic appeal, but, as a biological material, it can develop issues when exposed to moisture. Wood-destroying fungi can significantly reduce durability and structural integrity. Adequate moisture protection during construction is crucial for the longevity and performance of timber structures. This paper examines moisture protection practices on German construction sites and emphasizes the importance of proper on-site moisture management for sustainable timber construction. Visits to sites using timber construction revealed the status of moisture mitigation practices in conjunction with timber construction in Germany. A mixed-methods approach included photo documentation and protocol completion, yielding data for analysis to understand the depth and effectiveness of moisture protection strategies. The findings reveal a gap between problem awareness in the scientific community and practical handling on construction sites. Many sites exhibited disorganized structures and deficiencies in moisture protection strategies. While self-adhesive weathering membranes were used in nearly half the sites visited, less than one-third of the sites demonstrated sufficient moisture mitigation practices that protected the construction throughout the entire assembly process. This underlines the need to step up efforts in this area to ensure durable and high-quality timber construction that will be less reliant on the experience of designers or craftsmen.

Keywords: Assembly processes; Moisture; Timber construction; Mixed methods; Protection concept; Rainwater penetration; Prefabrication.

Introduction

As a renewable resource, wood can contribute to the attempts to counteract climate change by accumulating carbon dioxide (CO_2) throughout the lifespan of the growing tree (Tupenaite et al. 2023). When used in construction, this wood functions like a battery, storing the carbon it has absorbed over its lifetime (Sathre and O'Connor 2010; Mergel et al. 2024). Timber as a building material has the potential to maintain this storage function for a long time. However, wood is a biological material that can be degraded under certain conditions by fungi and insects. In particular, fungal decay typically occurs when the wood moisture content lies between cell wall saturation (about 25%) and the fully waterlogged condition, whereas in anoxic, permanently submerged environments most fungi are unable to decompose wood (Schrader et al. 2025). Thus, moisture management during construction is essential, as repeated wetting combined with periods of elevated moisture content creates a significant risk of biological degradation (Kalbe et al. 2022).

In contemporary German timber construction, the durability of the material is primarily determined by wood-destroying fungi and to a lesser extent by insects. The time and temperature profile of kiln drying leads to a reduction in protein and vitamins, making the wood less attractive to wood-destroying insects (Schmidt 2023). Consequently, insects rarely infest the wood and thus do not play a significant role in contemporary timber construction. This is especially important in the context

* Corresponding author
† Society of Wood Science & Technology member

of new buildings being erected. The only exception in this respect are termites, which—although at the moment pose a significant challenge in southern Europe—are generally not native to Germany based on current climatic conditions and occur only locally to a small extent (Scheiding et al. 2021; Kutnik et al. 2020). Therefore, moisture is the primary factor influencing the durability of state-of-the-art timber construction that we consider in this paper.

Fungi are generally unable to use water bound in the cell wall structure of the wood because it is held too strongly within the cell wall. For deterioration to occur, free water is needed. Because of this, most fungi require a moisture content above the fiber saturation point (around 25%) (Schrader et al. 2025). However, some fungi, like the dry rot fungus (*Serpula lacrymans*), are able to colonize timber, even though the moisture content is below the fiber saturation point, because they can transport water throughout their mycelium from a local moisture source to create an environment suitable for deterioration (Schrader et al. 2025). As fungal spores are present everywhere in the air (Scheiding et al. 2021; Wang et al. 2018), the greatest danger is therefore posed by mold and wood-destroying fungi. For mold to colonize a material, parameters such as moisture, temperature, ventilation, and exposure time are the influencing factors determining the climate conditions under which the mold growth occurs (Qiao et al. 2024).

Wang et al. (2018) stated that high relative humidities (RH) ranging from 80% to 95% or even short-term wetting of timber can lead to colonization by mold fungi (Schmidt and Riggio 2019), while Qiao et al. (2024) determined that most mold fungi developed best under conditions with RH between 60% and 90% and temperatures ranging between 5°C and 35°C. They also stated that temperature had less effect on the development compared to the moisture content.

While mold does not measurably affect wood properties, it is of concern because it can cause discoloration and is a potential allergen (Imken et al. 2020; Wang et al. 2018).

Unlike mold, rot fungi reduce wood properties through cell wall degradation (Imken et al. 2020). Exposure to moisture and its accumulation can lead to decay, mold growth, structural instability, and reduced indoor air quality (Wang et al. 2018; Cowled et al. 2023). There is even a risk that components may need to be completely replaced (Weinisch 2019). Hence, ensuring the protection of timber construction is a challenging task, requiring adequate moisture protection measures both during construction and throughout the lifespan of the actual building (Tengberg and Bolmsvik 2021). In this regard, preventing structures from becoming damp before completion and use is of paramount importance. As Udele et al. (2024) point out, this area has not yet been thoroughly investigated.

While the behavior of timber structures under the influence of moisture has been well studied, there is very little research dedicated to how in-situ moisture protection can be implemented or has been implemented up to now. Schmidt and Riggio (2019) found that the severity of exposure (e.g., free water) was largely determined by precautions taken by the designer and/or contractor. These precautions are influenced by their awareness of the issue and potential solutions, as well as by the construction system, schedule, and site conditions themselves. Wang et al. (2018) pointed out that there are several stages in wood construction where moisture ingress theoretically should not occur, but in reality, often does, resulting in prolonged suitable conditions for fungal attack. This typically happens because structural components are not yet operating under the conditions for which they were designed (Schubert et al. 2024)—for instance, in the absence of a completed roof or before elements have been structurally connected. In addition, the building materials themselves are not yet in their final state of use; for instance, concrete may still be curing and can introduce further moisture into the structure. Also, the protection of construction is closely related to a diversity of factors, such as water absorption, entrapment, and drying potential of the components (Wang 2015; Heinicke and Kehl 2024). Bolmsvik et al. (2023) conducted a case study on the effects of full weather protection on construction, examining moisture behavior, the likelihood of fungal growth, and its impact on the work environment (Tengberg and Bolmsvik 2021). The entire site was fully covered by a tent offering full weather protection, meaning that there was no exposure to the weather except for sunlight that could shine through the tent's tarpaulin. They found that no samples inside the weather protected area exhibited any mold growth, whereas 75% of the samples outside the protection did. This led to the conclusion that the implementation of full weather protection measures can lead to a substantial reduction in the risk of fungal damage.

Various factors during the construction process may contribute to an increase in moisture levels within a structure. These include insufficient ventilation, improperly planned or executed joints, and excess water released during the hydration process of floor slabs. Additionally, inadequate drainage due to rain and other external sources can contribute to moisture accumulation. It is widely acknowledged in the literature that wetting of timber components due to exposure to free water during construction is an issue of great importance (Kalbe et al. 2022; Heinicke

and Kehl 2024; Schubert et al. 2024). However, researchers have generally not agreed on how this should be dealt with. In Germany, DIN 68800-2:2022-02 Wood preservation – Part 2: Preventive constructional measures in buildings states that moisture content of timber should not change unfavorably during transport, storage, or assembly (Glauner et al. 2022). While the standard specifies that solid wood products are only allowed to have a moisture content of less than 20%, timber elements used in construction should not exceed a moisture content of 18% (Schmidt 2023). This implies the application of appropriate moisture control strategies throughout the construction process, but leaves much room for interpretation.

One effective way to document the moisture behavior of a building during the construction phase and beyond is to implement a monitoring system. This typically involves the use of either capacitive or sorption-based measurement techniques that directly (capacitive) or indirectly (sorption) measure wood moisture content (Flexeder et al. 2022). However, there are also a number of reasons why these systems are prone to error (Schmidt and Riggio 2019). Sensors can be affected by temperature and electromagnetic fields, as well as by losing contact inside the borehole. In addition, factors such as condensation or internal checking can also interfere with measurements, and these issues are often difficult to identify or isolate in practice (Schmidt and Riggio 2019).

Buildings in Canada and other regions have been equipped with sensor technology to track the moisture dynamics of mass timber components. These studies have shown that cross-laminated timber (CLT) elements, especially, tend to dry out much more slowly compared to how quickly they absorb moisture. This slow drying process can pose significant challenges, particularly for components that become inaccessible after construction, such as floors with concrete screed or encapsulated wall assemblies (Schmidt and Riggio 2019).

The aim of this paper is to provide insights into how moisture protection is organized on German construction sites. It seeks to contribute to the ongoing discourse about sustainable construction practices in Germany by addressing the significance of the problem associated with inadequate on-site moisture management. Proper moisture management throughout the building process, implemented and anticipated by all involved parties, will enhance durability, resilience, and long-term performance of timber structures in diverse environmental conditions.

Materials and methods

The aim of this study was to gain an overview of the extent to which contractors in Germany take weather protection into account during the construction phase. Therefore, a mixed-methods approach incorporating both qualitative and quantitative elements was used, involving on-site visits during the erection phase of timber construction projects. These visits were conducted using self-developed protocols and photo documentation. The observation checklist covered different phases of the construction process and included yes/no questions, multiple choice, and open-ended questions. There were two ways to complete the checklist: through direct observation or by gathering oral input from participants, such as foremen, architects, or craftsmen. This approach enabled direct observation and documentation of moisture mitigation practices and the conditions within real-world construction contexts.

Before the site visits, plans were requested from the respective design offices. Specifically, inquiries were made regarding everything related to moisture protection (e.g., planning documents indicating the extent of involvement in moisture protection and responsibilities, existing moisture protection concepts), detailed execution from wall to ceiling and foundation connections, as well as sections and views of the project. These data inquiries allowed attention to be focused on potential critical points during site visits. Anything that could not be understood on this basis was then clarified in a meeting with the foreman or site manager.

It was, however, not always possible to carry out moisture measurements on the wood components. On the one hand, access to the different sites was granted through different parties. Sometimes the access was made possible by the timber construction company, sometimes by the architect, and sometimes by the owner. This made it challenging to get permission for conducting moisture measurements. On the other hand, ensuring comparability would have required similar exposure conditions for the components, multiple measurement points, and repeated readings—ideally both before and after a rainfall event. Because our visits were non-repeating and not part of an ongoing monitoring program and the sites, systems, and buildings varied greatly (including differences in weather and season), we decided against moisture measurements.

The visits took place throughout Germany (Figure 1) when timber elements were assembled. The diversity of sites, construction methods, and handling practices observed allows the findings to be considered representative of a broad range of timber construction projects in the country. During each visit, systematic photo documentation was carried out to record on-site conditions and practices. The protocols were filled out to record the workflow as well as data concerning the construction form, methods, and other relevant information. Site visits

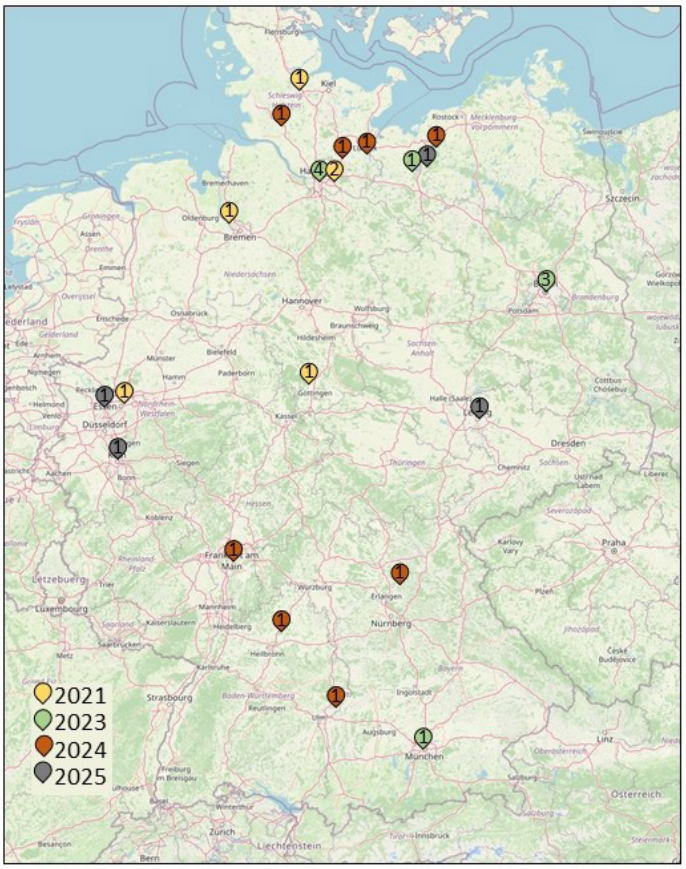

Figure 1. Map of construction sites visited. Map data © OpenStreetMap contributors, ODbL (openstreetmap.org/copyright).

were conducted once during the assembly phase, provided at least one of the following criteria were met:

a. The construction schedule was tight, the assembly process extended, or installation pauses were necessary—conditions under which exposure to rain was likely.

b. The project involved more than two residential units and/or more than two stories.

c. Special moisture protection efforts were employed, such as the use of a construction tent.

d. The construction was particularly sensitive to moisture, for example, glue-free assemblies or components with finished surfaces that are especially vulnerable to moisture exposure.

The protocols that were the primary data collecting instrument comprised eight topics. The topics covered fundamental aspects such as the building type, the place of prefabrication, and the construction site (I). They also addressed storage and shipping, focusing on how elements were transported, stored, and protected during these phases, as well as any inspections or tests conducted (II). Topics III to VI examined the structural system, the timber construction method, and the level of prefabrication. Finally, topics VII and VIII discussed special protection requirements and moisture mitigation concepts.

Every category (I-VIII) of the protocols was specified by subcategories This paper solely focuses on categories VII and VIII (Figure 2).

The data were analyzed to identify patterns, trends, and common practices in moisture protection during the assembly of timber construction. The protocols were designed to evaluate the extent to which the strategies were planned and executed.

In most cases, craftsmen were either not informed by their supervisors or unaware of the research objectives, and thus did not realize that moisture protection practices would be assessed. Consequently, it can be assumed that the sites were neither tidied up to create a better impression, nor did the craftsmen change their behavior concerning the handling of the elements.

Results and discussion

The findings presented in this article represent only the preliminary results of an ongoing investigation.

Assessment overview

The primary question when assessing construction sites in view of moisture protection was whether a clear and structured concept was evident or if the installation followed no discernible plan regarding weather protection.

Prior to the site visits, the building plans were thoroughly reviewed to determine whether weather protection measures had already been incorporated in the detailed planning phase. This preliminary step allowed for the completion of a significant portion of the assessment protocol in advance. Subsequently, the protocols were filled out according to the established order.

Through this assessment, insights were gained into the integration of protection measures within planning and execution, highlighting potential risks and best practices concerning moisture management throughout the construction process.

The assessment during site visits covered several fundamental and practical aspects relevant to moisture management and construction quality:

- **General exposure risks:** Evaluation of the construction method, where and how timber elements were at risk of moisture exposure, including the division of the site into construction phases to promote safer and more efficient substructures.
- **Storage methods:** Review of the different storage solutions. This included storage of components before

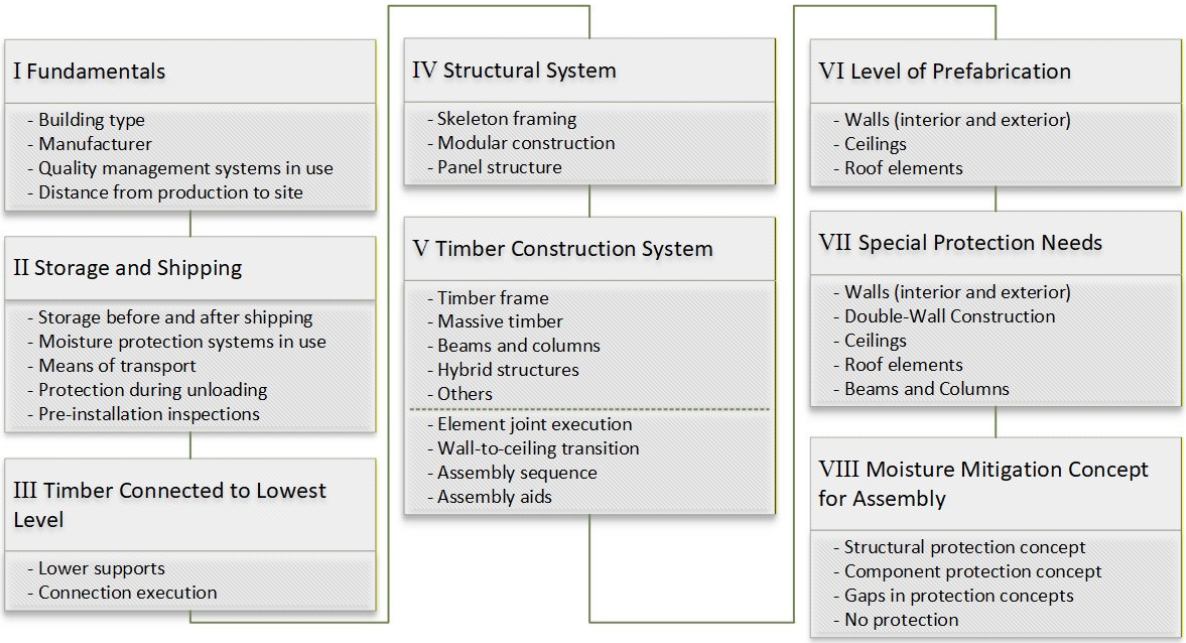

Figure 2. Site assessment protocol design.

and after transportation, including placement, elevation, and covering of materials to protect them from direct exposure to moisture. In addition, attention was paid to whether secondary materials, i.e., materials that were to be laid in a further work step, could hinder further protective measures due to their placement. For example, a pallet of bitumen sheets was placed on the roof without temporary weather protection underneath (Figure 3). That made it considerably more difficult for the craftsmen to carry out the protective measures before the roofer arrived. No crane was available at the later stages, so part of the roof stayed exposed to rain, which led to increased moisture levels in the connection joints of the ceiling components.

- **Adapting the installation conditions to the weather:** Analysis of how the sequencing of key tasks aligned with the weather, and whether unfavorable timing could increase risk of moisture ingress.
- **On-site handling of timber elements:** Observation of how timber components were transported, unloaded, and moved

Figure 3. Storage of construction materials for the roof prevented the implementation of temporary weather protection measures (author photograph).

around the site, with emphasis on practices that minimized surface wetting or damage. A typical question was whether or not the components were temporarily stored on the construction site or whether they were installed directly after shipment. Poorly planned or executed storage of construction components not only leads to a loss of quality during rainfall events, but also causes the entire construction site to become disorganized and cluttered (Figure 4). This can result in delays and errors.

- **Presence or absence of protective measures:** Documentation of weather protection strategies in use. Were weather protection strategies such as tents, tarpaulins, or temporary covers visible? This included identification of areas lacking adequate safeguards. These areas could be present because the work in question was either not (yet) carried out or not planned. Furthermore, it was necessary to evaluate whether protective measures for the components were carried out, even if these had not originally been included in the planning.
- **Protection during lifting and installation:** Assessment of procedures used when lifting and installing timber elements, ensuring these steps did not compromise material condition or introduce unnecessary moisture risks.
- **Communication and awareness:** Evaluation of the level of site awareness and communication regarding moisture-sensitive procedures, as well as training and involvement of all parties in maintaining protective measures.

This approach provided a comprehensive understanding of both planned and actual site practices, highlighting strengths and identifying potential areas for improvement in moisture protection and project execution.

Results

For this evaluation, protocol numbers VII and VIII were analyzed along with the documents provided by the planning offices. Subsequently, the photographic documentation was examined and included into the gatherings. As a result of this analysis, the scope of this examination does not include the entire process of manufacturing, storage, and shipping.

A total of 27 sites from different companies and design offices were evaluated. Identifying suitable sites for this research has presented a considerable challenge. Even though larger networks were willing to facilitate connections with their members, many larger timber construction companies appeared hesitant to permit external analysis of their projects. This reluctance may stem from concerns about disclosing operational inefficiencies or potential weaknesses, as well as a desire to protect competitive advantages by withholding insights into effective work strategies. Despite repeated inquiries, it often seemed that these companies sought to avoid the scrutiny associated with having their practices documented and evaluated. On the other hand, when we did gain access to sites, it was evident that, in numerous cases, the construction teams themselves did not appear particularly concerned about potential issues.

Figure 4. Disorganized construction site, inappropriate storing of mass timber elements (author photograph).

The on-site visits revealed a gap between problem awareness in the scientific community and the handling of components by the executing companies on site. It was striking how little attention was given to the possible consequences of inadequate or missing moisture protection measures, suggesting either a lack of awareness or a lower priority being placed on these critical aspects of construction. Structural-specific moisture protection, as discussed by Heinicke and Kehl (2024), seemed to be rare in Germany, as no construction sites with such a concept were found in this study. All sites that exhibited any form of conceptualization used the component protection concept (Heinicke and Kehl 2024).

Figure 5 summarizes a portion of the research results to date. It categorizes the sites based on the data evaluated. The evaluation aimed to identify where along this spectrum a site has to be located, with the following categorization:

- **No concept:** This refers to an absence of identifiable moisture protection strategies, resulting in a lack of logical order in the measures taken. For example, many sites used prefabricated CLT elements for ceilings that came with fully bonded membranes already applied at the factory, allowing for easy ordering from the manufacturer. However, if no additional measures were implemented to effectively manage and divert water away from the structure, it cannot be classified as a cohesive concept. Also, if these components with unprotected narrow sides were stored directly on the ground or left exposed to weathering without additional shielding, this demonstrated inadequate moisture protection. Proper intermediate storing measures are essential for preventing wetting and ensuring that the construction aligns with a comprehensive water management approach.
- **Planned but not implemented:** Analysis of the documents may reveal a defined concept through precise measures that were not applied on site, whether due to oversight, practical challenges or simply being overlooked. Non-application indicates a disconnect between planning and execution. The plans may showcase a clear strategy and a commitment to high-quality processes, yet the necessary information or the urgency to implement the measures was not effectively communicated from management to the installation team.

  For practical reasons or due to the sequence of work, there may be a bridging phase during which the measures cannot be carried out on site. (It is possible that there were time slots in which the elements were assembled; however, further application of measures had yet to be undertaken.). Nevertheless, it can be stated with certainty that in the absence of the prescribed measures for the site, there was a gap between the planned and actual outcomes. During a site visit where assembly had already progressed to the third and last floor, it quickly became apparent that not a single moisture protection measure intended in the planning to secure the intermediate construction stages had been implemented, apart from the application of membranes by the manufacturer in the factory.

  Although the ceiling element joints had been sealed to create a tight ceiling slab, water had intruded through the joints and stained the construction below. Additionally, the components had been improperly stored on the ground. By the time of the site visit several weeks of unsettled weather had passed, including heavy rain events, during construction from the ground level to the third floor.
- **Gaps in concept:** Indicated partial implementation, where certain aspects of moisture protection were in place, but significant areas of the construction were neglected. For instance, the lack of planned drainage for the ceilings throughout the entire building demonstrated a lack of comprehensive consideration for moisture management.

		2021						2023									2024								2025					
	Site Nr.	1	2	3	4	5	6	7	8	9	10	11	12	13	14	15	16	17	18	19	20	21	22	23	24	25	26	27	Σ:	%
No continuous protection	No concept					x	x				x	x			x							x						x	7	25.93
	Planned but not implemented							x	x								x												3	11.11
	Gaps in concept			x	x					x			x				x		x		x			x		x	x		10	37.04
	Full concept	x	x											x		x		x		x			x		x				8	29.63
	Particulary complex/ sensitive construction	x	x		x					x	x	x		x		x		x		x			x		x		x	x	14	51.85
	Simplified/resilient construction						x								x		x		x		x			x					6	22.22

Figure 5. Breakdown of projects following evaluation of overall moisture protection during construction.

This must be distinguished from accidentally forgotten work steps, which naturally arise during execution, whereas in our case, the lack of drainage reflected a deficiency in planning-compared to a single, unconnected drainage pipe.

- **Full concept:** This referred to a clearly structured and fully implemented moisture protection strategy. Each element followed a precise scheme, leading the water away from the structure. This ensured that water was captured, collected, and diverted, with all components protected from moisture intrusion throughout the installation process. The pathway for water was clearly defined at all times, ensuring comprehensive moisture management. The categorization was a structure based on organizational effort. Ultimately, moisture protection is a necessary organizational task that must be ensured by planners and producers. These three first rows and up to the sum of projects with: "No continuous protection". These were contrasted with sites where clear strategies were evident throughout the building process, labeled as "Full Concept".

To ensure comparability between construction sites, it was crucial to consider both conceptual differences and the complexity of the respective building projects. This approach was reflected in the last two rows of the table shown in Figure 5 (highlighted yellow), which categorized the sites into three groups:

- **Particularly complex/sensitive constructions:** Projects involving intricate or delicate structures that required enhanced protective measures during the construction phase to mitigate risks from environmental exposure. For instance, a hybrid ceiling constructed on site introduced specific challenges. The need to wire and place iron for concrete extended exposure times for walls beneath the ceiling to wind and weather. This contrasted with simpler scenarios, such as assembling prefabricated CLT elements, where the exposure period was significantly shorter.
- **Simplified/resilient constructions:** These projects were inherently robust or featured a lower degree of prefabrication, reducing their vulnerability to damage from rainwater. Such sites often demanded fewer resources for protective measures.
- **Ordinary constructions:** These were sites that fell between the extremes of complexity and simplicity or sensitivity and robustness. While they still required adequate moisture protection, the necessary measures aligned with standard practices rather than demanding extraordinary effort.

Figure 5 specifically highlights only the first two groups; the third group, ordinary constructions, is not explicitly shown. These sites were considered the residual category, encompassing all remaining projects after subtracting those classified as particularly complex or simplified. Their inclusion provided a holistic understanding of the spectrum of construction challenges and protection requirements. Classifying construction sites into these three groups made it evident that the level of protective effort required varied significantly based on the nature and complexity of each project. This classification highlighted the importance of tailoring moisture protection measures to the specific demands of each site.

Less than one-third (29.63%) of all sites had sufficient moisture mitigation practices and a complete concept. This means that, in the event of rain, the components were protected at every stage of construction, with the only exception being during their relocation by crane (Figure 6). This meant that a clear strategy of how the water was collected and diverted away from the structure was evident in the event of rain. There was no systematic gap where water could intrude on the construction other than by excessive rain events that could not be covered by state-of-the-art component protection measures. As Bolmsvik et al. (2023) highlighted, addressing this and other issues like crane relocation of elements, on site storage, wind deflection, or temperature control issues required a comprehensive structural protection concept. Interestingly, all of the sites found to have sufficient control over their processes had to deal with either particularly complex or vulnerable constructions. This included an office building constructed entirely with dowel-laminated timber (DLT), a method in which wooden panels are assembled using dowels instead of synthetic adhesives. Here, even minimal contact with moisture would automatically lead to warping and dimensional changes in the panels. It seems that the companies aware of the issue of moisture protection were developing greater expertise in handling such challenges. With growing awareness and skill, they may have felt more confident in tackling larger-scale or more complex projects. It could also be that these companies had previously faced moisture-related problems and were now more determined to prevent such failures in the future.

In 70.37% of projects, no continuous moisture protection was implemented. This meant that one of three situations existed: the planner did not include temporary moisture protection in the construction phase planning, the contractors on site did not recognize the need for moisture protection for building components, or the approach used did not cover all phases or did not include all parts of the construction.

Of the 70.37% (19 sites), 31.5% (6 sites) represented complex projects, of which only half (3 sites) had any conceptual approach. In 11.11% of cases, a specific moisture protection

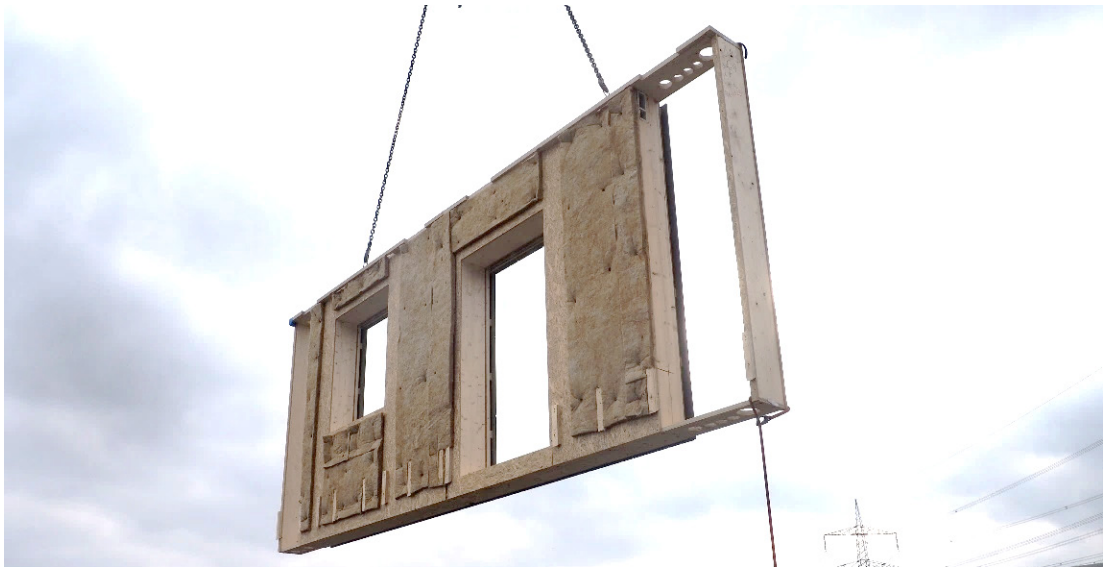

Figure 6. Element relocation by crane (author photograph).

strategy was planned for construction but somehow not executed. However, it does not seem that a connection existed between complexity and the enforcement of a planned concept. To draw any conclusions in this direction, further and more sophisticated studies would be needed, addressing more relevant factors and examining additional sites. Different reasons for the occurrence could, however, be found. In one instance, it was unclear what during erection led to the decision against implementing the planned measures. In another case, it was the lack of awareness regarding the conditions under which these specialized timber products could be used that contributed to the issue. In yet another case the responsibility for applying moisture protection was delegated to the client, who lacked the necessary expertise to implement a comprehensive protection strategy.

Two-thirds (66.67%, full concept + gaps in concept) of cases were found to have concepts in place, yet more than half of these concepts were incomplete by missing important components. This indicated that while moisture protection strategies were present in many cases, their implementation was often insufficient or incomplete. Further research and efforts, such as enhanced education, are necessary to ensure that future efforts are fully realized and effectively integrated into construction practices. Figure 7 shows a three-story semi-detached house with a low level of prefabrication. The concept involves fully covering all horizontal components. While the interior was sealed to prevent moisture from entering the cavities, the exterior was left open. This construction method requires a schedule that allows for drying measures before insulation is installed. Drying is possible due to the simplicity of the con-

Figure 7. Incomplete protection with possible entrapment of moisture (author photograph).

struction. Particularly critical in this case is the formation of troughs (red arrow) on one side of the structure to enable the waterproofing of the flat roof at the required height. Rainwater (during construction) not only drains poorly there but can also easily accumulate, while at the same time the moisture content is almost impossible to monitor.

As many as 25.93% of the sites surveyed to date had no systematic protection against moisture intrusion during assembly. Only two of these (seven in total) were especially simplified and resilient.

Until recently, timber construction in Germany was mainly limited to single-family or semi-detached houses. These projects were often completed within a "Schönwetterfenster"—a period where weather conditions were predictable and favorable for construction. This allowed for efficient execution within a narrow timeframe. However, the shift towards larger-scale timber construction projects, which demand extended assembly times, makes this approach less viable. There is a possibility that the mentality of adjusting construction schedules to the weather may not be as deeply ingrained in the minds of some workers. Larger and more complex projects requiring significantly longer assembly times mean that it is no longer an option to follow the same weather-dependent work patterns. The transition to larger projects with extended timelines may be presenting challenges for some workers, who are not yet accustomed to the level of planning and prolonged schedules these projects necessitate.

Conclusions

Our findings highlight the need for comprehensive moisture management in timber construction, from design to construction, to reduce the risk of decay, mold growth and structural instability. The number of uncontrolled situations, with constantly changing building standards and new requirements for quality and durability, make it clear that a new awareness and greater efforts are needed in the area of moisture protection. This research showed that timber construction is more than solely building with non-fossil materials, but a completely different approach to building.

While progress has been made, with some projects demonstrating robust moisture protection practices, a large portion of projects still lack adequate measures. Addressing these gaps will require a collaborative effort among designers, contractors, craftsmen, and the education sector to ensure that effective moisture protection strategies are integrated into every phase of wood construction. This collaborative approach is essential to overcoming existing challenges, as it allows for a more holistic understanding and application of construction methods, reducing the risk of moisture damage and ensuring the long-term durability of timber structures. Education plays a vital role in this process, as increasing awareness and knowledge among all stakeholders, from architects to builders, can help implement strategies that are tailored to the unique demands of timber construction.

In conclusion, ongoing research and industry efforts are crucial to enhancing moisture protection practices in wood construction, promoting more sustainable and resilient building practices that maximize wood's potential as a renewable and durable material.

Acknowledgements

The expenses incurred in traveling to the various construction sites were covered by 81fünf high-tech & holzbau AG.

References

Bolmsvik Å, Eriksson O, Tengberg CS, Johansson P (2023) Weather protection at the construction site: work environment and conditions for moisture and mould growth on massive timber. J Phys Conf Ser 2654:012042, 13th Nordic Symposium on Building Physics (NSB-2023) 12/06/2023–14/06/2023, Aalborg, Denmark. https://doi.org/10.1088/1742-6596/2654/1/012042

Cowled CJL, Slattery TP, Crews K, Brooke H (2023) Influence of Weathering on the Structural Performance of Sheathing-to-Timber Connections. Forests 14(4):734. https://hdl.handle.net/10453/178428

Flexeder N, Schenk M, Aondio P (2022) Moisture Monitoring Techniques for the Protection of Timber Structures. Proceedings of the 6th International Conference on Structural Health Assessment of Timber Structures SHATIS22, 7–9 Sept 2022 Prague, Czech Republic. https://doi.org/10.14459/2022md1687361

Glauner R, Grosser D, Melcher E (2022) Holzschutz; Praxiskommentar zu DIN 68800 Teile 1 bis 4, 3rd edn. Beuth Kommentar. Beuth Verlag. In German.

Heinicke R, Kehl D (2024) holzbau handbuch. Feuchtemanagement Witterungsschutz in der Bauphase. Holzbau Handbuch, Series 5, Part 1, Issue 1. In German.

Imken A, Brischke C, Kögel S, Krause KC, Mai C (2020) Resistance of different wood-based materials against mould fungi: a comparison of methods. Eur J Wood Prod 78 (4), S:661–671. https://doi.org/10.1007/s00107-020-01554-5.

Kalbe K, Kalamees T, Kukk V, Ruus A, Annuk A (2022) Wetting circumstances, expected moisture content, and drying performance of CLT end-grain edges based on field measurements and laboratory analysis. Build Environ 221:1–16. https://doi.org/10.1016/j.buildenv.2022.109245.

Kutnik M, Paulmier I, Ansard D, Montibus M, Lucas C (2020): Update on the Distribution of Termites and other Wood-boring Insects in Europe. IRG/WP 20-10960 Conference: 20-06-10/11 IRG51 Webinar Stockholm. The International Research Group on Wood Protection (IRG) (Proceedings IRG Annual Meeting (ISSN 2000-8953)). https://www.irg-wp.com/irgdocs/details.php?5b7ff8f0-0aee-ba2e-672c-f1b7008388f2

Mergel C, Menrad K, Decker T (2024) Which factors influence consumers' selection of wood as a building material for houses? Can J Forest Res

54:467–478. https://doi.org/10.1139/cjfr-2023-0197

Qiao J, Zhang X, Xiao F, Li Y, Gao W (2024) Experimental investigation of mold growth risk among typical residential indoor materials: Case study in coastal city, China. Energy Build 304 (Feb):113885. https://doi.org/10.1016/j.enbuild.2024.113885.

Sathre R, O'Connor J (2010) Meta-analysis of greenhouse gas displacement factors of wood product substitution. Enviro Sci Policy 13(2):104–114. https://doi.org/10.1016/j.envsci.2009.12.005.

Scheiding W, Grabes P, Haustein T, Haustein VH, Nieke N, Urban H, Weiß B (2021) Holzschutz: Holzkunde - Pilze und Insekten - konstruktive und chemische Maßnahmen - Technische Regeln - Praxiswissen, 3rd edn. Hanser eLibrary. Carl Hanser Verlag, München. In German.

Schmidt D, (2023) Holzbau Handbuch: Holzschutz Bauliche Massnahmen. holzbau handbuch, Series 5, Part 2, Issue 2. In German.

Schmidt E, Riggio M (2019) Monitoring moisture performance of cross-laminated timber building elements during construction. Buildings 9(6):144. https://doi.org/10.3390/buildings9060144

Schrader L, Brischke C, Trautner J, Tebbe C (2025) Microbial decay of wooden structures: actors, activities and means of protection. Appl Microbiol Biotechnol 109(1), S. 59. https://doi.org/10.1007/s00253-025-13443-z .

Schubert K, von Laar C, Bombeck H (2024) Understanding and Addressing On-Site Moisture Protection Challenges in Timber Construction: A Comprehensive Review of German Practices. Inżynieria Mineralna 1(2). https://doi.org/10.29227/IM-2024-02-58 .

Svensson Tengberg C, Bolmsvik Å (2021) Impact on a CLT structure concerning moisture and mould growth using weather protection. J Phys Conf Ser 2069(1):12017. https://doi.org/10.1088/1742-6596/2069/1/012017

Tupenaite L, Kanapeckiene L, Naimaviciene J, Kaklauskas A, Gecys T (2023) Timber Construction as a Solution to Climate Change: A Systematic Literature Review. Buildings 13(4):976. https://doi.org/10.3390/buildings13040976

Udele KE, Morrell I, Morrell J, Sinha A (2024) Biological durability of cross laminated timber connections. Data in Brief 55 (Aug):110698. https://doi.org/10.1016/j.dib.2024.110698 .

Wang J (2015) On-Site Moisture Management of Wood Construction. https://cwc.ca/wp-content/uploads/2016/01/Site-Moisture-Protection-Materials-for-Durability-website-V2.pdf. (02 May 2024).

Wang JY, Stirling R, Morris PI, Taylor A, Lloyd J, Kirker G, Lebow S, Mankowski ME, Barnes HM, Morrell JJ (2018) Durability of mass timber structures: A review of the biological risks. Wood Fiber Sci 50 (Special Issue):110–127. https://doi.org/10.22382/wfs-2018-045.

Weinisch KH (2019) Feuchteschutz im Geschossbau – eine Bilanz. 10. HolzBauSpezial Bauphysik & Gebäudetechnik 2019. https://events.forum-holzbau.com/pdf/16_HBS2019_Weinisch.pdf. (02 May 2024).

High heat resistance of adhesive bonds to wood and aluminum

Linda F. Lorenz *
Chemist
USDA, FS, Forest Products Laboratory
One Gifford Pinchot Dr.
Madison, WI 53726
Email: linda.f.lorenz@usda.gov

Charles R. Frihart
Volunteer
USDA, FS, Forest Products Laboratory
One Gifford Pinchot Dr.
Madison, WI 53726
Email: cfrihart4@gmail.com

Marco T. Lo Ricco
Research General Engineer
USDA, FS, Forest Products Laboratory
One Gifford Pinchot Dr.
Madison, WI 53726
Email: Marco.LoRicco@usda.gov

(Received 21 May 2025)

Abstract: Wood is preferred as a building material due to its high strength, low weight, and ability to retain many of its properties even at moderately high temperatures. However, numerous wood adhesives lose strength as the temperature increases, especially around 200°C. This study examined bond strength at temperatures above that required for initiation of wood degradation for bonds of wood-to-wood and wood-to-aluminum using two oil-based adhesives (resole phenolics and epoxies) and two bio-based adhesives (soy protein isolate and ovalbumin from egg whites). The phenolics not only gave the best strength in the wood-to-wood bonding, but also in the wood-to-aluminum bonding. The second best were the protein adhesives, and the epoxies were the weakest. This research reinforces the use of phenolic adhesives for wood exposed to high temperatures.

Keywords: Wood bonding; High temperature; Phenolic; Protein; Epoxy; Aluminum.

Introduction

For efficient use of wood resources, many wood manufacturers bond smaller wood elements (veneer, strands, particles, and fibers) to make useful larger wood assemblies (composites, various types of beams, and cross-laminated timber) (Frihart and Hunt 2010). Composite wood products need to resist bond failures to maintain structural integrity during extreme events for a sufficient time to allow people to escape injury or death. Heat resistance of wood bonds has been an ongoing issue (Yeh and Brooks 2006), whether it is the creep of structural bonds in hot and humid locations (ASTM 2011) or fire resistance (ANSI/APA PRG 320). For nearly half a century, the adhesives used in laminated wood products such as structural glulam were primarily phenol resorcinol adhesives that maintained bond integrity even when subjected to moisture and fire. The proliferation of mass timber products such as cross-laminated timber (CLT) over the last two decades, however, has resulted in the development of new adhesive formulations that facilitate the production of large-scale structural wood panels. The introduction of these new adhesive formulations has led to the development of new timber product standards and fire testing procedures. Recent research has focused on large-scale tests on thicker wood members (Zelinka et al. 2018), and the ANSI/APA PRG 320: Standard for Performance-Rated Cross-Laminated Timber standard requires full-scale fire qualification testing (ANSI/APA 2018). Because qualification testing at full scale is costly, Miyamoto et al. (2021) and Zelinka et al. (2020a) have demonstrated the validity of small-scale testing for precursory evaluation of adhesive performance at elevated temperatures.

One area not investigated is the resistance to elevated temperature of bonded thin veneers. Thin veneers are bonded into

* Corresponding author

products such as laminated veneer lumber (LVL) and plywood, both of which are produced at many scales, including mass timber panels that are comparable to the sizes of CLT. We used an economic small-scale apparatus (ASTM 2020) to address this gap in the literature by testing the strength of both bio-based and synthetic adhesives at temperatures above where wood starts to degrade. The adhesives were evaluated to determine if the thermal degradation of the wood caused the adhesive to de-bond or if the adhesives prevented the veneers peeling off prior to complete degradation of the veneer layer (Poletto et al. 2012). We also tested the wood bonding to aluminum under the same conditions, because aluminum is used in furniture, sporting equipment, and vehicular components. Especially in sporting and transportation applications, laminates need to be lightweight, which adds additional performance criteria for the adhesive. Bonding lightweight aluminum alloys to wood veneers with high strength-to-weight ratios is desirable, yet challenging because of material dissimilarities in porosity, thermal expansion, stiffness, moisture content, and chemical composition, among many other factors that potentially affect bond quality.

Aluminum-to-wood bonding is an area of particular concern with phenolics, which do not normally adhere to the metal platens in the pressing of composites. Historically, aluminum-to-wood bonding was investigated by the USDA Forest Service Forest Products Laboratory (1964) at a time when aircraft structures were made primarily from timber materials. Eickner et al. (1955) directly bonded 5-ply, birch-veneer plywood to aluminum alloy using several different adhesives and processes and tested the lap joints via 10 million cycles of prying to assess fatigue resistance. Black and Blomquist (1959) investigated the thermal degradation of various adhesives bonded to aluminum and stainless steel. Since these studies, new formulations and testing methods have been developed, which led to this current comparison of phenolic, epoxy, and bio-sourced adhesives.

The need to withstand high temperatures (such as 250°C) drastically limits the types of adhesives that can be used and eliminates adhesive types known for their mechanical or chemical thermal instability at higher temperatures: most polyurethanes, melamine-urea-formaldehyde, polyvinyls, and hydrocarbons (Liu et al. 2020; Zelinka et al. 2020b; and Miyamoto et al. 2021). This narrowed down the selection to three types that are known to have good heat resistance: phenolics, proteins, and epoxies (Frihart 2013). Phenolics are widely used in structural wood bonding because of their durability and heat tolerance. Proteins are not widely used in wood bonding mainly because of their limited moisture resistance and cost; however, they have long been used in wood fire door applications. Epoxies are not normally used in wood bonding, except in repairing delaminated wood beams and repairing spots of wood decay. Their advantage is that they are gap filling, and some formulations can bond at room temperature, but outside of wood applications, they are widely used for their durability and heat resistance.

Therefore, the objective of this study was to test the strength of both bio-based and synthetic adhesives at temperatures above where wood starts to degrade with wood-to-wood and wood-to-aluminum bonding.

Materials and methods

Specific adhesives were selected for minimal wood void filling to keep the bonded product weight low (Table 1). Glass Bubbles K15, which are hollow spheres of glass of 60 µ, were obtained from 3M™ (Minneapolis, MN) and added to the adhesives to reduce weight and density at 5%, 10%, or 20% of total solids.

The resoles and epoxies were used as received. The soy protein isolate (SPI, PRO-FAM™ 974) was from ADM (Decatur, IL), and the egg white (dried egg whites, H-40) was from Ballas Egg Products Corp. (Zanesville, OH). The protein adhesives were prepared by dissolving them in water at the concentrations specified and stirring until they were well mixed. The resoles were proprietary commercial aqueous PF adhesives with minimal wood penetration obtained from a major wood adhesive producer, stored at 5°C, and used within a month, according to the manufacturer's instructions. The epoxies were all selected because they were recommended as heat-resistant adhesives or had been previously tested for good wood bonds, and they were mixed with curing agents according to the manufacturers' instructions. Because the different types of adhesives interact differently with the wood surface and cure differently, the bonding conditions are discussed in the results and discussion section.

Veneers from five wood species, bigtooth aspen (*Populus grandidentata)*, yellow birch (*Betula alleghaniensis*), cherry (*Prunus* spp.), red maple (*Acer rubrum*), and yellow poplar (*Liriodendron tulipifera*) were obtained from Great Lakes Veneer (Marion, WI). The veneers were cut into 117 mm × 20 mm × 0.8 mm thick pieces. Aluminum pieces of 117 × 20 × 0.8 mm were cut from sheet stock. Half of the aluminum specimens were lightly sanded with medium grit sandpaper. To make a specimen, 5–10 mg of an adhesive was applied to the end of a piece of veneer and a second piece of veneer was

Table 1. List of adhesives evaluated for bonding wood and aluminum ABES samples.

Adhesive	Adhesive type and label	Details
PF 1	Resole phenol-formaldehyde	Concentration of 43.1% solids obtained from a commercial phenolic producer (Aqueous)
PF 2	Resole phenol-formaldehyde	Concentration of 42.3% solids obtained from a commercial phenolic producer (Aqueous)
	Epoxy 805	Aremco Products Inc (Valley Cottage, NY)
	Epoxy 526N	Aremco Products Inc (Valley Cottage, NY)
	Epoxy 2335	Aremco Products Inc (Valley Cottage, NY)
	EPON 162	Hexion (Houston, TX)
	EPON 862	Hexion (Houston, TX)
	D.E.R. 331	OLIN (Clayton, MO)
SPI 974	PRO-FAM™ 974	Soy protein isolate (SPI) from Archer Daniels Midland Company (Decatur, IL)
H-40	Egg white H-40	Ballas Egg Products (Columbus, OH)

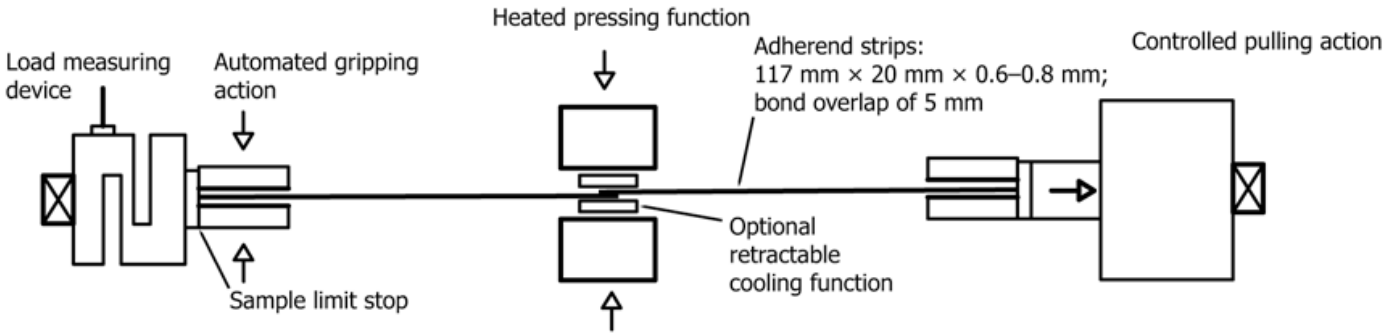

Figure 1. Schematic of the bonding and ABES testing system.

placed over the adhesive, resulting in a 5-mm overlap (Figure 1). The specimens were bonded at 120°C or 150°C for 120 s at 0.2 MPa using the ABES method (ASTM 2020) and tested the next day to ensure that the adhesives were fully cured. The ABES (Automatic Bond Evaluation System) from Adhesive Evaluation Systems, Inc. (Corvallis, OR) is an apparatus that can bond small samples and test them in a relatively short time.

The ABES test method was used for several reasons. The thin veneer ensured rapid heat transfer to the bondline both in the bonding step and 250°C heat treatment for 100 s. Good temperature and time control ensured repeatability in the bonding and heat treatment steps. The platens attain the higher temperatures for testing the heat resistance of the bond and the wood is degraded only near the bonded area. As soon as the platens are retracted, the tensile force is applied, with the bond still at the elevated temperature, and the force required to break the bond is measured in Newtons at the factory setting of 15 on the pull rate control (no unit specified). Using a smooth veneer ensures consistent testing of the bondline strength. The ABES instrument as described in ASTM D-7998-19R24 (ASTM 2024) is illustrated in Figure 1, and the procedure is described in detail (Frihart and Lorenz 2020). The small mass of wood and large mass of the platens assured that the bondline reached the set temperature quickly, as 0.2 MPa pressure was applied to the bondline. Five replicates were run for each test condition, and the mean and 95% confidence interval were calculated for each condition. The ABES is only a screening tool for eliminating the poor performers and not for setting the final adhesive formulations for production of full-scale laminates.

Results and discussion

Four important properties of the adhesives considered are that they need to bond wood laminates with minimum penetration, produce heat resistance bonds to 250°C, adequately bond with added glass bubbles to reduce the density and amount of adhesive used, and bond to aluminum. Wood is a porous material; thus, penetration of the adhesive is required to create strong bonds through mechanical interlock. In making lightweight products, a strong surface bond with minimum penetration is required, since the adhesive is much denser than the displaced air in the wood voids. Wood penetration can be judged by visual and microscopic examination of crosscut samples (Hare and Kutscha 1974). In this study, whether the bond failed because of wood or adhesive failure was not determined, because the

surface area of the bond in ABES testing is too small to identify and measure a definitive mode of failure.

Because the ABES data below are for screening purposes for the best wood species and adhesive formulation, the statistical differences were not examined by analysis of variance (ANOVA) and post-hoc tests. Instead, adhesive and veneer selections were made only when there were large and consistent differences apparent in graphs comparing the mean and error bar plots of bond strength at elevated temperatures. Although bond strength is critical, other factors like low adhesive application rates, resistance to peeling of thin veneers on heating, and availability of a consistent wood source were considered. Generally, bonds that exhibited the least change in strength at elevated temperatures, relative to room temperature, were considered top performers.

Phenol-formaldehyde adhesives

Phenol-formaldehyde (PF) adhesives are among the strongest and most durable wood adhesives that are often formulated as low molecular weight oligomers to improve penetration of the cell lumens and the cell walls for more water durable bonds (Frihart 2009). The two proprietary commercial aqueous resole PF adhesives (labelled PF 1 and PF 2) were bonded at 120°C using all five wood species and, in some cases, with glass bubbles added to reduce the adhesive density. The strengths at 21°C and after heating for 100 s at 250°C, without and with 5% glass bubbles, are provided in Figure 2. The strengths were similar for all the veneers, except for the cherry at 250°C. Even though the high temperature tests were above the temperature for the initiation of wood decomposition, there was no delamination in any of the samples at 250°C during the short hot-testing conditions. The 250°C test results were generally significantly lower than the 21°C test results, without and with the addition of glass bubbles, but these differences did not exist in every case. Significant differences were considered for conditions showing non-overlapping 95% confidence interval bars. The greater differences in the temperature effect on the cherry compared to the other species could indicate a greater heat sensitivity of this species.

Wood is often used because it is strong for its weight, but the adhesive has a higher density than the wood. Thus, low density glass bubbles were added to the PF 1 adhesive at 10% and 20%, in contrast to the 5% added previously. The bond shear strength decreased somewhat, and with 20% glass bubbles, this PF was very thick and difficult to spread on the wood. There was no delamination at 250°C, but the glass bubbles did not show any reinforcing effect leading to higher strength (Figure 3). At this point, the yellow poplar was selected based on its relative low density, greater uniformity, and high strength as the wood species to use beyond the preliminary test with each adhesive.

PF 1 (43.1% solids) was used to bond yellow poplar at 150°C, which is a more optimum temperature for bonding the PF adhesives (according to the manufacturer's guidelines), to compare with the samples bonded at 120°C. The 120°C was considered less promising for some applications due to it being difficult to attain in some pressing processes, especially for thicker plywood, which needs higher platen temperatures for all the bonds to reach this temperature. In Figure 4, the bond strengths tested at 21°C were 40% higher when bonded at 150°C, although the strengths tested at 250°C did not increase.

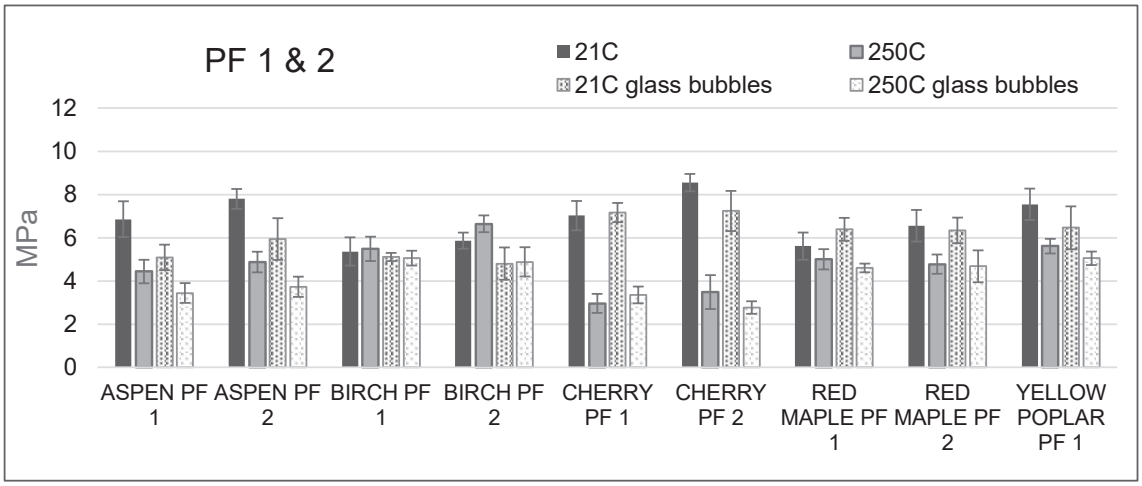

Figure 2. Room temperature (21°C) and high temperature (after 250°C heating for 100 s) bond shear strength of phenolics on five different wood species, without or with 5% glass bubbles, bonded at 120°C for 120 s using ABES. The values are the average of five replicates, and the error bars represent one standard deviation.

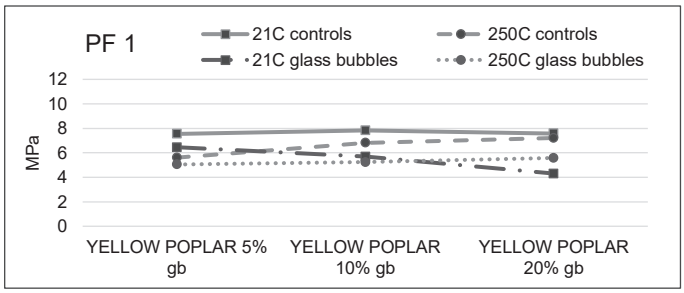

Figure 3. Room temperature (21°C) and high temperature (after 250°C heating for 100 s) bond shear strength of PF 1 with 5%, 10%, or 20% glass bubbles (gb) added, on yellow poplar bonded at 120°C for 120 s using ABES.

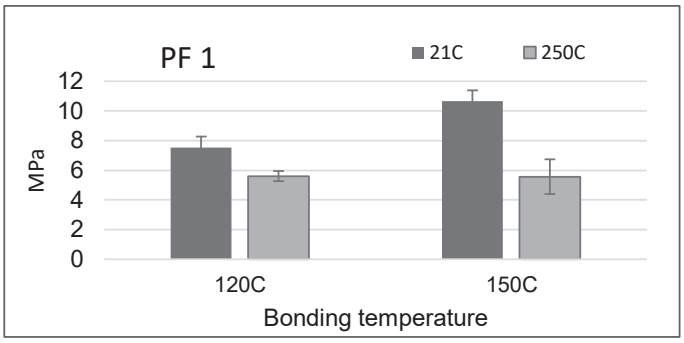

Figure 4. Room temperature (21°C) and high temperature (after 250°C heating for 100 s) bond shear strength of a phenolic on yellow poplar bonded at 120°C and 150°C for 120 s using ABES. The values are the average of five replicates, and the error bars represent one standard deviation.

Based on the results, we supposed that the adhesive is partially cured at 120°C and fully cured at 150°C, before reaching the 250°C test condition.

Proteins

In addition to the commercial phenolics that did very well as high temperature adhesives in the ABES tests, protein and epoxy adhesives were also studied. Protein adhesives were widely used for wood product assembly, including in fire door applications that continue today, until the introduction of synthetic adhesives that have better water resistance gained broader industry acceptance. Soybean proteins were the main commercial adhesives, but the ovalbumin from egg whites is also a good wood adhesive (Frihart and Lorenz 2018; Lorenz and Frihart 2023). Of the three adhesive types considered, the only fully bio-based option is protein adhesives. These adhesives come as powders and are dispersed in water at room temperature just prior to use.

A commercial soy protein isolate (SPI) was tested at 20% solids, which was a thick paste. As shown in Figure 5, the bond shear strengths at both 21°C and 250°C were similar for all the veneers, without and with 5% glass bubbles (based on the weight of soy solids). There was no delamination at 250°C of the SPI bonds, but their higher temperature bond strengths were considerably lower than those for the PF adhesives. The lower strength at higher temperatures may be due to less adhesive in the glueline (adhesive layer between the wood surfaces), since the solids content of the SPI adhesive was dramatically lower than the PF adhesive, at 20% versus 43%, respectively.

An egg white adhesive was tested at 50% solids, which was a thick liquid, but still pourable. In Figure 6, the bond strengths at both 21°C and 250°C were similar for all the veneers (except for the cherry), without and with 5% glass bubbles (based on the weight of egg white solids). There was no delamination at 250°C of the egg white bonds, and their 250°C bond strengths were above those with SPI and close to those with the PF adhesives, with cherry again providing lower strength.

Because of the low viscosity of the egg white dispersion, compared to the soy protein, glass bubbles were added to the egg

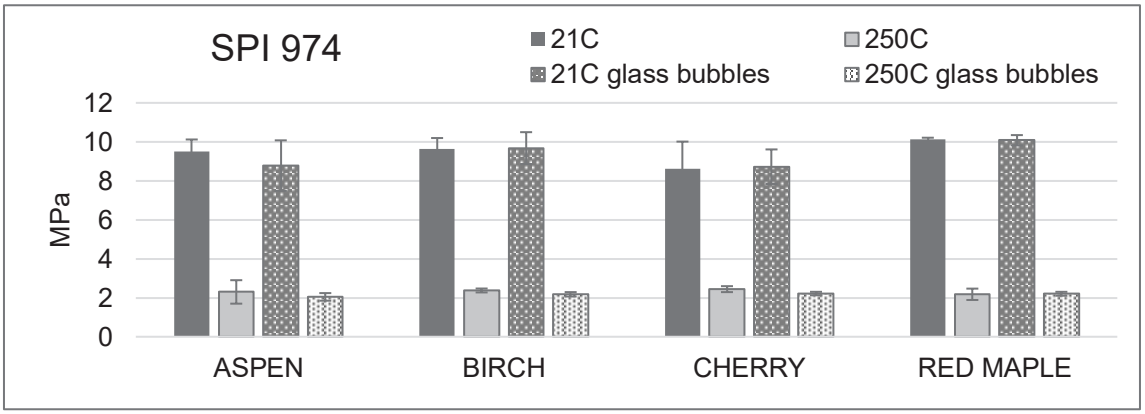

Figure 5. Room temperature (21°C) and high temperature (after 250°C heating for 100 s) bond shear strength of soy protein isolate on four different wood species, without or with 5% glass bubbles, bonded at 120°C for 120 s using ABES. The values are the average of five replicates, and the error bars represent one standard deviation.

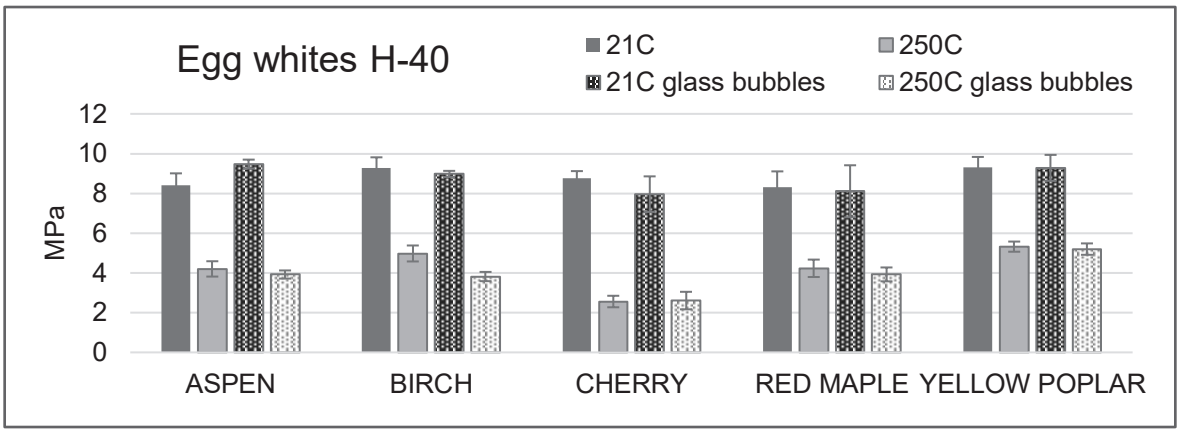

Figure 6. Room temperature (21°C) and high temperature (after 250°C heating for 100 s) bond shear strength of egg whites on five different wood species, without or with 5% glass bubbles, bonded at 120°C for 120 s using ABES. The values are the average of five replicates, and the error bars represent one standard deviation.

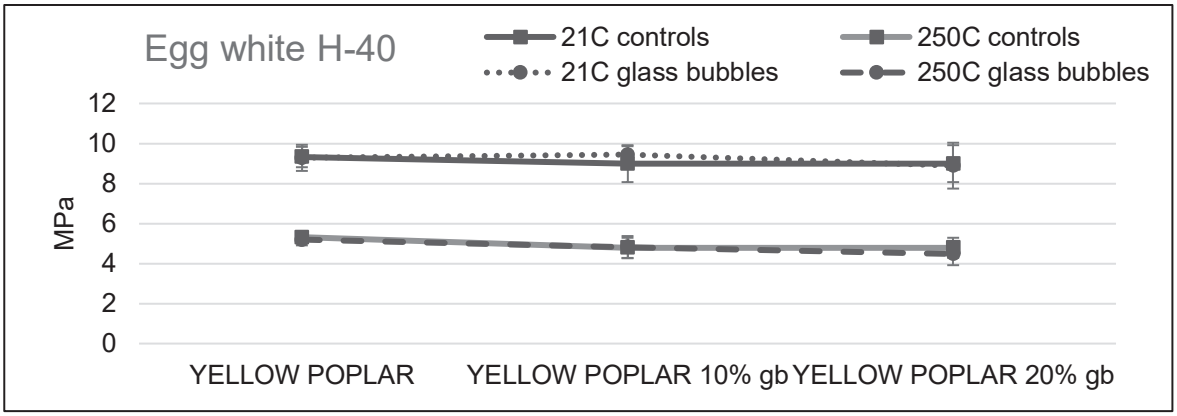

Figure 7. Room temperature (21°C) and high temperature (after 250°C heating for 100 s) bond shear strength of egg white adhesive with high amounts of glass bubbles (gb) on yellow poplar bonded at 120°C for 120 s using ABES.

white adhesive at 10% and 20% to compare with 5% added previously. The bond strength was about the same (Figure 7). With 20% glass bubbles the egg white was very thick and difficult to spread on the wood. There was no delamination at 250°C.

Although the protein adhesives performed sufficiently well in this application, the bonds at 250°C were lower than those of the phenolics. However, they could be suitable, with egg whites as the best option, if a bio-based adhesive was a necessary requirement.

Epoxy adhesives

Epoxies are well known as heat resistant adhesives and are widely used for bonds involving metals, composites, and other substrates involving high temperature applications. However, their use in wood bonding has been limited to specialty applications, such as bonding of wooden boats and aircraft, as well as for the repair of degraded, bonded wood products, because of their room temperature-curing and gap filling properties. An advantage of the epoxies is that they are usually not solvent- or water-borne; thus, there is no need to remove these liquids during the bonding process.

Most of the heat-resistant epoxies require bonding conditions at higher temperatures than are useful for wood and produce heavier weight gluelines than preferred. Of potentially useful epoxy adhesives, the most suitable were 805, 526N, and 2335 from AREMCO; these were tested as received and mixed according to the manufacturer's recommended ratios. The recommended cure schedules involving several hours at two different temperatures were not practical for the required veneer assembly and testing with ABES in 120 s, so bonding was tested at the recommended maximum temperature and adjusted depending on whether there was adequate bonding. Because of the porosity of wood, the 24 h at room temperature step was not used to avoid selective migration of adhesive components into the wood of the more polar curing agent,

which would have resulted in the wrong ratio for curing. The bond strengths at both 21°C and 250°C were similar for all the veneers, without and with 5% glass bubbles (based on the weight of the epoxy), as shown in Figure 8. There was no delamination at 250°C with any of the epoxies. At this point, the cherry had been dropped due to its poor performance with the other adhesives.

The recommended epoxy 805 cure schedule is room temperature for 24 h and then 93°C for 2 h. The bonding temperature had to be increased to 120°C for adequate bonding in 120 s. With 5% glass bubbles added, the adhesive became difficult to stir in about 20 minutes, and almost impossible to spread on the wood, which is why this data is not available for the last samples bonded, the yellow poplar and red maple.

The recommended epoxy 526N cure schedule is room temperature for 2 h and then 93°C for 2 h, cool to room temperature, then 163°C for 2 h. The bonding temperature had to be increased to 178°C for adequate bonding in 120 s. With 5% glass bubbles added, the adhesive became difficult to stir and spread on the wood after about 2 h. This adhesive provided adequate bond strength at 250°C, without and with glass bubbles (Figure 9).

The recommended epoxy 2335 cure schedule is 93°C for 2 h plus 177°C for 2 h. Bonding at 177°C resulted in good bonding in 120 s (Figure 10). With 5% glass bubbles added, the adhesive became difficult to stir and almost impossible to spread on the wood after about 2 h, which is why the data is incomplete for the aspen, the last samples to be bonded.

The epoxies above were selected because of their recommended heat resistance, but are not usually used for wood adhesion. Three additional epoxies, typically used for wood adhesion in marine and aircraft applications, were tested. The three epoxy adhesives (EPON 162 and 862 from Hexion, and

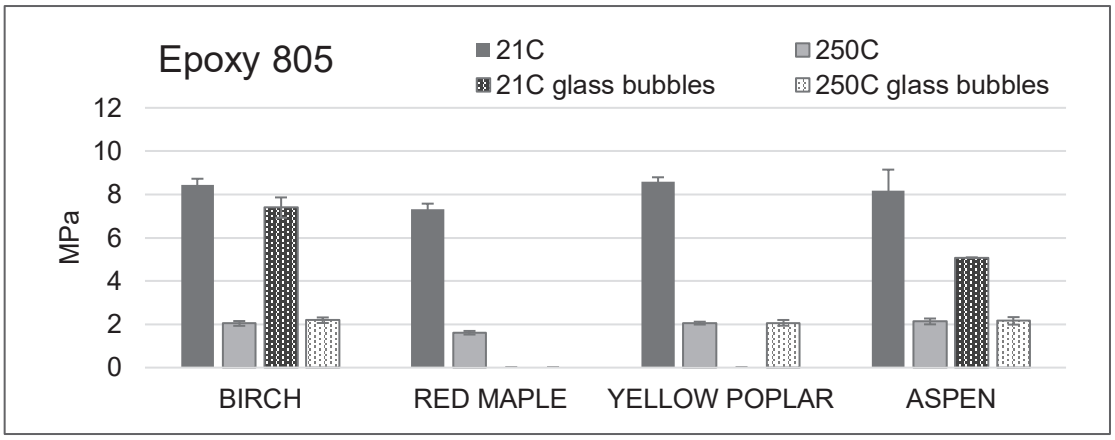

Figure 8. Room temperature (21°C) and high temperature (after 250°C heating for 100 s) bond shear strength of epoxy 805, without or with 5% glass bubbles, on four different wood species bonded at 120°C for 120 s using ABES. The values are the average of five replicates, and the error bars represent one standard deviation.

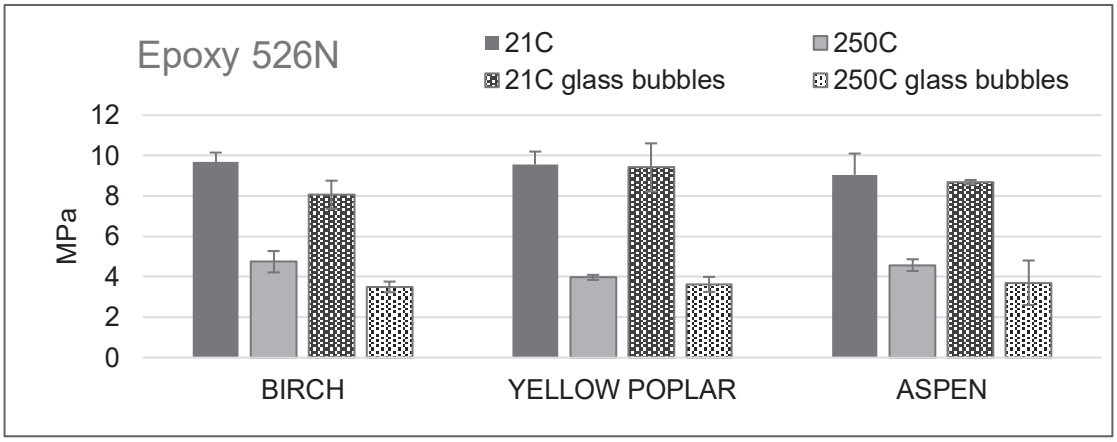

Figure 9. Room temperature (21°C) and high temperature (after 250°C heating for 100 s) bond shear strength of epoxy 526N, without or with 5% glass bubbles, on three different wood species bonded at 178°C for 120 s using ABES. The values are the average of five replicates, and the error bars represent one standard deviation.

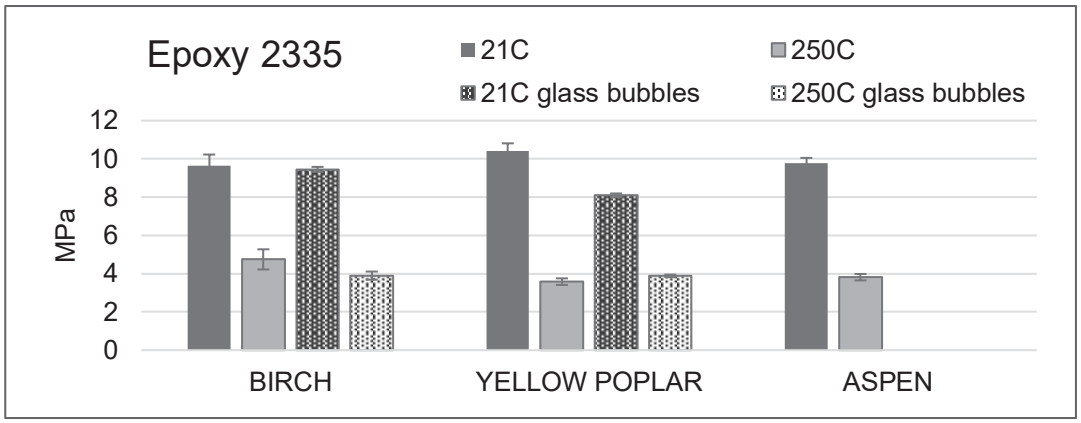

Figure 10. Room temperature (21°C) and high temperature (after 250°C heating for 100 s) bond shear strength of epoxy 2335, without or with 5% glass bubbles, on three different wood species bonded at 177°C for 120 s using ABES. The values are the average of five replicates, and the error bars represent one standard deviation.

D.E.R. 331 from Olin) were tested as received and mixed according to the recommended ratios with two different curing agents (Epikure W from Hexion and D.E.H. 24 from Olin). The Epikure W did not result in adequate bonding of yellow poplar until the temperature was increased to 200°C. All three epoxies had good strengths with D.E.H. 24 when bonded at 100°C for 120 s on yellow poplar. The strengths at both 21°C and 250°C were similar for all three epoxies, and better than or similar to, the epoxies tested previously (Figure 11). There was no delamination at 250°C with any of the epoxies.

Bonding to aluminum

Although the main part of the study was to bond wood-to-wood, there may be some applications that require wood-to-aluminum bonding. The aluminum was bonded to yellow poplar, since it gave good bonding results and was the least dense wood species, which helps to provide low weight composites.

Yellow poplar was bonded to untreated and treated (lightly sanded) aluminum at 160°C for 120 s with one of the phenolics. Sanding the aluminum did not increase the bond strength over the untreated aluminum (Figure 12). The aluminum was bonded to the wood at 160°C instead of 150°C, because the bonds were stronger than at 150°C. The epoxies Olin 331 and EPON 162 did not bond to the aluminum at 100°C, the temperature used in bonding the wood.

The wood-to-aluminum bonds with the phenolic were surprisingly strong and as good as the wood-to-wood bonds, even at high temperatures. Thus, the same phenolic could be used for bonding all the substrates.

Conclusions

The results of this evaluation of adhesive wood bonds at temperatures above where wood generally starts to lose strength

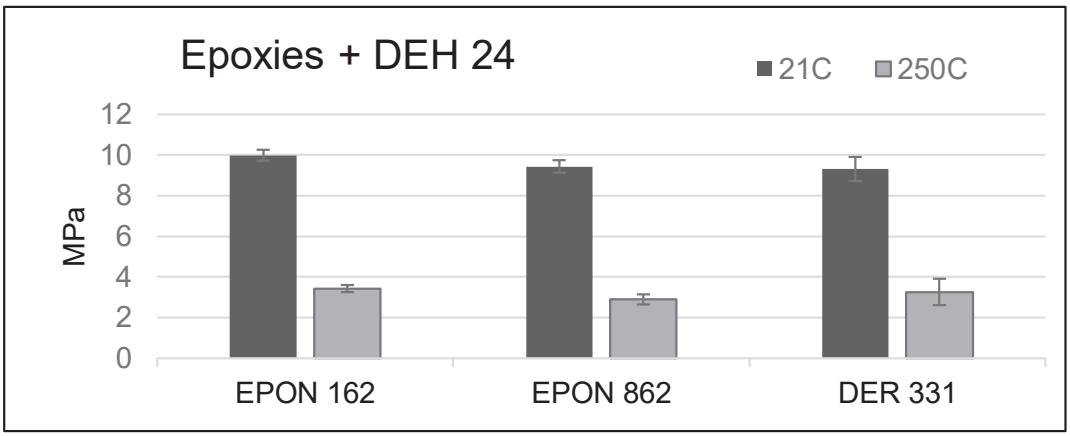

Figure 11. Room temperature (21°C) and high temperature (after 250°C heating for 100 s) bond shear strength of epoxies on yellow poplar bonded at 100°C for 120 s using ABES. The values are the average of five replicates, and the error bars represent one standard deviation.

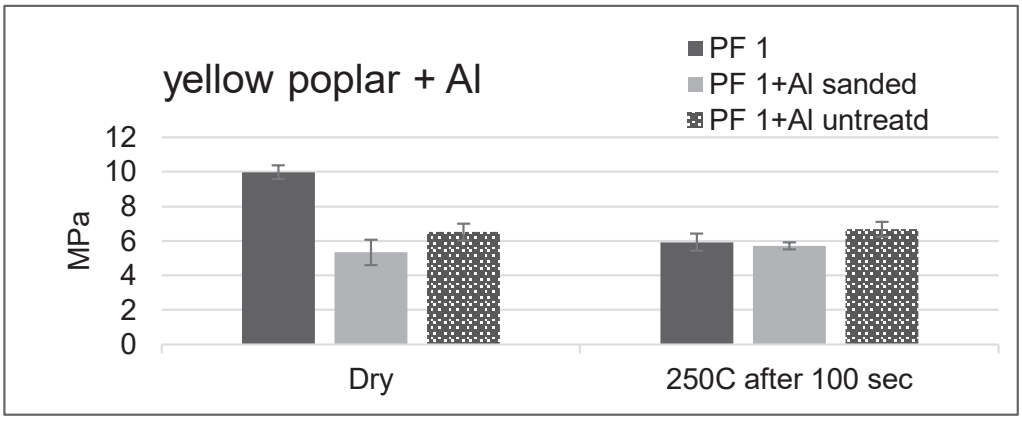

Figure 12. Yellow poplar was bonded to yellow poplar and aluminum (sanded and untreated) at 160°C for 120 s and tested at room temperature (21°C) and high temperature (after 250°C heating for 100 s). The values are the average of five replicates, and the error bars represent one standard deviation.

show that it is possible to make wood products with thin veneers and maintain bond integrity even at elevated temperatures. The lack of delamination indicated that the degradation of the wood would be the controlling factor for good product performance and that the thin laminates can replace solid wood whose properties are better understood. In addition, except for thickening of the adhesives, the glass bubbles generally decreased the 21°C bond shear strength, but had less effect on the 250°C bond test. The PF and egg white adhesives had the best shear strengths, without or with 5% glass bubbles, on the yellow poplar veneers. See Table 2 for the yellow poplar results, which was the preferred wood species due to its lower density and more uniform structure.

With the superior shear strength at 250°C and ease of use by many bonding methods, the PF1 adhesive provided the best results for producing and testing laminates on a larger scale. The proteins had good strengths, but they would require the bonding facility to prepare the adhesives, in contrast to the ready to use PFs. The epoxies were considered the least favorable of the adhesives, based on their lower strengths, thicker gluelines, and the difficulty in spreading them on the wood.

References

ANSI/APA (2018) PRG 320. Standard for Performance-Rated Cross-Laminated Timber. American National Standards Institute, New York, NY. https://www.apawood.org/Data/Sites/1/documents/standards/prg320/prg-320-2018.pdf

ASTM (2011) D 4502-92. Standard Test Method for Heat and Moisture Resistance of Wood-Adhesive Joints. American Society for Testing and Materials, West Conshohocken, PA. https://store.astm.org/d4502-92r11.html

ASTM (2024) D7998-19R24. Standard Test Method for Measuring the Effect of Temperature on the Cohesive Strength Development of Adhesives using Lap Shear Bonds under Tensile Loading. American Society for Testing and Materials, West Conshohocken, PA. https://doi.org/10.1520/D7998-19R24

Black JM, Blomquist RF (1959) Technical Note D-108: Relationship pf Polymer Structure to Thermal Deterioration of Adhesive Bonds in Metal Joints. USDA For Serv Forest Prod Lab, Madison, WI.

Table 2. Summary of adhesive shear strengths on yellow poplar.

	ABES shear strength in Pa without glass bubbles		ABES shear strength in Pa with 5% glass bubbles			
Adhesive	21°C	250°C	21°C	250°C	Comments	
PF 1 43.1% 120°C	754.3	560.6	645.7	504.5	Easy to use	
PF 2 42.3% 150°C	1066.6	556.5	NT	NT	Easy to use	
SPI 974 20%	1027.9	241.7	896.7	269.7	Easy to use	Thick paste
Egg whites H-40 50%	932.3	531.9	928.2	519.5	Easy to use	Pourable
Epoxy 805	858.6	205.5	NT	206.8	Very thick	With glass bubbles difficult
Epoxy 2335	1039.6	358.2	810.1	388.2	Very thick	With glass bubbles difficult
EPON 162	999.2	343.1	NT	NT	Very thick	With glass bubbles impossible
EPON 862	943.9	289.8	NT	NT	Very thick	With glass bubbles impossible
D.E.R. 331	931.3	326.6	NT	NT	Very thick	With glass bubbles impossible

NT = not tested

Eickner HW, Mraz EA, Bruce HD (1955) Report No. 1545: Resistance to Fatigue Stressing of Wood-to-Metal Joints Glued with Several Types of Adhesives. USDA For Serv Forest Prod Lab, Madison, WI.

Frihart CR (2009) Adhesive groups and how they relate to the durability of bonded wood. J Adhes Sci Technol 23(4):601–617. https://doi.org/10.1163/156856108X379137

Frihart CR (2013) Wood adhesion and adhesives. In: RM Rowell (ed), Handbook of Wood Chemistry and Wood Composites, CRC Press, Boca Raton, FL. 255–313.

Frihart CR, Hunt CG (2010) Adhesives with wood materials: bond formation and performance. In: Wood handbook - Wood as an engineering material. Gen Tech Rep FPL-GTR-190. USDA For Serv Forest Prod Lab, Madison, WI. Chapter 10.

Frihart CR, Lorenz LF (2018) Protein adhesives. In: Pizzi A and Mittal K (eds), Handbook of Adhesive Technology. CRC Press, Taylor & Francis Group, Boca Raton, FL, 145–176.

Frihart CR, Lorenz L (2020) Standard Test Method ASTM D 7998-19 for the Cohesive Strength Development of Wood Adhesives. JoVE, e61184. https://doi.org/10.3791/61184.

Forest Products Laboratory (1964) Research Note FPL-082: Adhesives for Bonding Wood to Metal. USDA For Serv Forest Prod Lab, Madison, WI.

Hare DA, Kutscha NP (1974) Microscopy of eastern spruce plywood gluelines. Wood Sci 6(3):294–304.

Liu J, Yue K, Xu L, Wu J, Chen Z, Wang L, Liu W, Lu W (2020) Bonding performance of melamine-urea–formaldehyde and phenol-resorcinol–formaldehyde adhesive glulams at elevated temperatures. Int J Adhes Adhes 98 (Apr):102500.https://doi.org/10.1016/j.ijadhadh.2019.102500

Lorenz LF, Frihart CR (2023) Ovalbumin has unusually good wood adhesive strength and water resistance. J Appl Polym Sci 140(3):e53332. https://doi.org/10.1002/app.53332

Miyamoto B, Bechle N, Rammer D, Zelinka S (2021) A small-scale test to examine heat delamination in cross laminated timber (CLT). Forests 12(2):232. https://doi.org/10.3390/f12020232

Poletto M, Zattera AJ, Santana RMC (2012) Thermal decomposition of wood: Kinetics and degradation mechanisms. Bioresour Technol 126 (Dec):7–12. https://doi.org/10.1016/j.biortech.2012.08.133

Yeh B, Brooks R (2006) Evaluation of adhesive performance at elevated temperatures for engineered wood products. In: Proceedings of the 9th World Conference on Timber Engineering, Portland, OR.

Zelinka S, Pei S, Bechle N, Sullivan K, Ottum N, Rammer D, Hasburgh L (2018) Performance of wood adhesive for cross laminated timber under elevated temperatures. In: Proceedings, WCTE 2018-World Conference on Timber Engineering. Korean Institute of Forest Science. Seoul, Republic of Korea.

Zelinka SL, Miyamoto B, Bechle N, Rammer D (2020a) Small scale test to measure the strength of adhesives at elevated temperatures for use in evaluating adhesives for cross-laminated timber (CLT). In: Makovicka Osvaldova L, Markert F, Zelinka S (eds), Wood & Fire Safety, WFS 2020, Proceedings of the 9th International Conference on Wood & Fire Safety, Springer, Cham, pp. 3–8. https://doi.org/10.1007/978-3-030-41235-7_1

Zelinka SL, Hasburgh L, Bourne K (2020b) Overview of North American CLT fire testing and code adoption. In: Makovicka Osvaldova L, Markert F, Zelinka S (eds), Wood & Fire Safety WFS 2020, Proceedings of the 9th International Conference on Wood & Fire Safety, Springer, Cham, pp. 232–237. https://doi.org/10.1007/978-3-030-41235-7_35

Manufacturing of oriented strand board from olive tree pruning residues

Antypas Imad Rezakalla *
Associate Professor
Don State Technical University
Gagarin Square 1, Rostov-on-Don
Russian Federation
E-mail: imad.antypas@mail.ru

(Received 14 September 2025)

Abstract: This study investigated the feasibility of manufacturing eco-friendly flakeboard from olive tree pruning residues using three concentrations of a tannin-formaldehyde adhesive, where the condensed tannin was extracted from pomegranate peels. The research evaluated the effects of adhesive concentration (11%, 12%, and 13%) on the physical and mechanical properties of panels to verify their compliance with European standards. Panels were tested for moisture content, density, water absorption, thickness swelling, modulus of rupture (MOR), internal bond (IB) strength, and screw withdrawal resistance. While moisture content and density were not significantly affected by adhesive ratio, water absorption and thickness swelling after 24 h decreased significantly with higher resin content. Mechanically, the 13% adhesive sample exhibited superior performance, achieving the highest values for MOR (18.8 MPa), IB strength (0.61 MPa), and screw withdrawal resistance (680 N), representing improvements of 7%–10%, 16%, and 10%, respectively, over panels with the lower resin content. All produced panels met the relevant European standard specifications. The results showed that olive tree pruning waste can be successfully valorized to produce sustainable oriented strand board (OSB) panels using a bio-based tannin-formaldehyde adhesive. The panels, which also feature an attractive natural appearance, are suitable for applications in furniture manufacturing, interior cladding, and structural uses, offering a promising solution to reduce reliance on synthetic adhesives and minimizing agricultural waste.

Keywords: Olive tree waste; Flakeboard; Tannin-formaldehyde adhesive; Pomegranate peels; Mechanical properties; European standards; Sustainable manufacturing.

Introduction

The manufacturing of composite panels relies on the use of industrial adhesives such as urea-formaldehyde (UF), phenol-formaldehyde (PF), or melamine-urea-formaldehyde (MUF) at rates ranging from 10% to 18%, relative to the dry wood material (Pizzi et al., 1994). The global production and consumption of engineered wood materials have seen a steady upward trend. For instance, global particleboard production reached 96 million cubic meters in 2020 (FAOSTAT 2022). However, this growth has been accompanied by the persistent problem of formaldehyde (HCHO) emissions from products bonded with synthetic adhesives, particularly those containing UF resin (Roffael 1982, 1993). The health risks associated with these emissions, which include irritation of mucous membranes and increased cancer risk, prompted significant regulatory action, most notably the California Air Resources Board's (CARB) Airborne Toxic Control Measure (ATCM) in 2009 (CARB 2009). This ruling established stringent formaldehyde emission limits for composite wood products, effectively setting a new, stricter standard that had a global impact on manufacturing practices.

At the industrial level, formaldehyde is emitted into the factory air during drying and pressing processes, exposing workers to harmful health effects, such as inflammation of the mucous membranes, eye irritation, an increased risk of cancer, and detrimental effects on the central nervous system (Tappler et al. 2008). These harmful effects occur at formaldehyde concentrations exceeding 0.1 parts per million (ppm), equivalent to 0.12 mg/m³ (Roffael 1982; Tappler et al. 2008; Rader, 1974).

At the domestic level, formaldehyde is emitted from furniture and building materials made from a variety of engineered wood products. These include particleboard, medium-density fiberboard (MDF), laminated veneer lumber (LVL), and oriented strand board (OSB). Emissions can be particularly pronounced during winter when colder temperatures reduce ventilation and

* Corresponding author

air-exchange rates in homes. Formaldehyde levels exceeding 0.1 ppm may be associated with acute health effects like eye inflammation, as well as chronic risks including cancer and adverse effects on the central nervous system (Roffael 1982; Tappler et al. 2008; Hameed et al. 2007; Rader 1974).

These risks have prompted researchers to develop formaldehyde scavengers, such as melamine and resorcinol, formaldehyde-free industrial adhesives, like polymerized diphenylmethane diisocyanate (pMDI) or natural adhesives derived from polyphenols, such as tannin-formaldehyde resin (TF-resin) (Roffael 1981). These risks have also prompted researchers to develop alternative adhesive systems. Among the most promising are bio-based adhesives, such as tannin-formaldehyde (TF) resins, which can be synthesized from condensed tannins extracted from renewable agricultural wastes like tree barks, prunings, and fruit peels (Pizzi 2006). While the potential of TF-resins is established in some engineered wood products like particleboard, their application in OSB remains relatively unexplored, particularly when using a combined system of non-wood strands and a non-conventional tannin source. Therefore, this study investigates the feasibility of manufacturing OSB panels from olive tree pruning residues using a novel TF-resin, where the condensed tannin is extracted from pomegranate peels. This approach directly addresses the dual challenge of reducing reliance on synthetic formaldehyde-based adhesives and valorizing agricultural waste streams.

The use of alternative raw materials, such as agricultural biomass and recycled wood waste, aligns with the principles of the circular economy and represents a promising avenue for diversifying the raw material base for wood-based panels (Lee et al. 2022). While much of the research in this area has focused on particleboard, the feasibility of applying these materials to OSB requires specific consideration. The production of high-quality, engineered flakes suitable for OSB is more challenging than producing particles for particleboard, as it demands longer strands with a specific geometry to ensure effective orientation and mechanical performance. Therefore, a key objective of this study was to evaluate whether olive tree pruning residues could be technically processed into viable flakes and successfully utilized in OSB production, thereby testing the boundaries of agricultural biomass for higher-value structural composites.

Several recent studies have established the viability of agricultural waste for wood panel manufacturing, demonstrating that various pruning residues can serve as effective raw materials. Wong et al. (2020) showed that incorporating 10% grapevine prunings with 90% pine produced hybrid panels with excellent mechanical properties and improved density, reducing dependence on natural wood while lowering carbon emissions. Complementing this, Şahin (2020) found that panels with 30% grapevine pruning residues met European standard specifications, and that increasing urea-formaldehyde resin content from 10% to 12% enhanced durability while maintaining suitable mechanical and physical properties. These findings collectively validate the approach of using woody, non-traditional biomass in panel production and directly support our hypothesis that olive tree prunings—a similar agricultural waste—possess suitable structural characteristics for engineered wood panels. Furthermore, these studies confirm the importance of resin content optimization, which informed our experimental design to test tannin-formaldehyde adhesive at 11%, 12%, and 13% concentrations for manufacturing panels from olive pruning residues.

In another study, Özlüsoylu (2023) successfully produced low-density wood panels from recycled wood bark using adhesive mixtures of varying densities. Subsequently, the panels were coated with three types of varnish (water-based, polyurethane, oil/wax) to study their effects on surface properties. Results showed that the oil/wax varnish yielded the highest roughness values and greatest color change, while water-based and polyurethane varnishes produced smoother and glossier surfaces, especially in high-density panels (420 kg/m³). The study concluded that using a higher density (420 kg/m³) with 4% adhesive content provides the best results in terms of smoothness and gloss, making it the optimal choice for applications requiring high surface quality.

Research by Ferrández-García et al. (2022) presents a method to transform olive tree pruning waste into adhesive-free eco-boards via hot pressing. The effects of leaf type (whole/shredded), temperature (130–150°C), and pressing time (4–12 min) on board properties were analyzed. The boards exhibited low water uptake, high thermal insulation, and enhanced mechanical performance with optimized processing conditions. This study is highly relevant to our work, as it confirms the fundamental suitability of olive tree pruning residues as a raw material for panel production. However, while Ferrández-García et al. (2022) focused on binderless boards for specific properties, our research explores a different pathway: utilizing these residues as a substitute for conventional wood flakes in structural OSB, which requires the addition of an adhesive to achieve the necessary mechanical strength for load-bearing applications. This comparison highlights the versatility of olive pruning

waste and the novelty of our approach in targeting a different product segment.

In the work by Chia-Ju Lee et al. (2021), a formaldehyde-free tannin-based adhesive (AcBTanGlu) for the production of oriented bamboo scrimber board (OBSB) is presented. The scientific novelty of their work lies in the demonstration that this adhesive not only eliminates harmful emissions but also surpasses traditional synthetic resins in key performance indicators: mechanical strength, dynamic modulus of elasticity (MOE), and dimensional stability.

Wenjing Hu et al. (2025) proposed a method of photocatalytic degradation to reduce the mean degree of polymerization (mDP) of larch tannins, which solves the problem of high viscosity and low strength of tannin-based adhesives. The resulting modified tannin, with a formaldehyde mass fraction of only 10%, enabled the creation of an adhesive that meets strength and water resistance standards while minimizing formaldehyde emission.

Collectively, the literature demonstrates a clear trend toward utilizing agricultural residues and developing bio-based adhesives to mitigate the environmental impact of wood-based panels. Building upon these insights, particularly the proven suitability of olive tree pruning residues as a raw material and the successful use of condensed tannins as a resinous component, this research aims to bridge a specific knowledge gap. Therefore, this study investigates the feasibility of manufacturing eco-friendly OSB by combining two underutilized waste streams: using strands from olive tree pruning residues bonded with a tannin-formaldehyde adhesive, where the condensed tannin is extracted from pomegranate peels.

The specific objectives of this study were to evaluate the potential of utilizing olive tree pruning residues in combination with a tannin-based adhesive for panel production by

- Quantifying the effect of three condensed tannin-adhesive concentrations (11%, 12%, and 13%) on the physical, mechanical, and hygroscopic properties of the manufactured panels.
- Verifying compliance of the panel properties with relevant European technical standards to assess their suitability for commercial applications.
- Providing a sustainable environmental solution based on the simultaneous valorization of agricultural waste streams—olive tree prunings and pomegranate peels—and reducing reliance on conventional synthetic adhesives.
- Contributing to the development of an environmentally conscious wood composite industry that aligns with circular economy principles without compromising product quality and performance.

Materials and methods

Dried pomegranate peels (*Punica granatum* L.) were obtained as agricultural waste from local fruit processing facilities in Alanya, Türkiye. The raw material was processed using a Fritsch Pulverisette 19 laboratory cutting mill (Fritsch GmbH, Türkiye) equipped with a 1.0 mm sieve to achieve consistent particle size distribution. For extraction, 1 kg of the resulting powder was mixed with 12 L of distilled water preheated to 87°C (±2°C) in a temperature-controlled reactor (Isılab ISI-90, Türkiye). The suspension was maintained under continuous mechanical stirring at 200 rpm for precisely 75 min using an Hei-TORQUE Precision 100 overhead stirrer (Heidolph, Türkiye)—with parameters previously optimized through response surface methodology to maximize tannin yield from this specific biomass source. Following extraction, the mixture was cooled to ambient temperature (23±2°C) and sequentially filtered through Whatman No. 1 filter paper, followed by a 0.45 μm membrane filter.

The clarified filtrate was immediately concentrated using an IKA RV 10 rotary evaporator (IKA, Türkiye) at 55°C (±5°C) under reduced pressure (100–150 mbar) until reaching a total solids content of 42.5% (±2.5%), as determined by gravimetric analysis using a Precisa XR 205SM-DR analytical balance (Precisa, Türkiye). The mild temperature conditions were specifically maintained to prevent thermal degradation of polyphenolic compounds, while ensuring efficient solvent removal. The concentrated tannin extract was stabilized with 0.1% sodium metabisulfite and stored at 4°C in amber glass containers with nitrogen headspace until resin synthesis.

Resin synthesis

The concentrated tannin extract (42.5% ± 2.5% solids content) was transferred into a three-necked round-bottom flask (Jsil Glasstek, China) equipped with a mechanical stirrer (IKA RW 20 digital, IKA China), reflux condenser, and digital thermometer. For resin formulation, 35 g of paraformaldehyde (95% purity, Merck China) and 80 g of urea (ACS reagent, Sigma-Aldrich China) were added sequentially to 200 g of tannin extract under continuous stirring at 300 rpm. The reaction mixture was gradually heated to 83°C (±2°C) using a programmable heating mantle (Heidolph, China) to ensure

complete reagent dissolution and initiate the polycondensation reaction between tannin, urea, and formaldehyde components.

The reaction was maintained at 82–85°C for 150 min (±15 min) under reflux conditions. Reaction progress was monitored through periodic viscosity measurements using a Brookfield DV2T viscometer (Brookfield China) with RV-06 spindle at 20 rpm. Polymerization was considered complete when the dynamic viscosity reached 450–550 mPa·s, corresponding to a homogeneous, viscous syrup-like consistency suitable for strand coating and subsequent hot-press curing. The resulting tannin-urea-formaldehyde (TUF) resin was immediately cooled to 25°C (±3°C) in a water bath and stored in sealed HDPE containers (Nalgene China) at 4°C for subsequent panel manufacturing within 24 hours.

Wood preparation

Olive tree branches (*Olea europaea*) were collected from agricultural pruning operations in the Mediterranean region of Turkey. Selected branches measuring 80–200 mm in length, with straight grain and minimal knots, were processed into strands using a laboratory-scale rotary lathe (Pallmann, China). The strands were precision-cut to dimensions of 70–120 mm in length and 1.0–2.0 mm in thickness, with a target width of approximately 15 mm. The resulting strands were then conditioned in a forced-air drying oven (Memmert, China) at 40°C for 24 h to achieve a uniform moisture content of 5.0% (±0.5%) as verified by a moisture analyzer (Sartorius, China). This strand geometry and moisture content were selected to optimize both resin adhesion and panel formation characteristics during panel manufacturing.

Panel manufacturing

The process of manufacturing prototype panels from olive tree pruning strands using a tannin-urea-formaldehyde (TUF) adhesive was conducted with reference to the German standard DIN-T 60 (1999) for wood-based panels. Strands were resinated using an industrial-scale pneumatic spray system (SATA, China) with a 1.3 mm nozzle diameter at 3.5 bar pressure, applying adhesive for 90 s with continuous mechanical mixing to ensure uniform distribution. The strands were sprayed with 11%, 12%, and 13% TUF resin content (based on dry wood weight), achieving consistent resin coverage without strand surface saturation.

The resinated strands (2.6 kg per panel) were manually formed into a single-layer mat within a forming frame (430 × 430 × 300 mm) placed on a caul plate. The mat was pre-pressed at 0.5 MPa for 30 s using a wooden platen to facilitate handling. Hot-pressing was conducted in a laboratory hydraulic press (Carver, China) at 170°C for 7 min under 3.5 MPa pressure, using 16-mm thick metal stops to control panel thickness. After 24-h conditioning at 20°C and 65% RH, panels were trimmed to final dimensions of 410 × 410 × 16 mm. Three replicate panels were manufactured for each resin concentration, totaling nine experimental panels (Figure 1).

The panels were cut into sections appropriate for assessing moisture content according to standard EN 322 (1993), density according to standard EN 323 (1993), water absorption capacity after 24 h according to standard DIN EN 322 (1993-08), and thickness swelling after 24 h of water immersion according to standard EN 317 (1993; Table 1, Figure 2).

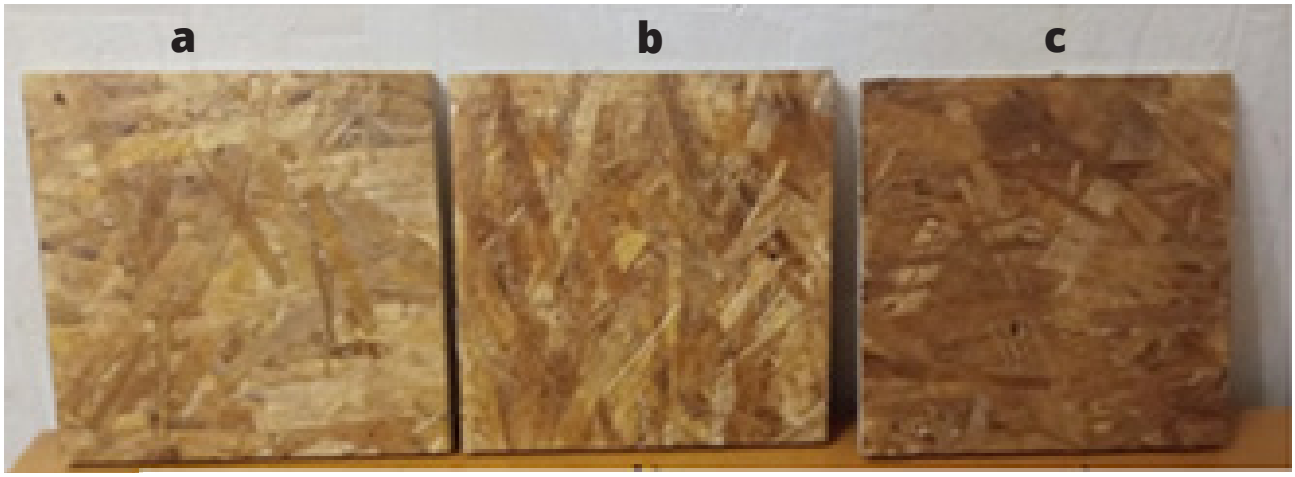

Figure 1. Examples of wood panels constructed using (a) 11%, (b), 12%, and (c) 13% condensed tannin adhesive.

Table 1. Dimensions and replicates used to evaluate various panel properties.

Property measured	Specimen dimensions	Replicates	Test method
Moisture content	50 × 50 × 16	3/panel	EN 322 (1993)
Density	50 × 50 × 16	3/panel	EN 323 (1993)
24 h water absorption	50 × 50 × 16	3/panel	EN 317 (1993)
24 h Swelling	50 × 50 × 16	3/panel	EN 317 (1993)
Flexural properties	250 × 50 × 16	3/panel	EN 310 (1993)
Internal bond strength	50 × 50 × 16	3/panel	EN319 (1993)
Screw withdrawal capacity	150 × 50 × 16	3/panel	EN 319 (1993)

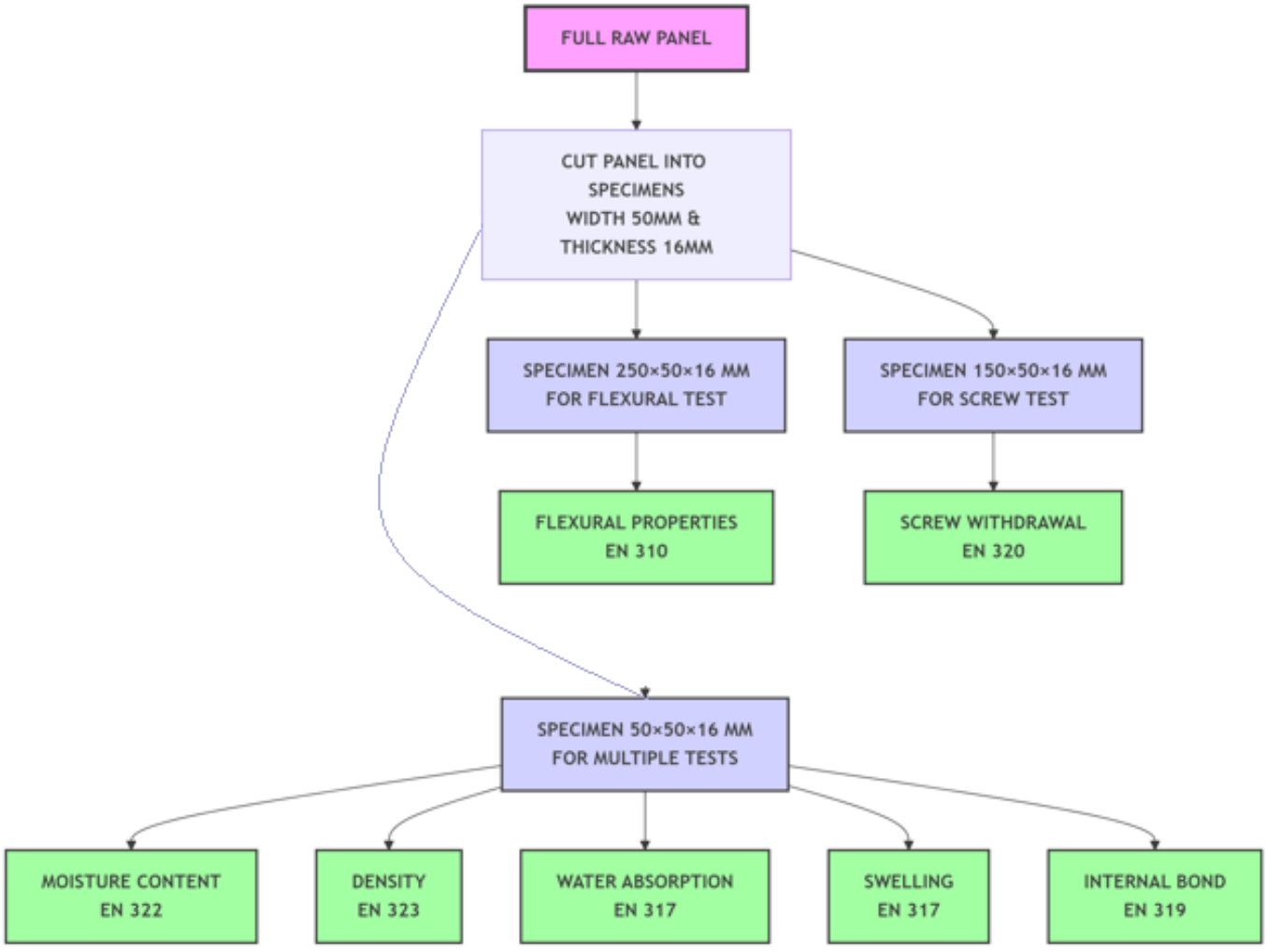

Figure 2. Cutting scheme and testing protocol for wood-based panels according to European standards (EN).

Flexural properties testing

Panel flexural properties were evaluated using a Universal Testing Machine (Jinan Testing Equipment IE-5020, China) equipped with a 10 kN load cell. Testing was performed according to EN 310 (1993) standard employing a three-point bending configuration with a 200-mm span length. Specimens were loaded to failure at a constant crosshead speed of 5 mm/min.

Load-deflection data were continuously recorded at 10 Hz sampling frequency through the machine's integrated data acquisition system. The modulus of rupture (MOR) was calculated from the maximum load at failure, while the MOE was determined from the slope of the initial linear portion of the load-deflection curve (specifically between 10% and 40% of maximum load). Three replicate specimens were tested from each of the three panels for every resin concentration, yielding a total of nine measurements per resin treatment for both MOR and MOE.

The MOR and MOE values were calculated using the following equations from the standard EN 310 (1993):

$$MOR = (3 \times F_{max} \times L)/(2 \times b \times h^2) \quad [1]$$

$$MOE = (L^3 \times \Delta F)/(4 \times b \times h^3 \times \Delta y) \quad [2]$$

Where: F_{max} = maximum load (N); L = span length (mm); b = specimen width (mm); h = specimen thickness (mm); ΔF = load increment in the elastic region (N); and Δy = deflection increment corresponding to ΔF (mm).

Internal bond strength (IB) was assessed by gluing blocks to the face of each panel and pulling the section apart at a rate of 0.5 mm/min. Maximum load at failure was recorded as IB. Three samples were tested from each of the three panels for each resin concentration.

Screw withdrawal tests were performed by inserting a 3.5 mm diameter by 40 mm long screw to a depth of 15 mm into the panel. The screw was then inserted into a specially designed apparatus that applied the load while constraining the panel. The load at failure was recorded. Three samples were tested from each of the three panels for each resin concentration.

All statistical analyses were conducted using R software version 4.3.1 (Beijing R Foundation for Statistical Computing, China) with the following packages: tidyverse (version 2.0.0) for data manipulation and visualization, car (version 3.1-2) for ANOVA assumptions testing, and agricolae (version 1.3-7) for post-hoc comparisons. The data were subjected to a one-way analysis of variance (ANOVA) at $\alpha = 0.05$ significance level to determine the effects of tannin-adhesive concentration (11%, 12%, 13%) on all measured panel properties.

Prior to ANOVA, data normality was verified using Shapiro-Wilk tests ($p > 0.05$) and homogeneity of variances was confirmed with Levene's tests ($p > 0.05$). When ANOVA indicated significant main effects, means were separated using Tukey's Honest Significant Difference (HSD) test at $\alpha = 0.05$. All results are presented as mean ± standard deviation based on nine replicates per treatment group (three specimens from each of three panels per resin concentration).

Results and discussion

Panels were increasingly darker with increased resin content, but appeared similar otherwise (Figure 1).

Physical properties

Moisture content

The moisture content of all panels after pressing ranged from 6.76% to 6.77%, meeting the requirement of the European Standard DIN-T-60 (1999), which specifies a maximum moisture content of 12% for wood-based panels. Statistical analysis confirmed that adhesive concentration had no significant effect on moisture content ($F = 0.011$, $p = 0.989$), which reflects the consistent initial moisture content of the resinated strands (11%) and the standardized pressing conditions applied to all panels. (Tables 2, 3).

Density

Densities were slightly below the EN 323 (1993) standard (0.80 g/cm^3), but there was no significant effect of resin concentration (Tables 1, 2). The slightly lower density may reflect the characteristics of the pruned material, which contained more internal voids. Branch wood in olives is typically denser than stem wood, owing to slower growth rates. Higher pressing pressure might have improved this property, although this would have resulted in a thinner panel. The use of a thicker mat coupled with higher pressing pressures would likely be necessary to utilize these materials.

Water absorption

Resin concentration demonstrated a highly significant effect on both 24-h water absorption ($F(2, 33) = 50713$, $p < 0.0001$) and thickness swelling ($F(2, 33) = 10962$, $p < 0.0001$). Increased resin content from 11% to 13% resulted in a progressive decrease in both properties, with water absorption declining

Table 2. Effect of different levels of a tannin-formaldehyde resin on physical properties of oriented strand board panels[a].

Adhesive concentration	Moisture content (%)	Density (g/cm³)	Water absorption 24h (%)	Thickness swelling 24h (%)
11%	6.760 ± 0.15	0.7558 ± 0.008	68.93 ± 0.52	15.88 ±0.41
12%	6.764 ± 0.14	0.7561 ± 0.007	67.90 ± 0.48	15.05 ±0.36
13%	6.766 ± 0.13	0.7563 ± 0.006	66.36 ± 0.44	14.46 ±0.39

[a]Values represent means of nine replicates per adhesive concentration plus or minus one standard deviation

Table 3. Analyses of variance examining the effects of adhesive concentration on panel moisture content, density, 24-h water absorption, and thickness swell.

	Effect	SS	Df	MS	F	P
Moisture content	Type	0.000	2	0.000	0	0.457
	Error	0.012	33	0.000		
Density	Type	0.000	2	0.000	0	0.875
	Error	0.00019	33	0.00001		
24-h water absorption	Type	40.1	3	20.0	50713	<0.0001
	Error	0	33	0		
Thickness swell	Type	12.213	2	6.107	10962	<0.0001

from 68.93% to 66.36% and thickness swelling reducing from 15.88% to 14.46%. These improved hygroscopic properties reflect enhanced strand coating and more complete coverage at higher resin levels, which creates a more effective barrier against water penetration and improves interfacial bonding between strands. The results align with established principles of composite wood panel behavior, where increased resin content typically enhances dimensional stability through improved matrix formation and reduced capillary water uptake (Lelis 1992).

Mechanical properties

The mechanical properties demonstrated significant improvement with increasing resin content. The MOR increased from 17.10 MPa to 18.80 MPa, while the MOE rose from 3750 MPa to 4180 MPa as the resin concentration increased from 11% to 13%. One-way ANOVA confirmed that resin content had a statistically significant effect on both MOR ($F(2, 24) = 22.85$, $p < 0.001$) and MOE ($F(2, 24) = 15.12$, $p = 0.0003$).

Similarly, IB strength significantly improved with increased resin content ($F(2, 24) = 18.90$, $p < 0.001$), rising from 0.52 MPa to 0.61 MPa, reflecting enhanced inter-strand bonding through more complete surface coverage and improved adhesive bridging.

Screw withdrawal resistance also showed statistically significant improvement with higher resin content ($F(2, 24) = 25.45$, $p < 0.001$), increasing from 615 N to 680 N. This improvement occurred despite the absence of significant density variation among panels, indicating that enhanced resin-strand interactions and improved matrix cohesive strength—rather than bulk density—contributed to better resistance against lateral forces during screw insertion and withdrawal.

Table 4. Effect of resin concentration on modulus of rupture (MOR), internal bond strength (IB) and screw withdrawal resistance of oriented strand board.[a]

Resin concentration	Modulus of rupture (MPa)	Internal bond strength (MPa)	Screw withdrawal resistance (N)
11%	17.10 ±0.45	0.52 ±0.03	615 ± 12
12%	17.60 ±0.38	0.55 ±0.02	635 ± 10
13%	18.80 ±0.42	0.61 ±0.03	680 ± 14

[a]Values represent means of nine samples per resin concentration plus or minus one standard deviation.

Detailed statistical results

Tukey's multiple comparisons test

Tukey's test revealed that differences between all resin content levels (11%, 12%, 13%) were statistically significant ($p < 0.05$) for all tested mechanical properties, confirming a gradual and continuous performance improvement with each increase in resin content.

These results confirm that increasing the tannin-formaldehyde resin content leads to statistically significant improvements in all mechanical properties of panels manufactured from olive tree pruning residues.

Table 5. Analysis of variance and mean values of mechanical properties of experimental panels manufactured with different tannin-formaldehyde resin concentrations.

Property	F-value	Degrees of freedom	P-value	Statistical significance
MOR	22.85	(2, 24)	<0.001	Significant
MOE	15.12	(2, 24)	0.0003	Significant
IB	18.90	(2, 24)	<0.001	Significant
Screw withdrawal	25.45	(2, 24)	<0.001	Significant

Conclusions

Oriented strand board panels produced from olive branch prunings were fully compliant with relevant European standards. Increased resin content produced significant improvements in water absorption, swelling, IB, and screw withdrawal resistance. Panel appearance, coupled with panel properties would make these materials highly suitable for a variety of applications, including furniture manufacturing, interior wall cladding for halls and auditoriums, and interior structural applications.

Single-layer panels manufactured from olive tree pruning strands using a tannin-urea-formaldehyde adhesive derived from pomegranate peels demonstrated compliance with key European standard requirements for wood-based panels. Statistically significant improvements ($p < 0.05$) were observed in critical performance properties with increasing resin content from 11% to 13%: 24-h thickness swelling decreased by 9.0%, IB strength increased by 17.3%, and screw withdrawal resistance improved by 10.6%.

The enhanced mechanical performance, coupled with the aesthetically pleasing natural appearance of the panels, suggests strong potential for commercial applications in furniture manufacturing, interior wall cladding for architectural spaces, and non-structural interior applications. The successful valorization of two agricultural waste streams—olive tree prunings and pomegranate peels—provides a sustainable manufacturing pathway that reduces dependence on conventional wood resources and synthetic formaldehyde-based adhesives, supporting circular economy principles in the composite panel industry.

Recommendations

Based on the findings of this study, it is recommended to adopt the 13% tannin-formaldehyde resin concentration for manufacturing panels from olive tree pruning residues, as it demonstrated superior mechanical performance and dimensional stability. Future research should focus on developing multi-layer panel structures to meet standard OSB specifications and exploring formaldehyde-free cross-linkers to enhance the environmental profile. Further investigation into the long-term durability and economic feasibility of this approach is essential for commercial implementation.

References

CARB-California Air Resources Board- (2009) Appendix A. State of California, Air Resources Board Resolution (CARB) 09-31, April 23. https://ww2.arb.ca.gov/sites/default/files/classic/fuels/lcfs/bioguidance/biodocs/xabiores.pdf

DIN Standards - DIN-T 60 (1999) European Standard, Holzfaserplatten, Spanplatten und Sperrholz- Beuth Verlag. https://api.pageplace.de/preview/DT0400.9783410316275_A47132175/preview-9783410316275_A47132175.pdf

EN 310 - DIN EN 310 (1993) Wood-based panels; determination of modulus of elasticity in bending and of bending strength; German version EN 310:1993, August 1, 1993. https://standards.globalspec.com/std/195563/din-en-310

EN 317 - DIN EN 317 (1993) Particleboards and fibreboards; determination of swelling in thickness after immersion in water; German version EN 317:1993, August 1, 1993. https://standards.globalspec.com/std/639415/din-en-317

EN 319 - DIN EN 319 (1993) Particleboards and fibreboards; determination of tensile strength perpendicular to the plane of the board; German version EN 319:1993, August 1, 1993. https://standards.globalspec.com/std/583969/din-en-319

EN 322 - DIN EN 322 (1993) Wood-based panels; determination of moisture content; German version EN 322:1993, August 1, 1993. https://standards.globalspec.com/std/983588/din-en-322

EN 323 - DIN EN 323 (1993) Wood-based panels; determination of density; German version EN 323:1993, August 1, 1993. https://standards.globalspec.com/std/964615/din-en-323

Ferrández-García A, Ferrández-Garcia, MT, Ortuño TG, Mata-Cabrera F, Ferrández-Villena M (2022) Analysis of the manufacturing variables of binderless panels made of leaves of olive tree (*Olea europaea* L.) pruning waste, Agronomy 12(1):93. https://doi.org/10.3390/agronomy12010093

FAOSTAT (2022). Food and Agriculture Organization of the United Nations. World Food and Agriculture – Statistical Yearbook. 380. Rome. https://doi.org/10.4060/cc2211en

Hameed M, Roffael E, Kraft R (2007) On the formation of formaldehyde, furfural and formic acid by thermo hydrolytic treatment of monomeric sugars (xylose, arabinose and galactose). Contribution to the formation of volatile organic compounds (VOC) during thermo-mechanical pulping. Holztechnologie 48(3):15–18. Retrieved from https://urn.kb.se/resolve?urn=urn:nbn:se:lnu:diva-41663

Hu W, Zhang Y, Zhou Zhang Y, Han S. (2025) Tannin formaldehyde wood adhesives synthesized by photocatalytic degradation larch tannins to avoid the harm of formaldehyde. J Hazard Mater 490:137754. https://doi.org/10.1016/j.jhazmat.2025.137754

Lee CJ, Chang T-C, Chung M-J (2021) Effects of gluing conditions for formaldehyde-free tannin adhesive on the oriented bamboo scrimber board properties. Eur J Wood Wood Prod 79 (5):1623–1631. https://doi.org/10.1007/s00107-021-01701-6

Lelis R. (1995) On the reactivity of sap- and heartwood of Douglas fir as well as their water extractives towards formaldehyde. European Journal of Wood and Wood Products, 53(1), 12-16. https://www.researchgate.net/publication/248156568_On_the_reactivity_of_sap-_and_heartwood_of_Douglas_fir_as_well_as_their_water_extractives_towards_formaldehyde

Özlüsoylu I (2023) The effect of varnish type, glue amount, and density on the surface properties of low density particleboards produced from waste wood bark. BioResources 18(4):7025–7040. https://doi.org/10.15376/biores.18.4.7025-7040

Pizzi A, Mtsweni B, Parsons WJ (1994) Wood-induced catalystic activation of PF adhesives auto polymerization vs. PF/wood covalent bonding. J Appl Polym Sci 52, 1847–1856. https://doi.org/10.1002/app.1994.070521302

Pizzi, A. (2006) Recent developments in eco-efficient bio-based adhesives for wood bonding: Opportunities and issues. J Adhes Sci Technol 20(8):829–-846. https://doi.org/10.1163/156856106777638635

Rader J. (1974) Reizwirkung von irect Ehyde in Praepariersaelen, Analytische und Experimentelle Untersuchungen Inaugural dissertation, Wuerzburg-Germany.

Roffael E, Parameswaran N (1981) Thermochemische Aktivierung desEigenbindevermögens von Eichenholzspänen. Adhäsion 25:286–289. https://publica.fraunhofer.de/handle/publica/253038

Roffael E (1982) Die Formaldehydabgabe von Spanplatten und anderen Werkstoffen. DRW-Verlag, Stuttgart 328.

Roffael E (1993) Formaldehyde release from particleboards and other wood based panels. Forest Institute Malysia 281.

Lee SH, Lum WC, Boon JG, Kristak L, Antov P, Pędzik M, Rogoziński T, Taghiyari HR, Lubis MAR, Fatriasari W, Yadav SM, Chotikhun A, Pizzi A (2022) Particleboard from agricultural biomass and recycled wood waste: a review. J Mater Res Technol 20:4630–4658. https://doi.org/10.1016/j.jmrt.2022.08.166

Tappler P, Twrdik F, Damberger B, Mitterer K, Hutter HP (2008) Pilotstudie zur Untersuchung des Luftwechsels in Innenräumen. Gefahrstoffe, Reinhaltung der Luft 68(3):87–91.

Wong MC, Simone IS, Hendrikse PC, Sherrell PC, Ellis AV (2020) Grapevine waste in sustainable hybrid particleboard production. Waste Manag 118:501–509. https://doi.org/10.1016/j.wasman.2020.09.007

Copper migration from treated wood garden boxes into soil and vegetable biomass Part II: The third and fourth growing seasons after installation

*G. N. Presley**†
Associate Professor
Department of Wood Science and Engineering
Oregon State University
gerald.prelsey@oregonstate.edu

M. J. Konkler
Senior Faculty Research Assistant II
Department of Wood Science and Engineering
Oregon State University
Matthew.Konkler@oregonstate.edu

(Received 15 September 2025)

Abstract: Concerns about the safety of preserved wood as a garden box frame material persist in the public stemming from fears about chemical contamination of homegrown food. This study describes the third and fourth years of a long-term study to measure copper migration from copper azole-treated garden bed frames into garden soil and vegetable biomass (Presley and Konkler 2024). Garden bed frames made of Douglas-fir lumber untreated or pressured treated with copper azole were planted with common garden vegetables over two growing seasons. Vegetables and soil samples were collected and analyzed for copper concentration. Average copper levels in vegetables collected from treated or untreated beds were not distinguishable, except for radish roots grown in year 4 which contained higher copper levels (7.5 PPM) when grown in untreated wood beds compared to those grown in treated wood beds (3.7 PPM; $p < 0.05$ Tukey's HSD). At the end of each growing season, average copper concentrations in soil were significantly elevated in soil in direct contact (0–25 mm) with the treated wood (77.8–101 PPM) over copper levels found at equivalent locations in untreated wood beds (21.1–33.2 PPM) ($p < 0.05$, Tukey's HSD). No differences in average copper concentrations were observed in soils taken from any other sampling location, indicating that measurable copper accumulation was limited to within 25 mm of the bed edge. This study shows that the use of treated wood as a bed frame material has no impact on vegetable copper content and the impacts of copper migration are small and spatially limited.

Keywords: Metal leaching; Bioaccumulation; Wood durability; Copper azole.

Introduction

Wood is a popular material for the construction of raised beds for vegetable gardens because of its wide availability, workability, and ease of construction. However, wood is susceptible to biodegradation by wood-destroying fungi, particularly in a ground-contact application with regular wetting, such as a garden box frame. Pressure treatment of wood commodities with copper containing biocides is commonly used to improve the resistance of wood to decay by fungi in residential applications such as garden box frames (Kirker and Lebow 2021).

The use of chemical preservatives for the protection of raised bed garden frames has raised concern among the general public because of the proximity of these materials to homegrown vegetables. These concerns have arisen from the past use of chromated copper arsenate (CCA) as a wood preservative for residential applications and from concerns of arsenic contamination in gardens and bioaccumulation in food. While these concerns have not been substantiated by scientific data (Quarles et al. 2004), CCA was voluntarily discontinued as a residential-use wood preservative over 20 years ago (EPA 2002). Today, arsenic-free copper-based wood preservatives such as copper azole (CA-C), micronized copper azole (MCA), and alkaline copper quaternary (ACQ) dominate the residential pressure-treated wood market. Despite this, fears in the

* Corresponding author
† Society of Wood Science & Technology member

general public remain about the risks of metal contamination of produce grown in close proximity to pressure-treated wood.

Fears of copper contamination from treated wood in garden boxes are based on concerns related to human and plant health. High levels of metals in soil or hydroponic growth medium can inhibit the ability of common vegetables to grow and result in poor vigor. These problems are cited in relation to chemically contaminated soils with relatively high levels of copper (over 200 PPM), often exceeding those found in soil naturally (Yang et al. 2002; Chiou and Hsu 2019). Additionally, many vegetables can bioaccumulate copper when grown in soil with copper levels that are high enough to consider it a contaminant (Sharma et al. 2021).

Chemical migration from wood-preservative systems currently available in the residential market in the United States has been widely studied and, in the case of modern residential wood preservatives, copper is the primary chemical component that has the potential to migrate from the wood (Kennedy and Collins 2001). It is well known that measurable copper migrates from these treated wood commodities when exposed to water. Whether or not these losses translate into physiological changes in plants in the context of a vegetable garden box is another question. The impacts of CCA and copper alone have been assessed on grapevines grown in hydroponic chambers with mixed results showing no metal accumulation (Ko et al. 2007) or measurable copper accumulation when soluble copper was added to plant cultures (Shabbir et al. 2020). Amending soil with CCA-treated sawdust resulted in some increases in metal concentrations in beetroot, albeit at levels below toxic thresholds for animals (Speir et al. 1992). While informative, these in vitro studies do not represent treated wood's impact as it is used by residential consumers.

A previous study of the impact of treated wood on metal concentration in garden vegetables showed mixed results and had a limited sample size (Love et al. 2014). A recent study that reported the impacts of copper azole-treated wood on copper content in garden soils and vegetables over 2 years of planting showed that the only measurable impact of treated wood in this context was a small increase in copper concentrations in soil in direct contact with the bed material (Presley and Konkler 2024). The study presented here is a continuation of a long-term investigation of the impact of copper azole-treated wood on garden soil and vegetable metal content when it is used as a bed frame material. Data for the third and fourth growing seasons after garden bed construction are described below.

Methods

Garden box planting and maintenance

Previously constructed garden box frames were maintained and planted for a third and fourth growing season of a long-term study started in 2021 in Albany, Oregon (Presley and Konkler 2024) (Figure 1). The study included two beds made with wooden frames of each type: untreated or pressure-treated 5.1 × 30.5 cm (2 × 12-inch) nominal Douglas-fir. The treated beds were incised and pressured treated to American Wood Protection Association standard ground contact retentions of 2.4 kg/m^3 with copper azole type C (AWPA 2024). Before planting commenced for each growing season, the beds were all topped with a ~5 cm layer of compost, which was mixed in with the top layer of garden soil.

The four beds were planted in patterns identical to one another in each year, and planting diagrams showing the distribution of vegetable types in each planting year are shown in Figures 2 and 3. Vegetable types and the varieties grown in years 3 and 4 of this study are summarized in Table 1. Vegetables were either seeded into the beds directly or were planted as juvenile plant starts that were raised from seed indoors prior to being planted. Vegetables were planted at appropriate times for USDA hardiness zone 8b, in which the study area resides. The beds were watered using treated municipal water by drip irrigation fed through 12.5 mm polyethylene tubing in response to seasonal weather patterns. Trellising for peas consisted of a wooden lattice made of strips of untreated Douglas-fir. Trellising for tomatoes in year 3 consisted of the same wooden lattice, and in year 4 it consisted of a 4.8 m galvanized cattle panel bent over the beds and affixed to either side of the beds (Figure 1). No copper input was expected from any of the trellising materials.

Vegetable and soil collection

Vegetables were collected from the garden beds throughout the growing season as they reached harvestable sizes. Three replicate samples of each vegetable large enough to provide sufficient test material were collected from each bed, for a total of 6 replicates per bed type. This was the case for all vegetables except for radishes grown in untreated beds in year 4, which only had a total of four replicates due to crop failure in one untreated bed. The number or total mass of vegetables collected for each replicate sample varied because of variation in vegetable size and the total number of available plants for each vegetable type. Sufficient biomass was collected in each replicate to make three replicate extracts for copper analysis.

Figure 1. Treated and untreated garden boxes in October of the third (left) and September of the fourth (right) growing seasons.

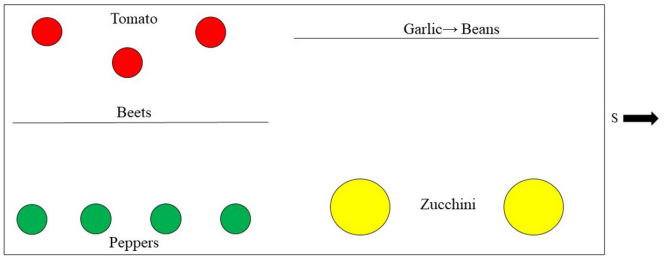

Figure 2. Planting diagram for year 3 for treated and untreated raised beds. Varieties grown for each vegetable are listed in Table 1 and circles indicate an individual plant. Beans were succession planted after garlic.

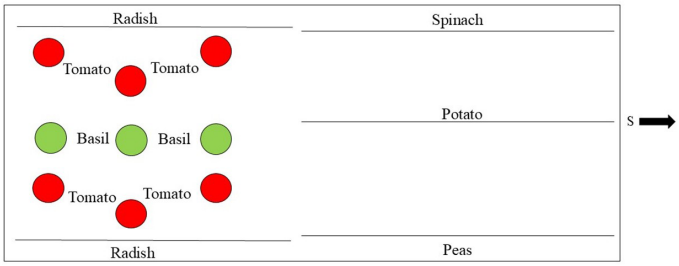

Figure 3. Planting diagram for year 4 for treated and untreated raised beds. Varieties grown for each vegetable are listed in Table 1 and circles indicate an individual plant.

In most cases the edible portion of the plant was reserved for analysis of copper concentration only. For root crops beets and radishes, the leaves were also analyzed for copper concentration.

Soil samples were collected from each bed at the beginning and end of each growing season. At the start of each growing season, compost was added to each bed and worked into the top layers of soil prior to planting, as noted above. A sample of the compost was retained for analysis of copper concentration. Soil samples for the start of the season were collected after the compost addition. A soil corer of 25 × 305 mm was used to collect samples 0–25 mm from the bed edge, 76–102 mm from the bed edge, and at the bed center. The corer was plunged into the soil to capture a ~305 mm soil core representative of soil held by the bed frames. Four soil samples from each location were taken per bed, and these were analyzed as replicate samples (Figure 4).

Measurement of copper

Soil or vegetable biomass was microwave digested in triplicate from comingled samples and analyzed for copper content us-

Table 1. Description of vegetable samples harvested from the raised beds in year 3 and year 4 and which plant parts were analyzed.

Vegetable	Part analyzed	Variety *
Planting year 3		
Garlic	Bulb	Russian Red
Garlic	Leaves	Russian Red
Beet	Root	Early Wonder Tall Top
Beet	Leaves	Early Wonder Tall Top
Zucchini	Fruit	Mexicana
Bush bean	Fruit	Oregon 91G bush bean
Bell pepper	Fruit (flesh only)	Wonder Bell F1
Tomato	Fruit	Carmello
Planting year 4		
Basil	Leaf	Emily
Pea	Pod	Sugar Daddy Snap Pea
Potato	Tuber	Vivaldi
Radish	Leaf	Cherry Belle
Radish	Root	Cherry Belle
Spinach	Leaf	Lakeside F1
Tomato	Fruit	Pozzano

* Seed source for all plantings: Territorial Seed Company.

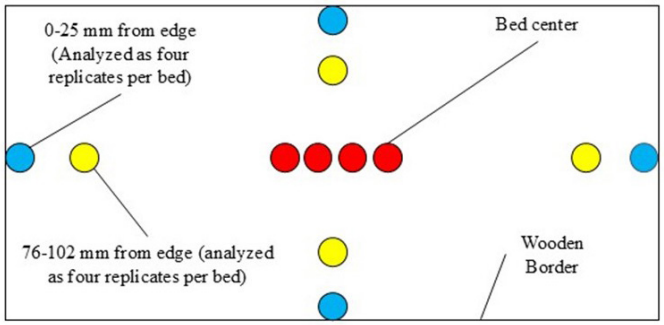

Figure 4. Sampling diagram for soil samples taken at the beginning and end of each growing season adapted from Presley and Konkler (2024).

ing atomic absorption spectrophotometry (AAS). Soil or plant biomass samples were homogenized, oven dried, and digested according to EPA method 3052 (EPA 1996). Briefly, 0.25 g of soil or 0.5 g of plant biomass was placed into PTFE microwave extraction tubes and 10 mL of concentrated nitric acid was added. Samples were digested for 9.5 minutes at 180°C, with a total microwave digestion time of about 15 minutes. Each replicate sample was digested in triplicate to generate three separate technical replicates per replicate sample. The resulting digestate was rinsed from the tube with DI water and brought up to a volume of 35 mL with DI water. It was then analyzed for copper using AAS and as µg/g (PPM) in the original oven-dried biomass.

Samples were loaded onto a Shimadzu AA-7000 and analyzed using Flame Atomic Absorption Spectroscopy for copper. Copper analysis was performed at 324.8 nm. The lamp current was set to 6mA, the slit width was 0.7 nm, the flame type was a mixture of air and acetylene (atomic absorption grade) with an acetylene flow rate of 1.8 liters per minute, and the burner height was 7 mm. Each sample was analyzed four times with a total per sample analysis time of approximately 1 minute. The recorded absorbance was plotted against a five-point standard curve to calculate concentration. The detection limit using this method for copper was 0.006 PPM for the liquid extracts.

Statistical comparisons were made between copper levels in treated and untreated beds using a single factor ANOVA and a Tukey's honestly significant difference post hoc test, $\alpha = 0.05$.

Results and discussion

Copper concentrations for vegetables harvested in years 3 and 4 after bed installation are shown in Figures 5 and 6, respectively. Copper concentrations in the vegetable biomass were the same in vegetables grown in treated and untreated beds in most cases, with no statistically significant differences ($p > 0.05$, Tukey's HSD). One exception was for radish roots grown in year 4, where radishes harvested from the untreated beds had significantly higher average copper levels (7.5 PPM) than those harvested from treated beds (3.7 PPM; $p = 0.027$, Tukey's HSD). Higher average copper levels in radishes grown in the untreated beds was not expected, but it may be due to the lower sample size for radishes obtained in year 4, due to a poor crop during that growing season. Additionally, it is important to note that the copper levels measured here may just represent natural variation in the plant biomass. The United State Department of Agriculture (USDA) Food Central database for food nutrients lists radishes as having about 10.6 PPM copper on a dry weight basis (USDA 2019). Levels measured here are lower than the USDA's typical average copper level for radishes and, despite some variability between populations, copper levels measured in this study are not of concern for human consumption.

Similarity among copper concentrations from vegetables originating from treated or untreated beds is in line with previous observations from earlier growing seasons that were part of this study (Presley and Konkler 2024). Some prior observations suggested that copper may accumulate in carrot tops when grown in treated wood beds (Love et al. 2014), but none of the root crops grown in years 3 and 4 of this study showed increased copper levels resulting from the treated bed frame materials. Other studies have shown that vegetables will accumulate copper if grown in soils amended with or contaminated with copper, but generally copper levels required to generate that effect are much higher than are observed in soils found in treated wood garden beds (Apodaca et al. 2017; Intawongse and Dean 2007; Presley and Konkler 2024).

Copper levels taken from soils at three locations in each bed were measured at the beginning and the end of years 3 and 4 after installation (Figure 7). At the start of year 3, average copper levels in soil from untreated and treated beds were similar, and no statistically significant differences were detected ($p > 0.05$, Tukey's HSD). At the end of year 3, soil samples taken 76–102 mm from the bed edge and the bed center similarly showed no significant differences in average copper concentrations. At the 0–25 mm sampling point taken at the end of year 3, soils taken from treated beds had higher average copper concentrations (101 PPM) compared with soil samples from equivalent locations in untreated boxes (33.2 PPM). This pattern was consistent with what was observed

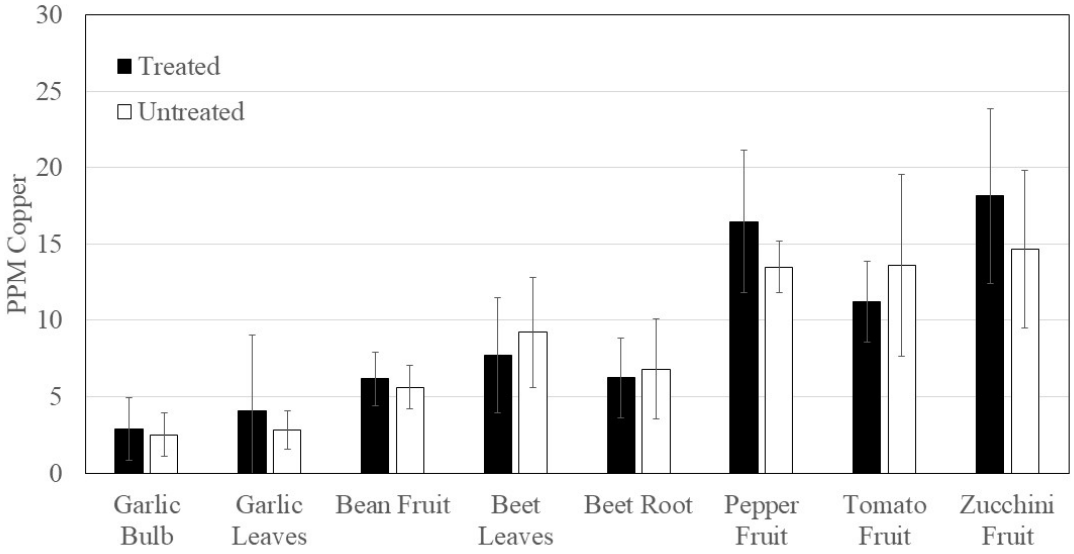

Figure 5. Copper levels found in vegetable biomass taken from the raised beds in year 3. Error bars are plus or minus one standard deviation of six replicate extracts, three taken from each replicate bed of each type.

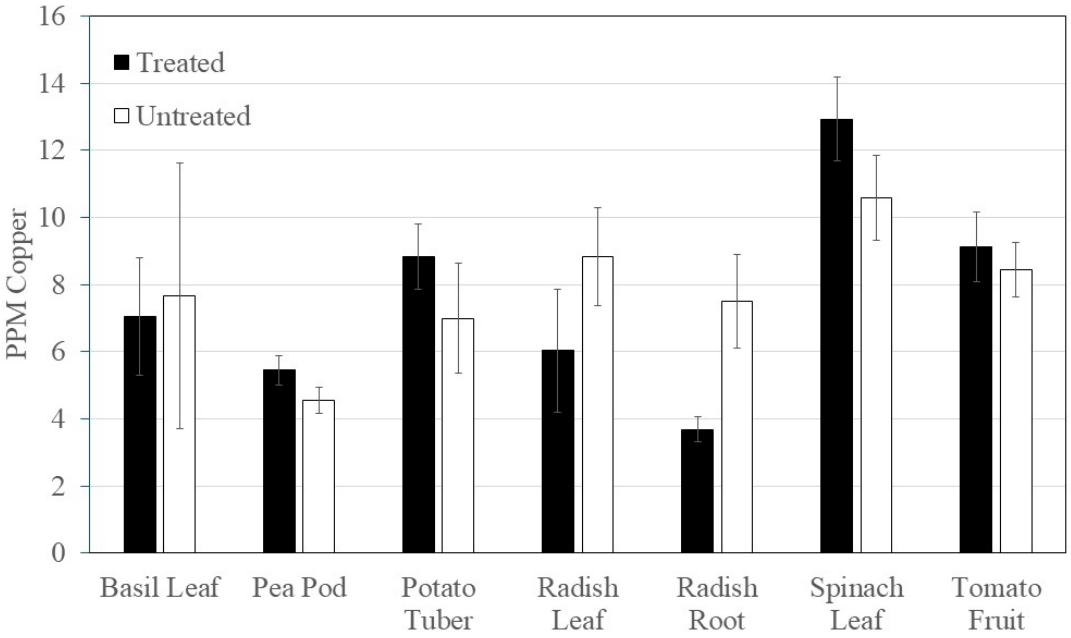

Figure 6. Copper levels found in vegetable biomass taken from the raised beds in the year 4 season. Error bars are plus or minus one standard deviation of six replicate extracts, three taken from each replicate bed of each type, except for radishes from untreated beds, which only had four replicates in total due to crop failure in one bed.

in the first two growing seasons, where copper accumulation was only measurable in soils in direct contact with the treated wood bed frame (Presley and Konkler 2024).

At the start of the fourth growing season, soil isolated from 76–102 mm from the bed edge and the bed center showed no significant differences in average copper concentrations between equivalent samples taken from treated and untreated beds ($p > 0.05$, Tukey's HSD; Figure 7). Soils taken from the 0–25 mm sampling location in the treated beds showed significantly higher average copper concentrations (44.4 PPM) compared to the same location in untreated beds (26.2 PPM; $p < 0.05$, Tukey's HSD). Compost addition reduced the average

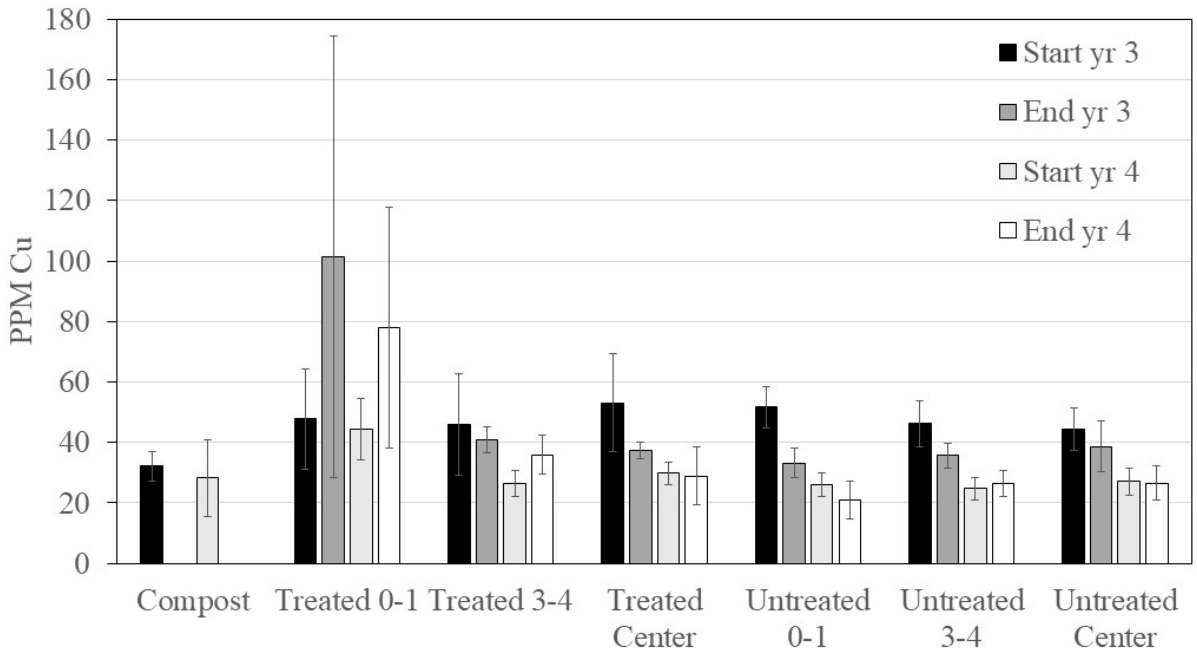

Figure 7. Copper levels found in soils taken from treated and untreated garden boxes at the start and the end of the third season, as well as the start and the end of the fourth season of growth. Error bars are plus and minus one standard deviation of eight replicate extracts, four from each of two garden beds of each type. Figure labels 0–1 for both treated and untreated boxes refer to the 0–25 mm sampling locations; labels 3–4 refer to the 76–102 mm sampling locations.

copper concentration from 101 to 44.4 PPM from the end of the third growing season to the start of the fourth. However, in year 4, average copper levels in soils from the 0–25 mm sampling location in treated beds were still higher than the 0–25 mm sampling location in untreated beds. In earlier sampling points, compost addition was enough to equalize copper average copper concentrations after a year of accumulation in soils in direct contact with the bed edges (Presley and Konkler 2024). At the end of year 4, soils taken 76–102 mm from the bed edges as well as those from the bed center were similar in the treated and untreated beds ($p > 0.05$, Tukey's HSD). Average copper concentrations were higher in soils taken from the 0–25 mm sampling location in treated beds (77.8 PPM) than those found at the same location in untreated beds (21.1 PPM; $p < 0.05$, Tukey's HSD).

Data from years 3 and 4 are consistent with previous observations in years 1 and 2 of this study (Presley and Konkler 2024). Treated wood results in copper increases in soil only in direct contact with the bed material and is not widely observed throughout the garden bed soil.

Additionally, average copper concentrations in soils measured in years 3 and 4 ranged from 21.1 to 101 PPM across all bed types and sampling locations, which fall well below 140 PPM, the level considered elevated above natural soil levels found in the Willamette Valley (DEQ 2013). Soils in other parts of the United States naturally can contain up to about 500 PPM copper (Rehman et al. 2019). While treated wood does result in copper increases in some of the garden box soil, levels measured in this study to date are not unnaturally high.

The primary issue among those who are concerned about treated wood's impact on garden vegetables centers on bioaccumulation and downstream health impacts. Copper concentration in soil is important in determining whether or not vegetables grown in that soil bioaccumulate levels of copper and copper that can impact human health (Sharma et al. 2021). Contaminated soils levels that may cause issues with crop contamination are much higher than have been observed in this study. In a study performed in Italian agricultural soils, soil with copper concentrations as high as 217 PPM showed no dietary risks to consumers (Fagnano et al. 2020). Another study of bioaccumulation of copper in Chinese cabbage, pakchoi, and celery showed that soil concentrations of total copper must reach 430–835 PPM before bioaccumulation becomes a health risk (Yang et al. 2002). The highest average copper levels observed in soils in this study to date (101 PPM) are much lower than those that have been shown to result in copper bioaccumulation in food crops.

Another concern centers on the impact of copper on the viability and vigor of garden vegetables. Copper contaminated soils can also result in changes to plant physiology and reduced crop vigor. Soil copper levels above 250 PPM have been shown to reduce the growth of four different leafy vegetables (Chiou and Hsu 2019). The copper threshold in soil at which Chinese cabbage, pakchoi, and celery showed growth inhibition is about 150 PPM (Yang et al. 2002). Previous observations indicate that toxicity thresholds for many vegetable crops are considerably higher than the highest copper levels measured in this study. Additionally, the highest copper levels observed in the treated wood garden boxes in this study were limited to a thin, ~25 mm band around the bed margins.

The sampling regime for the third and fourth growing seasons was changed to include greater sampling replication (four soil samples per bed per location and triplicate extracts of each soil sample). This change resulted in improved data quality compared with the previous report (Presley and Konkler 2024) and enables greater confidence in the findings. Soil, as well as wood, is a highly variable matrix of organic and inorganic matter; metal migration through these matrices can be highly varied from one location to another. Still, this study only included two beds of each material type, and future long-term studies are needed to provide a greater sampling of the conditions gardeners face.

Conclusion

This shows that use of copper azole-treated wood as a garden bed frame material does not cause an increase in copper concentrations in vegetables grown in those garden boxes. Copper accumulation in soil was limited to within a ~25 mm distance from the treated wood bed material, up to an average of just over 100 PPM at the end of year 3. The magnitude of copper accumulation was modest, with the highest concentrations still falling within natural copper levels for the region in which the beds are located.

Acknowledgements

This work was funded by the Oregon State University Environmental Performance of Treated Wood Research Cooperative.

References

AWPA-American Wood Protection Association (2024). American Wood Protection Association 2024 Book of Standards, Birmingham, AL.

Apodaca SA, Tan W, Dominguez O, Hernandez-Viezcas JA, Peralta-Videa JR, Gardea-Torresdey JL (2017) Physiological and biochemical effects of nanoparticulate copper, bulk copper, copper chloride, and kinetin in kidney bean (*Phaseolus vulgaris*) plants. Sci Total Environ 599-600; 2085-2094. https://doi.org/10.1016/j.scitotenv.2017.05.095

Candan F, Ozturk M, Altay V, Yalcin IE (2023) An experimental study on the effects copper and lead on the seedlings of some economically important vegetable species. Notulae Botanicae Horti Agrobotanici Cluj-Napoca 51(4):13158. https://doi.org/10.15835/nbha51413158

Chiou W-Y, Hsu F-C (2019) Copper toxicity and prediction models or copper content in leafy vegetables. Sustainability 11(22):6215, https://doi.org/10.3390/su11226215

Environmental Protection Agency-EPA (2002). Notice of Receipt of Requests to Cancel Certain Chromated Copper Arsenate (CCA) Wood Preservative Products and Amend to Terminate Certain Uses of CCA Products. Federal Register February 22, 2002, OPP-66300.

Environmental Protection Agency-EPA (1996). SW-846 Method 3052: Microwave Assisted Acid Digestion of Siliceous and Organically Based Matrices. https://www.epa.gov/hw-sw846/sw-846-test-method-3052-microwave-assisted-acid-digestion-siliceous-and-organically-based

Fagnano M, Agrelli D, Pascale A, Adamo P, Fiorentino N, Rocco C, Pepe O, Ventorino V (2020) Copper accumulation in agricultural soils: Risks for the food chain and soil microbial populations, Sci Total Environ 734, 139434. https://doi.org/10.1016/j.scitotenv.2020.139434

Intawongse M, Dean JR (2006) Uptake of heavy metals by vegetable plants grown on contaminated soil and their bioavailability in the human gastrointestinal tract. Food Addit Contam 23(1):36–48. https://doi.org/10.1080/02652030500387554

Kennedy MJ, Collins PA (2001) Leaching of preservative components from pine decking treated with CCA and copper azole, and interactions of leachates with soils, Proceedings of the IRG annual meeting, Document No. IRG/WP 01-50171, International Research Group on Wood Preservation. https://www.irg-wp.com/irgdocs/details.php?8b7f9528-a03d-4d0a-8d94-e7ba8146b260

Kirker GT, Lebow ST (2021) Chapter 15: Wood preservatives. In: Wood handbook—wood as an engineering material. General Technical Report FPL-GTR-282. USDA Forest Service, Forest Products Laboratory, Madison, WI. 26 p. https://research.fs.usda.gov/treesearch/62200

Ko B, Vogeler I, Bolan NS, Clothier B, Green S, Kennedy J (2007) Mobility of copper, chromium and arsenic from treated timber into grapevines. Sci Total Environ 388(1–3):35–42. https://doi.org/10.1016/j.scitotenv.2007.07.041

Love CS, Gardner B, Morrell JJ (2014) Metal accumulation in root crops grown in planters constructed from copper azole treated lumber. Eur J Wood Wood Prod 72:411–412. https://doi.org/10.1007/s00107-014-0789-5

United States Department of Agriculture (2016). National Organic Program (NOP), Treated Lumber (Draft Guidance) NOP 5036. United States Department of Agriculture Agricultural Marketing Service, Washington, DC. https://www.usda.gov/guidance-documents/nop-5036/ams/treated-lumber-draft-guidance

Oregon Department of Environmental Quality (DEQ) (2013). Development of Oregon Background Metals Concentrations in Soil, Technical Report. Land Quality Division, Cleanup Program, Portland, OR. https://digitalcollections.library.oregon.gov/nodes/view/121431

Presley GN, Konkler MJ (2024) Copper migration from treated wood garden boxes into soil and vegetable biomass Part I: The first two growing seasons after installation. Wood Fiber Sci 56(2):91–99. https://doi.org/10.22382/wfs-2024-09 https://wfs.swst.org/index.php/wfs/article/view/3287

Rehman M, Lui L, Wang Q, Saleem MH, Bashir S, Ullah S, Peng D (2019) Copper environmental toxicology, recent advances, and future outlook: a review, 26: 18003–18016. https://doi.org/10.1007/s11356-019-05073-6

Schmitt OJ, Andriolo JL, Silva ICB, Tiecher TL, Chassot T, Tarouco CP, Lourenzi CR, Nicoloso FT, Marchezan C, Casagrande CR, Drescher GL, Kreutz MA, Brunetto G (2022). Physiological responses of beet

and cabbage plants exposed to copper and their potential insertion in human food chain. Environ Sci Pollut Res 29:44186–44198. https://doi.org/10.1007/s11356-022-18892-x

Shabbir Z, Sardar A, Shabbir A, Abbas G, Shamshad S, Khalid S, Murtaza G, Dumat C, Shahid M (2020) Copper uptake, essentiality, toxicity, detoxification and risk assessment in soil-plant environment. Chemosphere 259(Nov):127436. https://doi.org/10.1016/j.chemosphere.2020.127436

Sharma N, Bakshi A, Sharma A, Kaur I, Nagpal AN (2021) Health risk associated with copper intake through vegetables in different countries. IOP Conf Ser Earth Environ Sci 889:012071. https://doi.org/10.1088/1755-1315/889/1/012071

Speir TW, August JA, Feltham CW (1992) Assessment of the feasibility of using CCA (copper, chromium and arsenic) -treated and boric-acid treated sawdust as soil amendments. Plant Soil 142:235–248. https://doi.org/10.1007/BF00010969

Quarles SL, Kobzina JW, Geisel PM (2004) Using CCA Preservative-Treated Lumber in Gardens and Landscaping, University of California Division of Agriculture and Natural Resources, Publication 8128. https://doi.org/10.3733/ucanr.8128

United States Department of Agriculture (2019) FoodData Central Food Details Database, SR Legacy data, FDC ID 169276. https://fdc.nal.usda.gov/

Yang XE, Long XX, Ni WZ, Ye ZQ, He ZL, Stofella PJ, Calvert DV (2002). Assessing copper thresholds for phytotoxicity and potential dietary toxicity in selected vegetable crops. J Environ Sci Health - B Pestic Food Contam Agric Wastes 37(6):625–635. https://doi.org/10.1081/PFC-120015443

SWST accreditation: Shaping the future of wood science and technology education and its role in the forest products industry

*Judith Gisip**†
Senior Lecturer
Faculty of Applied Sciences
School of Industrial Technology
Universiti Teknologi MARA
Shah Alam, Selangor, Malaysia
E-mail: judith@uitm.edu.my

Eric Hansen†
Professor and Department Head
Department of Wood Science and Engineering
Oregon State University
Corvallis, OR
Email: eric.hansen@oregonstate.edu

(Received 5 October 2025)

Abstract: Society of Wood Science and Technology (SWST) accreditation plays a crucial role in ensuring that wood science and technology programs remain relevant, industry-aligned, and future-ready. As the forest products sector evolves with shifting global markets and growing sustainability demands, the need for highly skilled professionals in areas like bio-based materials and advanced manufacturing is critical. SWST accreditation establishes rigorous standards, equipping graduates with the technical and professional skills necessary to thrive in the industry. However, awareness of accreditation's full potential remains limited, and many programs could better leverage it to enhance curriculum, strengthen industry connections, and boost global recognition. This paper provides an overview of SWST accreditation and its role in shaping the future of wood science and technology education by maintaining program quality, fostering interdisciplinary approaches, and supporting the development of a workforce that drives innovation and competitiveness within the forest products industry.

Keywords: SWST accreditation; Accreditation standards; Wood science education; Internationalization; Forest products industry.

Introduction

The Society of Wood Science and Technology (SWST) is an international professional society dedicated to advancing the knowledge and profession of wood science and technology and related disciplines. SWST began exploring a potential role in accreditation of wood science programs in the late 1970s (Armstrong and Shmulsky 2008), and accreditation of educational programs has been an important function of SWST, with the first Wood Science and Technology undergraduate program at North Carolina State University accredited in 1984 (VL Herian, personal communication, December 2025; Rice 2010). SWST seeks to enhance the quality of education at the Bachelor of Science and Master of Science levels by ensuring that graduates are exposed to relevant and current topics in wood science and technology. SWST also recognizes that multiple terms (Table 1) may be used to describe a universal concept or program name that benefits its mission and helps develop consensus among accredited programs and constituencies.

Wood science and technology programs have experienced significant evolution over recent decades. Many programs have changed traditional names like "wood science and technology" or "forest products" to more contemporary titles like "bioproducts," "renewable materials," or "sustainable construction management and engineering" (Armstrong et al. 2013), as well as "wood innovation for sustainability." These changes reflect a broader trend in higher education to adapt to evolving industry needs and student interests.

* Corresponding author
† Society of Wood Science & Technology member

Table 1. Recognized terminology in wood science and technology for accredited programs (SWST 2025).

Terminology
• Wood Science and Technology
• Forest Products
• Lignocellulosic Materials
• Renewable Materials
• Sustainable Materials
• Bio-based Materials

This paper provides an overview of SWST accreditation, its standards and procedures, its role in shaping the future of wood science and technology education, and its impact on the forest products industry.

History and evolution of SWST accreditation

SWST started developing accreditation guidelines and standards in the 1960s (Rice 2012). The original standards covered most of the topic areas specified by institutional accrediting bodies. It began accrediting university-based, undergraduate-level wood science and technology programs in 1984. Early evaluations of wood science and technology education emphasized accreditation as the appropriate mechanism for strengthening academic programs. A broad survey of North American wood science programs reported strong support for accreditation as a means to enhance program quality, visibility, and institutional leverage, while licensing of wood technologists was viewed as inappropriate for the discipline. These findings reinforced the role of professional societies such as SWST in safeguarding educational standards, particularly at the undergraduate level (Barnes 1979).

At the same time, early commentary cautioned against rapid adoption of highly formalized accreditation models. Drawing on extensive experience with Society of American Foresters (SAF) accreditation, Kaufert (1979) highlighted the financial and administrative burdens associated with national accreditation systems and questioned their immediate feasibility for SWST. These concerns contributed to a cautious, evolutionary approach to accreditation, emphasizing program review and gradual standards development rather than rigid prescriptive requirements.

Until recently, only programs in North America were considered for accreditation, but SWST expanded to programs outside the region with the accreditation of a program at the University of Bio Bio in Chile in 2009. Since that time, programs have received accreditation in Indonesia, China, and Mexico. There were, and remain, professional standards that are detailed, prescriptive, and narrow in scope. In the early 2000s, SWST began a major revision of its accreditation standards aimed at shifting from course-based requirements to outcomes-based assessment, aligned with parallel reforms by SAF and regional higher-education accreditors, while preserving independent, discipline-specific standards (SWST 2001).

Subsequent assessments of wood science education programs reinforced the need for accreditation and continuous program evaluation. Despite increasing interdisciplinarity and curricular diversification, consensus remained that core competencies in wood anatomy, physical and mechanical properties, and processing technologies constitute the foundation of wood science education. These findings underscored the importance of discipline-specific accreditation frameworks capable of accommodating program diversity, while preserving essential scientific rigor (Gardner et al. 2005).

In the past decade, there have been several publications on the status of wood science and technology education and on the need for SWST accreditation to address the changes through revising its guidelines. Table 2 summarizes the publications that address these issues.

As wood science programs broadened to encompass bio-products, sustainability, and renewable materials, concerns emerged that highly prescriptive accreditation standards no longer reflected the diversity of contemporary curricula. Calls to reframe and modernize wood science education emphasize flexibility, international relevance, and outcomes-based evaluation, while retaining a clearly defined disciplinary core. These perspectives further justified SWST's shift toward outcomes-based accreditation as a mechanism for supporting innovation without diluting disciplinary identity (Shupe 2011).

Advantages and impacts of SWST accreditation

Wood science and technology evolved from formal forestry education systems into a recognized interdisciplinary scientific discipline with wood physics as its core, supported by over a century of dedicated research institutions and international collaboration (Sandberg and Niemz 2025). This historical and scientific foundation underpins the need for rigorous, discipline-specific accreditation of undergraduate wood science programs.

Society of Wood Science and Technology accreditation provides numerous benefits for educational institutions, students, and

Table 2. Status and changes in wood science and technology education and SWST accreditation.

Main Points	Authors
Challenges and opportunities facing wood science programs in the United States, particularly the need to adapt to changing student interests and industry needs and rebranding the discipline to highlight its relevance to sustainability, environmental issues, and the bioeconomy.	Smith and Valverde (2019)
The challenge of low enrolment in Wood Science and Technology (WST) programs, and various strategies to address the challenge.	Armstrong et al. (2013)
SWST should change responding to the evolving needs of its members and the broader society. It should pursue initiatives which include enhancing student membership and developing educational material for accredited programs.	Cloutier (2012)
Evolution and refocusing of accreditation standards for programs and disciplines, particularly within the Society of Wood Science and Technology (SWST).	Rice (2012)
Broadening SWST accreditation guidelines to meet the evolving demands of the wood products industry to include renewable or sustainable materials, green building materials, environmental and ecological concerns, renewable materials processing, physical properties of renewable materials, bioenergy, bioenergy systems, and business and entrepreneurship.	Rice (2010)

the forest products industry, globally. In addition to publishing peer-reviewed literature, SWST archival records document the development and operationalization of its accreditation system. Accreditation Committee reports published in newsletters describe formal multi-year program reviews, site visits, joint evaluations with SAF, the transition toward outcomes-based assessment, standards revision through public consultation, and the SWST Executive Board oversight, providing primary evidence of the rigor and continuous improvement embedded in SWST accreditation.

Accreditation enhances the reputation of wood science and technology programs, signaling to prospective students, employers, and the public that the program meets high standards of quality and relevance. This can lead to increased student enrollment; increased quality of graduates; improved faculty recruitment; increased exposure and potential for collaboration with peer institutions, industry and government research organizations; and greater recognition of the program's achievements.

It should be noted that SWST accreditation is discipline-specific and does not replace licensure-based or national engineering accreditation systems. While its visibility may not be extensive outside the wood science community, this reflects a focused, outcome-based evaluation against wood science and technology standards. Unlike prescriptive engineering accreditation schemes, SWST accreditation emphasizes disciplinary coherence, scientific foundations, industry relevance, sustainability, and continuous improvement. This focus makes it particularly well-suited to academic programs in which wood science forms the central intellectual and professional foundation.

As for student outcomes, SWST accreditation enhances the employability of graduates by ensuring programs provide them with the knowledge, skills, and credentials that employers seek. Accredited programs ensure that students are well-prepared for careers in the forest products industry and related fields and professional networks. These opportunities can enhance their educational experiences, broaden their horizons, and connect them with potential employers. In terms of industry impacts, SWST accreditation streamlines workforce training by ensuring that graduates possess the necessary skills and knowledge for the forest products industry. This reduces the extent of necessary on-the-job training and allows employers to hire graduates that are more workforce ready. Accredited programs produce graduates who are equipped to drive innovation, develop new technologies, and contribute to the growth and sustainability of the forest products industry.

Finally, SWST accreditation plays a crucial role in promoting sustainable practices in the forest products industry globally. SWST-accredited programs incorporate principles of sustainable forestry into the curriculum, educating students about responsible forest management, conservation, and biodiversity. The standard encourages coverage of development topics such as life-cycle assessment, a tool used to evaluate the environmental impact of products and processes throughout their entire life cycle. Similarly, circular economy is a topic being

embraced by programs in their course coverage, emphasizing to students the topics of waste reduction, reuse, and recycling in the forest products industry.

SWST accreditation aligns with the United Nations Sustainable Development Goals (SDGs), particularly SDG 9 (industry, innovation, and infrastructure), SDG 12 (responsible consumption and production), and SDG 15 (life on land) (United Nations General Assembly 2015). It helps ensure that curricula include aspects of the SDGs so that graduates can contribute to achieving those goals. By promoting sustainable practices, accredited programs contribute to global sustainability efforts.

Accreditation standards, procedures, and guidelines

SWST independently evaluates programs that choose to undergo the accreditation process. The evaluation process is flexible to accommodate recognition of professional bachelor's degrees, bachelor's degrees, and master's degrees and how these degrees can vary based on program characteristics and requirements, country, etc. The three objectives of these evaluations are: (1) improve the quality of education through self-assessment and external review; (2) recognize global institutions that meet or exceed minimum requirements set by SWST; and (3) promote and encourage coverage of knowledge essential for practicing scientists and technologists (SWST 2025). Accreditation assessment ensures that the environment, facilities, faculty, and infrastructure are sufficient for a program to produce competent graduates with a firm grasp of the tenets of materials science and technology and with a well-rounded education. The core of an SWST-accredited program requires inclusion of a fundamental understanding of renewable materials as well as basic materials science, including raw materials biology, physical properties, mechanical properties, and chemical characteristics and properties. It is also suggested that the program covers other materials and includes properties of these materials in their basic materials science coursework. Table 3 outlines several key areas in which students in an accredited program may focus. The standard requires students to develop a foundation in at least one of these areas (SWST 2025).

The essential components of SWST-accredited programs include a rationale and purpose, as well as goals and objectives to achieve its mission; educational objectives that are consistent with the institution's mission and SWST accreditation standards; a process for establishing educational objectives that responds to the needs of program constituencies; and an evaluation process that measures performance based on the SWST accreditation standards and uses the results to improve the effectiveness of the program.

In terms of the procedures for the accreditation to take place, a renewable materials program may request review for initial accreditation by SWST when it has operated a professional bachelor's, bachelor's, or master's program meeting SWST criteria for at least five years. Comprehensive self-study and self-evaluation are essential first steps in the accreditation process. The goal of the self-evaluation is to demonstrate compliance with SWST accreditation standards, determine accountability, and form the basis for program planning and improvement. To be valuable, a self-evaluation must be candid, realistic, and assesses all aspects of the program(s) under review. An annual report is required from each accredited program, which includes a summary of important changes and accomplishments that have occurred during the past year.

Table 3. Key areas in which students must build foundational knowledge (SWST 2025).

	Topic Areas	Description
1.	Harvesting, processing and manufacturing of renewable materials	Processing renewable materials from harvest into valuable products.
2.	Environmental impacts, assessment and sustainability	Covers life cycle analysis, carbon storage, certification, safety, standards, and legal issues.
3.	Bioenergy and bioconversion	Processing renewable materials is energy-intensive but offers efficiency gains. Understanding energy delivery, environmental impacts, life cycle analysis, and policies is essential.
4.	Business and entrepreneurship	Covers business, finance, marketing, and entrepreneurship in renewable materials.
5.	Growth and management of renewable materials (e.g., forestry/forest sciences)	Managing renewable materials for sustainability while meeting societal needs.
6.	Sustainable building materials and construction methods and management	Explores renewable construction materials, their impact on daily life, business, health, and the environment.
7.	Renewable materials science and engineering	Deepens science and engineering knowledge for graduate studies or research careers.
8.	Pulp, paper and packaging sciences	Pulp, paper, and packaging studies cover processes, sustainability, and engineering for industry operations.

The role of SWST accreditation in the forest products industry

SWST accreditation plays a significant role in ensuring the competence and readiness of graduates entering the forest products industry (Rice 2010). By setting standards for curriculum and competencies, SWST ensures that graduates possess a firm grasp of materials science and technology and a well-rounded education. Accreditation helps to improve the quality of professional education in wood science and technology through self-assessment and external review. Accreditation also recognizes institutions that meet or exceed minimum requirements set by SWST. Accreditation standards define a profession and provide accountability to those standards and promote competency among the graduates of those programs (SWST 2025).

SWST accreditation standards can incorporate needs assessments to identify gaps in innovation capacities and skills within the forest sector. Innovation is crucial for tackling global challenges and achieving SDGs within the forest sector, as emphasized in the "State of the World's Forests 2024" report of the UN Food and Agriculture Organization (FAO 2024). This provides a strong rationale for the importance of high-quality wood science and technology education that can foster such innovation. Global wood production is at record levels, approximately 4 billion m^3 per year. Projections indicate significant increases in wood demand by 2050 (FAO 2024). These data points underscore the need for a skilled workforce to manage forest resources and production sustainably, which can be enhanced through SWST accreditation.

The world forest sector has developed unequally across regions, with North America and Europe leading in the forestry value chain. Developed countries have achieved higher production efficiency through advanced technologies, enabling them to create more income with fewer jobs, compared to developing countries (Li et al. 2019). This suggests that wood science and technology education should be tailored to regional needs and focus on improving production efficiency and value addition in developing economies.

Ultimately, accreditation is a signal to employers that graduates from a program possess foundational knowledge of wood as a material, a knowledge base lacking from graduates of almost any other program. While employees with other backgrounds learn about wood through on-the-job experience, their lack of foundational wood science and wood technology knowledge limits their effectiveness in problem solving when faced with the idiosyncrasies and complexities of wood as a material.

Internationalization of SWST accreditation

The Society of Wood Science and Technology strives to uphold its vision of becoming the world leader in advancing the profession of wood science. Its initial focus on only North America has now become global in nature (Armstrong 2014). SWST is poised to expand its global reach. As of February 2025, there were a total of 12 SWST accredited programs worldwide (Table 4). China is an important country with three accredited programs and one undergoing evaluation in 2025. There are seven accredited programs in the United States and one in Mexico. Accreditation is active for the duration of 10 years, with re-accreditation required at that time. A yearly update report is required of all programs to maintain accreditation.

SWST accreditation standards are comparable to regional frameworks, such as the European Higher Education Area,

Table 4. SWST accredited programs worldwide.

Program reviewed	Country	Initial accreditation	Most recent	Expires
North Carolina State University, Raleigh	USA	1984	2015	2025
Virginia Polytechnic Institute and State University, Blacksburg	USA	1985	2015	2025
Mississippi State University, Starkville	USA	1987	2023	2034
West Virginia University, Morgantown	USA	1989	2019	2029
Oregon State University, Corvallis	USA	1990	2023	2024
University of Maine, Orono	USA	1993	2013	2024
University of Idaho, Moscow	USA	1996	2015	2025
Nanjing Forestry University, Nanjing, Jiangsu	China	2017	2017	2027
Zhejiang A & F University, Lin'an, Hangzhou	China	2018	2018	2028
South China Agricultural University, Guangzhou	China	2019	2019	2029
Inner Mongolia University, Hohhot, Inner Mongolia	China	2024	2024	2034
University of Guadalajara, Guadalajara*	Mexico	2024	2024	2034

* Accredited MS degree only

ensuring that accredited programs meet international benchmarks for quality and relevance. Additionally, SWST accreditation plays a role in reducing skill gaps across emerging and developed economies by providing a standardized framework for wood science and technology education. This ensures that graduates possess the skills and knowledge needed to contribute to the global forest products industry.

Lessons learned from SWST accreditation reviews

This section presents a synthesis of accreditation visit reports, offering insights into how these evaluations are shaping educational practices and fostering stronger connections with the forest products industry. The following reflects observations from site visits to five programs (three in the U.S., two outside U.S.) that were accredited during 2023–2024. It is important to note that these observations should be interpreted in context. The accreditation visits involved different accreditation teams, institutions with varying missions, resources, and institutional policies, and programs operating within distinct national, regulatory, and cultural contexts. As such, the observations are not intended for direct comparison or generalization, but rather to provide illustrative insights into recurring themes and experiences encountered during recent accreditation activities.

The accreditation journey begins with an extensive self-study, where institutions document their strengths, challenges, and strategic visions in aligning with SWST standards. This preparatory phase includes data collection, stakeholder engagement and pre-visit readiness. This foundational work sets the stage for on-site evaluations, which are crucial for validating self-reported data and offering real-time feedback. During the accreditation visit, evaluation panels conduct detailed tours of facilities and research laboratories, observe live demonstrations of teaching practice, and hold interviews with key stakeholders. Evaluation panels use a set of well-defined SWST criteria to systematically assess institutional performance. This dual focus on recognition and constructive feedback underscores the accreditation process as both an evaluative tool and a roadmap for continuous improvement.

Table 5 is a summary of general strengths and areas for improvement among SWST-accredited programs, based on evaluation data collected from December 2023 to December 2024. A checkmark (✓) indicates that the respective strength or improvement area was identified during the program's self-assessment, site visit, or peer review process. The "Total (✓)" column represents the number of programs reporting each item.

SWST accreditation reviews across various institutions have revealed both shared strengths and recurring challenges that can serve as valuable guidance for prospective or developing programs. Among the most notable strengths are strong stakeholder relationships, where programs typically maintain close ties with partners, alumni, and government bodies. This results in robust internship pipelines, collaborative research opportunities, and enhanced student employability. Another strength lies in the provision of adequate resources and facilities, including up-to-date laboratories and dedicated spaces for hands-on learning. Additionally, faculty members are typically described as dedicated, collaborative, and committed to student success, forming a strong backbone for academic quality.

Table 5. Summary of general strengths and areas for improvement of SWST accredited programs during the period of December 2023 to December 2024.

Strengths	U.S. 1	U.S. 2	U.S. 3	Non-U.S. 1	Non-U.S. 2	Total (✓)
Strong stakeholder relationships	✓	✓	✓	✓	✗	4
Adequate resources and facilities	✓	✓	✗	✓	✗	3
Dedicated and collaborative faculty	✓	✓	✓	✗	✗	3
Areas for improvement	U.S. 1	U.S. 2	U.S. 3	Non-U.S. 1	Non-U.S. 2	Total (✓)
Low enrollment numbers	✓	✓	✓	✓	✗	4
Need for recruiting strategies	✓	✓	✗	✓	✗	3
Curriculum enhancement	✓	✓	✓	✗	✗	3
Faculty development and diversity	✓	✗	✗	✗	✗	1
Administrative and program support	✗	✓	✗	✓	✗	2
Assessment and evaluation	✓	✗	✗	✗	✗	1
Facilities	✗	✗	✗	✗	✓	1

(✓) = the respective strength or improvement area was identified during the program's self-assessment, site visit, or peer review process. "Total (✓)" column represents the number of programs exhibiting each item.

However, several key areas for improvement emerge. Low enrollment remains a common concern, often driven by limited public awareness of the discipline. While accreditation alone does not directly increase enrollment, SWST accreditation can serve as a strategic asset for programs seeking to enhance visibility and student recruitment. Accreditation provides an externally validated mark of quality that can be leveraged in institutional marketing, industry engagement, and students advising to differentiate wood science programs from broader or less specialized offerings. In addition, alignment with SWST standards can strengthen industry partnerships, internship pipelines, and graduate employability narratives, which are increasingly important factors influencing student enrollment decisions. Programs are encouraged to invest in targeted outreach and digital engagement strategies. Curriculum modernization is another pressing need, with calls to better integrate emerging topics such as circular economy principles, digital fabrication, and renewable materials innovation. Faculty development and diversity are also flagged as critical areas, requiring support for professional growth and inclusive hiring practices.

Administrative limitations, including understaffing and communication gaps, can hinder program efficiency and growth. Strengthening internal communication channels and clarifying staff roles can mitigate these issues. Lastly, a consistent need for improved assessment practices has been noted, underscoring the importance of clear learning outcomes, robust data collection, and continuous quality enhancement.

By understanding and proactively addressing these lessons from past accreditation reviews, new and existing programs in wood science and renewable materials can position themselves for long-term success and impactful contributions to the field.

Prospective programs in wood science and renewable materials can thrive by proactively addressing these common challenges. Leveraging strengths such as stakeholder partnerships and faculty dedication, while planning strategically around enrollment, curriculum, and program infrastructure, will position new or evolving programs for long-term success and meaningful impact.

Future trends

SWST accreditation ensures the relevance and future-readiness of wood science and technology education by addressing contemporary issues such as sustainable development, bioeconomy, and technological advancements. As sustainability and bioeconomy gain importance, there is a growing demand for professionals skilled in materials science, industrial ecology, markets, biomaterials, bioenergy, regulatory policies, green building materials, and business management (Rice 2010). Programs are evolving to incorporate biomaterials, bioproducts, green materials, and biosystems engineering, while addressing environmental and ecological concerns. Recognizing wood's key role in bioeconomy, SWST has highlighted its significance in the building sector, which has one of the highest ecological footprints and the greatest potential for reducing climate impacts.

As for technological advancements, Industry 4.0 and the emerging Industry 5.0 technologies provide significant potential in the wood sector to extract relevant information and improve the management of the entire supply chain (Weiss et al. 2021). These optimization technologies are applied to material science such as wood-based materials, including wood modification, real-time monitoring of wood properties, and defect detection using sensor-based monitoring. The use of technology can optimize sawing and production processes (Molinaro and Orzes 2022). Furthermore, the integration of augmented reality in the harvesting process can help optimize the harvesting process and improve efficiency.

When adapting to changing demands, SWST accreditation standards will continue to require a fundamental understanding of wood as a material. SWST changed its guidelines in 2005 to what is termed "outcomes-based" assessment for programs. Under this approach, the program being accredited must show "demonstrated competencies" in specific areas. The challenges cited have resulted in several programs in the United States revamping their curricula (Rice 2010). A 2023 change to the standard allowed accreditation of MS-level programs, with the University of Guadalajara being the first to achieve MS degree accreditation. This change was partially motivated by a focus on the multiple MS programs across Europe. Accordingly, greater efforts will be placed on identifying potential institutions across Europe, and globally, with MS programs focused on wood.

Acknowledgments

The authors would like to thank Victoria L. Herian, former Executive Director of the Society of Wood Science and Technology, for providing valuable historical facts and information that were crucial to the preparation of this manuscript. The authors also gratefully acknowledge Universiti Teknologi MARA (UiTM) for its contribution to the publication of this manuscript.

References

Armstrong JA (2014) SWST: Advancing the profession internationally. Wood Fiber Sci 46(1):127–130. https://wfs.swst.org/index.php/wfs/article/view/382

Armstrong JP, Busto C, Barnes HM (2013) Education in wood science and technology: An update. Wood Fiber Sci 46(1):3–14. https://wfs.swst.org/index.php/wfs/article/view/1102

Armstrong J, Shmulsky R (2008). Accreditation: Elevating programs, the profession, and SWST. Wood Fiber Sci 40(4):481–483. https://wfs.swst.org/index.php/wfs/article/view/1343/1343

Barnes HM (1979). Education in wood science and technology: A status report. Wood Fiber Sci 10(4):243–258. https://wfs.swst.org/index.php/wfs/article/view/98

Cloutier A (2012) Adapting to change, responding to needs. Wood Fiber Sci 44(3):241– 242. https://wfs.swst.org/index.php/wfs/article/view/276

FAO-Food and Agriculture Organization of the United Nations (2024) The State of the World's Forests 2024 – Forest-sector innovations towards a more sustainable future. Rome. https://doi.org/10.4060/cd1211en

Gardner DJ, Kurjatko S, Kúdela J, Paule L (2005) The status of wood science education programs. Wood Fiber Sci 37(2):189–91. https://wfs.swst.org/index.php/wfs/article/view/296

Kaufert FH (1979) Accreditation and SWST. Wood Fiber Sci 10(4):239–240. https://wfs.swst.org/index.php/wfs/article/view/2085

Li Y, Mei B, Linhares-Juvenal T (2019). The economic contribution of the world's forest sector. Forest Policy Econ 100:236–253. https://doi.org/10.1016/j.forpol.2019.01.004

Molinaro M, Orzes G (2022). From forest to finished products: The contribution of Industry 4.0 technologies to the wood sector. Comput Ind 138:1–15. https://doi.org/10.1016/j.compind.2022.103637

Rice RW (2012) SWST Program accreditation: Our foundations, our past and our future. Wood Fiber Sci 44(1):1–4. https://wfs.swst.org/index.php/wfs/article/view/1231

Rice RW (2010) Wood science and technology program accreditation in the United States- history, guidelines, processes and changing demand. Proceedings of the International Convention of Society of Wood Science and Technology and United Nations Economic Commission for Europe – Timber Committee. 1–9.

Sandberg D, Niemz P (2025) From forestry schools to wood physics as a scientific discipline: a review of historical milestones and future directions of wood science. Holzforschung 79(11):582–602. https://doi.org/10.1515/hf-2025-0033

Shupe TF (2011) Rebranding wood science academic programs. Wood Fiber Sci 43(4):345. https://wfs.swst.org/index.php/wfs/article/view/872

Smith RL, Valverde PF (2019) The current and future state of wood science education in the United States. Wood Fiber Sci 51(2):221–230. https://doi.org/10.22382/wfs-2019-022

Society of Wood Science and Technology (2001). SWST Newsletter (May–June 2001). Society of Wood Science and Technology, Madison, WI.

Society of Wood Science and Technology (2025) Accreditation handbook: SWST Standards, procedures and guidelines for accrediting educational programs. Society of Wood Science and Technology, Monona, WI. https://www.swst.org/wp/wp-content/uploads/2023/08/Accreditation-Handbook-1-July-2023.pdf

United Nations General Assembly (2015) Transforming our world: The 2030 Agenda for Sustainable Development. https://sdgs.un.org/goals

Weiss G, Hansen E, Ludvig A, Nybakk E, Toppinen A (2021) Innovation governance in the forest sector: Reviewing concepts, trends and gaps. For Policy Econ 130:1–11. https://doi.org/10.1016/j.forpol.2021.102506

Experimental characterization of basic connection properties of Hinoki and Sugi

*Arijit Sinha**†
Professor & JELD-WEN Chair
Department of Wood Science & Engineering
Oregon State University, Corvallis, OR 97331
Email: Arijit.sinha@oregonstate.edu

Samuel Ayeni†
Graduate Research Assistant
Department of Wood Science & Engineering
Oregon State University, Corvallis, OR 97331
Email: samuel.ayeni@oregonstate.edu

Anthony Newton
Graduate Research Assistant
Department of Wood Science & Engineering
Oregon State University, Corvallis, OR 97331
Email: anthony.newton@oregonstate.edu

Yuichi Sato
Managing Director
Japan Lumber Inspection and Research Association, JLIRA
2-3-13 Kanda Ogawamachi,
Chiyoda-ku, Tokyo, 101-0052 JAPAN
sato@jlira.jp

Tyler Deboodt
Senior Faculty Research Assistant
Department of Wood Science & Engineering
Oregon State University, Corvallis, OR 97331
Email: tyler.deboodt@oregonstate.edu

Ian Morrell†
Assistant Professor
Department of Civil & Environmental Engineering
Tennessee Technological University, Cookeville, TN 38505
E-mail: imorrell@tntech.edu

(Received 11 November 2025)

Abstract: Hinoki (*Chamaecyparis obtusa*) and Sugi (*Cryptomeria japonica*) are two promising softwood species gaining attention beyond their traditional use in Japanese residential construction. Following the establishment of design values through in-grade testing and their inclusion in the American Wood Council (AWC) National Design Specification (NDS) Supplement, further evaluation of their connection performance is essential to increase the information about the two species of wood and support broader adoption, particularly in the U.S. construction market. This study characterized the connection performance of these species through a series of standardized tests: withdrawal resistance, lateral resistance, and dowel bearing strength. The objectives were to characterize the yield behavior, withdrawal capacity, and bearing strength of fasteners embedded in the species, and to evaluate the relevance of the predictive equations provided in the NDS for wood construction within the context of the experimental findings. The experimental results demonstrated species-specific differences in withdrawal and lateral resistance performance, with both species exhibiting consistent failure modes in agreement with NDS yield mode predictions, primarily modes IIIs and IV. Dowel bearing strength showed a similar trend to withdrawal behavior, with the species generally exhibiting higher bearing strength values that those predicted by current design equations. While the results were conservative, they indicate that designers can safely employ the current equations for connections in both Hinoki and Sugi. These findings contribute essential connection performance data to support the structural application of Hinoki and Sugi in mainstream construction.

Keywords: Connection performance; Dowel bearing strength; Withdrawal resistance; National Design Specification.

* Corresponding author
† Society of Wood Science & Technology member

Wood and Fiber Science, 58(2), 2026, pp. 107–116
https://doi.org/10.22382/wfs-2026-12

Introduction

In the United States, wood has long served as one of the most versatile building materials and the backbone of residential construction, where nearly all new single-family houses and low rise multifamily residential structures are constructed using wood framing and sheathing (McKeever 2009). The structural performance of wood combined with its environmental benefits, such as carbon sequestration, secure its place in modern sustainable building strategies. Timber structures can be prefabricated for on-site assembly or traditionally built in place using conventional framing methods and mechanical fasteners. As in all structural systems, the load-bearing capacity of timber constructions is usually governed by the capacity at the joints (Harte 2009).

Connections are central to the structural integrity of wood-based constructions. The performance of these connections determines the overall performance of the structure. The American Wood Council (AWC) National Design Specification (NDS) for wood construction (AWC 2024) prescribes methods to design dowel-type fasteners, including nails, bolts, and wood screws. A dowel-type fastener commonly undergoes two kinds of loading scenarios: one is dominated by lateral loading of connections and the other leads to withdrawal from the framing member. The NDS (AWC 2024), as well as the Forest Products Laboratory (FPL) Wood Handbook (FPL 2021), provide empirical equations for determining allowable withdrawal strength and fundamental methods for designing and evaluating dowel connections. They include design criteria such as yield mode equations and empirical relationships between dowel bearing strength, specific gravity (G), and the bending yield strength of common dowel-type fasteners. The underlying formulations are based on the European Yield Model (EYM), proposed by Johansen (1949), and were later incorporated into the NDS (AWC 2024). Studies have evaluated the lateral load carrying capacity, withdrawal and dowel bearing strength of common and novel wood-based building material to foster their use in structural applications (Miyamoto et al. 2020; Morris et al. 2018; Sinha and Avila 2014; Sinha and Miyamoto 2014; Zarnani and Quenneville 2014)

Hinoki, or Japanese cypress (*Chamaecyparis obtusa*), and Sugi, or Japanese cedar (*Cryptomeria japonica*), are being considered for construction application beyond Japan. Combined, the two species are the most planted coniferous species in Japan, with their production volume by tree species totaling 73.4% in 2022 (Annual Report on Forests and Forestry in Japan 2023). Both species have been utilized in residential construction, particularly for wall paneling and structural posts (Huang et al. 2021). Recently, they were approved by the American Lumber Standards Committee to be included in the National Design Specification supplement as per the Pacific Lumber Inspection Bureau (PLIB 2024). To expand their application potential, particularly in the United States construction market, additional evaluation of their structural performance is required. One such evaluation is to characterize connection behavior for these species.

The overarching goal of this study was to evaluate the connection properties of Hinoki and Sugi for use in U.S. wood construction. Although both species are currently recognized in U.S. building codes, existing research has largely focused on their fundamental mechanical properties, with little to no investigation on the performance of structural connections involving these species. This study aimed to address that gap by experimentally characterizing the performance of common wood connections fabricated using these species and evaluate how well the results correlate with predictive methods based on specific gravity, as applied in U.S. specifications and contexts. The specific objectives of this study were as follows:

1. Characterize dowel withdrawal from Hinoki and Sugi at the single-fastener level with common dowel connections.
2. Characterize the dowel bearing behavior of Hinoki and Sugi using a range of dowel sizes up to 25 mm.
3. Characterize the performance of Hinoki and Sugi single-fastener framing connection using a sheathing side member and common framing nails.
4. Determine failure modes and connection strength for both species using standardized methods, including ASTM D5764 Standard Test Method for Evaluating Dowel-Bearing Strength of Wood and Wood-Based Products (ASTM International 2024) and NDS-based methods (AWC 2024), to generate experimentally validated data supporting the reliable use of Hinoki and Sugi in U.S. structural design applications.

Materials and methods

Materials used in this study included Hinoki and Sugi lumber imported from Japan for a separate, larger research project. Specimens were fabricated from defect-free sections of panels previously tested in that project, with knots, splits, and other defects excluded. As per reporting from the Pacific Lumber Inspection Bureau (PLIB), the specific gravities of the two species are 0.45 (Hinoki) and 0.36 (Sugi) for design (PLIB

2024). Identical test procedures, fastener types, side material, and numbers of test repetitions were applied to both species (Table 1)

Withdrawal test

Fasteners used for withdrawal tests consisted of nails and screws: 8d common nail (64 mm × 3.3 mm), 16d box nail (89 mm ×x 3.4 mm), 20d common nail (101 mm × 5.16 mm), 16d ring-shank nail (89 mm × 4.11 mm), and #6 wood screw (50 mm × 2.7 mm). The withdrawal tests involved nails being pulled individually across the edge face of the specimen.

Withdrawal tests were carried out across a large specimen's edge face measuring 38 mm × 184 mm (2 × 8 inches) with the fastener installed in the 38 mm face of the wood section. As specified in ASTM D1761 Standard Test Methods for Mechanical Fasteners in Wood and Wood-Based Materials (ASTM International 2020), all fasteners were installed to a minimum depth of nine times the diameter. The wood screw was tested at this depth, while the nails, both smooth and ring-shank, were tested such that approximately 25 mm of the fastener was exposed above the wood. Testing was conducted using an Instron Universal Testing Machine (UTM) with a 100 kN capacity by applying a displacement-based loading protocol (Figure 1a). The moving crossarm of the UTM was connected to the nail head and raised at a constant rate of 2.54 mm/min, per ASTM D1761 (ASTM International 2020). Testing was stopped after the peak load was attained and the load subsequently declined.

Table 1. Test matrix for connection tests for Hinoki (*Chamaecyparis obtusa*) and Sugi (*Cryptomeria japonica*).

Test	Fastener	Side Material	Number of Tests
Withdrawal	8d common nail	N/A	36
	16d box nail	N/A	36
	20d common nail	N/A	36
	16d ring-shank nail	N/A	36
	#6 wood screw	N/A	36
Lateral resistance	8d common nail	12.5 mm (1/2") plywood	10
Dowel bearing	3.5 mm dowel parallel	N/A	10
	3.5 mm dowel perpendicular	N/A	10
	6 mm dowel parallel	N/A	10
	6 mm dowel perpendicular	N/A	10
	13 mm dowel parallel	N/A	10
	13 mm dowel perpendicular	N/A	10
	19 mm dowel parallel	N/A	10
	19 mm dowel perpendicular	N/A	10
	25 mm dowel parallel	N/A	10
	25 mm dowel perpendicular	N/A	10

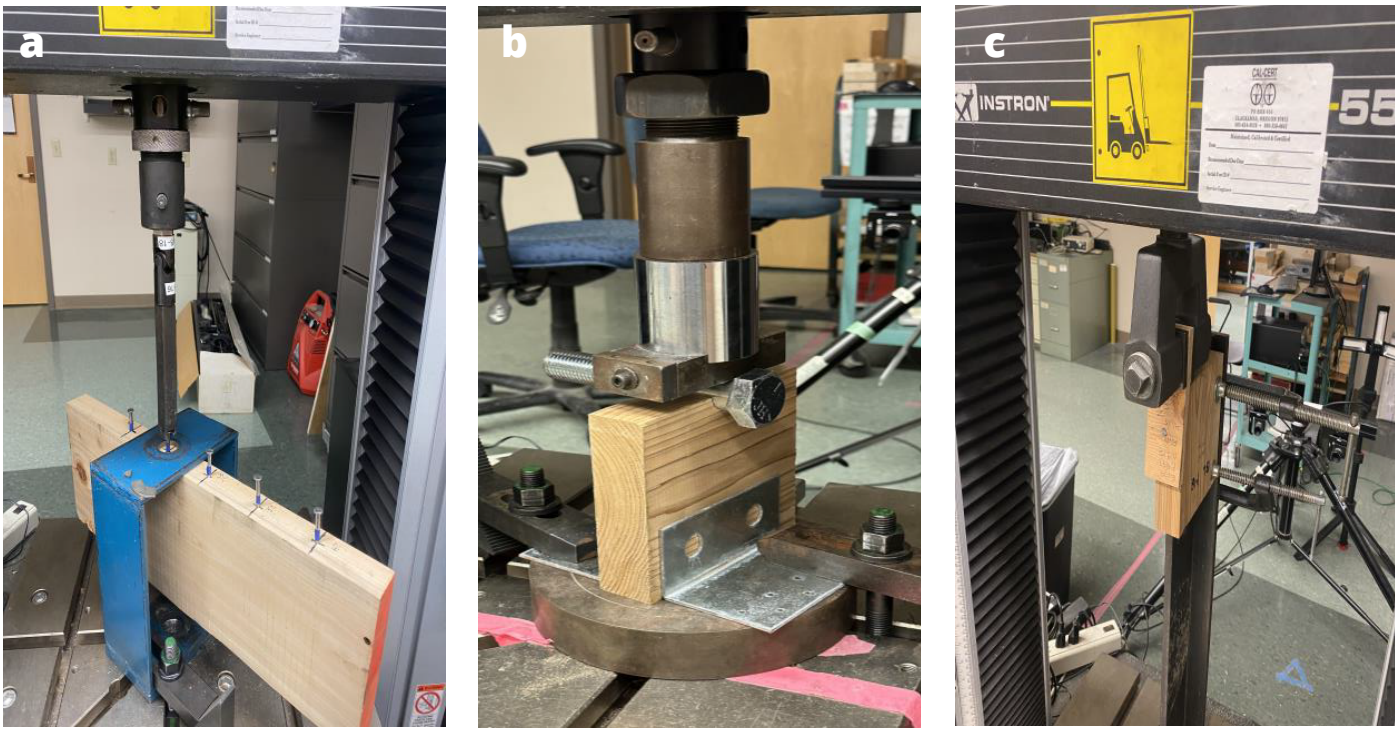

Figure 1. Connection tests set up (a) withdrawal; (b) dowel bearing; (c) lateral resistance.

The withdrawal strength (*WS*) was calculated using the expression per ASTM D5764 (ASTM International 2024).

$$WS = \frac{P_{peak}}{L} \quad [1]$$

where P_{peak} = max force observed in withdrawal test; and L = length of the nail that was embedded into the wood specimen.

Lateral resistance test

Lateral resistance tests were conducted by securing the lumber to the fixture and applying a transverse load to the fastener or member until failure. Sheathing used for lateral testing was derived from 12.5 mm plywood 2440 mm × 1220 mm sheets. The lateral resistance test specimens consisted of the defect-free sections of both Hinoki and Sugi species of 38 × 140 mm (2 × 6 inches) and a side member of 13 mm (1/2 inch) plywood. An 8d common nail was driven through the plywood side member into the narrow 38-mm wide face of the lumber. The nail was installed fully into both members, with care to avoid any overdriving into the plywood. This study closely follows ASTM D1761 (ASTM International 2020) to ensure comparability with existing data for North American wood species (Figure 2).

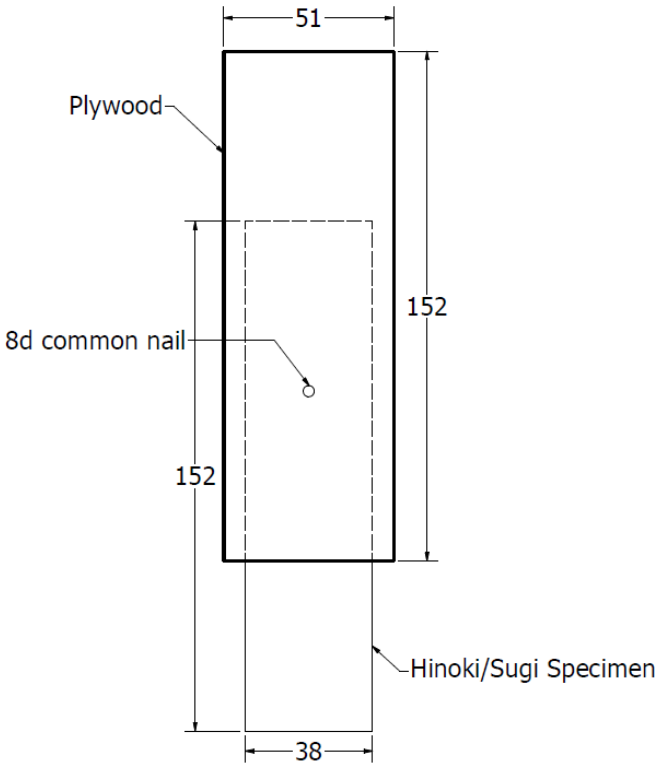

Figure 2. Schematic of lateral connection (dimensions in mm).

The tests were conducted using an Instron UTM with a 100 kN capacity by applying a displacement-based loading protocol (Figure 1b). The moving crossarm of the UTM was attached to the plywood side member and was raised at a constant rate of 2.54 mm/min, per ASTM D1761 (ASTM International 2020) until force resistance in lateral testing reached 80% of peak load. At this stage, testing was halted and the corresponding failure modes were documented.

The yield load is determined using the 5% offset method prescribed in the NDS (AWC 2024) as shown in Figure 3. In the 5% offset method, first the initial stiffness is determined as the slope of the linear portion of the load deflection profile. That slope is offset by 5% of the dowel diameter on the x-axis. The yield point is then defined as the intersection between the offset line and the test data.

Dowel bearing test

Dowel bearing strength was determined following ASTM D5764 using the half-hole method (ASTM International 2024). Due to the orthotropic nature of wood, the dowel strength can differ with respect to the grain direction. As such, tests were conducted with the dowel bearing both parallel and perpendicular to the grain direction for dowel diameters of 3.5 mm, 6 mm, 13 mm, 19 mm, and 25 mm. All specimens were prepared in accordance with geometric guidelines outlined in ASTM D5764.

Dowel bearing tests were conducted using the previously mentioned UTM (Figure 1c). Each specimen was prepared from clear lumber sections with a half-hole routed into the edge that was of equal diameter to the dowel for that test series. The crossarm of the UTM compressed the dowel into the half-hole at a rate of 1 mm/min, per ASTM D5764 (ASTM International 2024). Testing was concluded when the dowel became fully

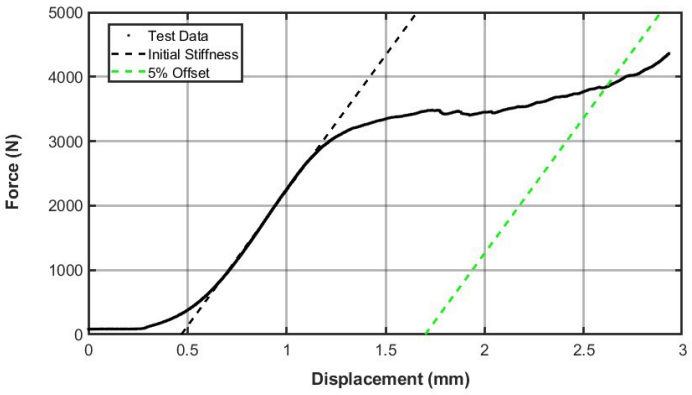

Figure 3. Graphical depiction of 5% offset method used for both lateral resistance and dowel bearing.

embedded within the wood specimen. This stage was identified by the onset of a second region of approximately constant stiffness in the force–displacement response, as illustrated in Figure 3. Dowel bearing (DB) strength was calculated using the 5% offset method, following ASTM D5764 (ASTM International 2024).

$$DB = \frac{F_{yield}}{DL} \quad [2]$$

where *DB* is the dowel-bearing strength (MPa); F_{yield} = yield load (N) determined at the point at which the 5% offset line intersects with the experimental data; *D* = diameter (mm) of the dowel; and *L* = length (mm) of the specimen (ASTM International 2024).

Predictions based on NDS equations

The equations and parameters used to calculate yield performance for each mode are presented in the National Design Specification developed by AWC's Wood Design Standard Committee (AWC 2024), based on the EYM. The yield performance of both Hinoki and Sugi connections were estimated using the six yield modes presented in Table 12.3.1A of the NDS (AWC 2024), with each mode corresponding to specific components of the connection undergoing deformation. To calculate yield strength and identify yield modes, several input parameters are required. These include the geometry of the main (framing) and side (sheathing members), the geometry and material properties of the dowel, the dowel bearing strengths of both main and side members, and the geometry of the connection. All six yield modes are analyzed, and failure is anticipated to occur following whichever yield mode is calculated with the lowest value. This critical mode and associated load are the predicted yield mode and strength.

Results and discussion

Withdrawal

Hinoki

Fastener withdrawal resistance of Hinoki was determined using the peak force from testing (Table 2). These values were determined on a per embedment length basis and were compared to equations using the geometry and type of dowel fastener and the proposed specific gravity of Hinoki (0.44). Experimentally determined withdrawal resistance of Hinoki was compared with the NDS withdrawal design values given on Table 12.2D of the NDS (AWC 2024). For 8d and 16d box nails, the average withdrawal capacities for Hinoki were 34.7 N/mm and (coefficient of variation [COV] = 21.8%) and 24.3 N/mm (coefficient of variation [COV] = 17.8%), respectively. Corresponding values predicted by the NDS equation were 23.3 N/mm and 23.8 N/mm, respectively. For 20d common nails and 16d ring-shank nails, the average withdrawal resistance was 29.2 N/mm (coefficient of variation [COV] = 21.8%) and 69.8 N/mm (coefficient of variation [COV] = 10.6%), respectively, while the NDS equation predicted 33.3 N/mm and 54.7 N/mm, respectively. In comparison, studies have reported average nail withdrawal capacities of 26.78 N/mm for juniper wood (Morris et al. 2018) and 28.75 N/mm for Douglas-fir (Wang et al. 2011). For wood screws, the average withdrawal resistance was 92.7 N/mm (coefficient of variation [COV] = 8.2%), whereas the NDS equation predicted a withdrawal capacity of 73.3 N/mm (AWC 2024). As shown in Table 2, the predicted values for both nails and wood screws were in close agreement with the observed values.

Sugi

Fastener withdrawal resistance of Sugi was determined using the peak force from testing and is presented in Table 3. These values were determined on a per embedment length basis and were compared to equations using the geometry and type of dowel fastener and the specific gravity of 0.36. The withdrawal strength comparison between experiment results and predictions derived from NDS equation can be seen in Table 3. The experimentally determined withdrawal resistance of fasteners in Sugi was compared with the NDS withdrawal design values presented in Table 12.2D of the NDS (AWC 2024). For 8d and 16d box nails, average withdrawal capacities of 13.6 N/mm (COV = 33%) and 11.6 N/mm (COV = 20.4%) were measured, respectively, while the corresponding NDS predictions were

Table 2. Hinoki withdrawal summary.

Fastener Type	Avg. withdrawal resistance (N/mm)	COV (%)	NDS predicted values (N/mm)
8d box nail	34.7	21.8	23.3
16d box nail	24.3	17.8	23.8
20d common nail	29.2	21.8	33.3
16d ring-shank nail	69.8	10.6	54.7
#6 wood screws	92.7	8.2	73.3

Table 3. Sugi withdrawal summary.

Fastener Type	Avg. withdrawal resistance (N/mm)	COV (%)	NDS predicted values (N/mm)
8d box nail	13.6	33	13.8
16d box nail	11.6	20.4	13.6
20d common nail	14.4	20.6	16.8
16d ring-shank nail	40.0	10.3	26.5
#6 wood screw	54.3	8.1	45.9

13.8 N/mm and 13.6 N/mm, respectively (AWC 2024). Average withdrawal resistances for 20d common nails and 16d ring-shank nails were 14.4N/mm (COV = 16.8%) and 40.0 N/mm (COV = 26.5%), respectively, compared with NDS-predicted values of 16.8 N/mm and 26.5 N/mm, respectively. The values observed in this study are comparable to the average withdrawal resistance of 16.03 N/mm reported for hybrid poplar by Sinha and Avila (2014) and 14.2 N/mm reported by OWIC (2011). Wood screws exhibited an average withdrawal resistance of 54.3 N/mm (COV = 8.1%), whereas the NDS equation predicted a withdrawal capacity of 45.9 N/mm (AWC 2024). Overall, as summarized in Table 3, the NDS-predicted values (AWC 2024) were in reasonable agreement with the experimentally measured withdrawal resistance for Sugi, with close agreement for most fasteners and more conservative estimates observed for the 16d ring-shank nails and wood screws.

Dowel bearing

Dowel bearing (Hinoki)

A summary of results and associated COVs from the dowel bearing tests for Hinoki (at an average specific gravity of 0.44) in the parallel and perpendicular direction are presented in Table 4. The dowel bearing tests were analyzed using the 5% offset method to determine the dowel bearing strength. The dowel bearing strength showed a similar trend to the previous withdrawal results, with the Hinoki typically exhibiting higher dowel bearing values than those predicted by equations from the NDS (AWC 2024), as shown in Figure 4. Strengths parallel to grain tend to be greater than those perpendicular; this is a common trend because of the anatomy of wood.

The results for dowel bearing between 6 mm and 25 mm in the parallel direction aligned well with the values from the empiric equations, with in total a 3% difference between the experimental and analytical results. Tests completed with 3.5 mm diameter dowels did not show a difference of 60%. These results were unexpected due to previous models suggesting that the direction is insignificant at small dowel sizes. The larger dowel (6-25 mm) bearing strength diverged for the perpendicular direction, with smaller diameter fasteners aligning well with the equation and diverging as diameter increased. The dowel bearing strength observed for Hinoki was comparable to the dowel bearing strength of Douglas-fir (37.12 MPa) reported by Kent et al. (2004). While the results for this were conservative, this would suggest that a designer could safely design connections in Hinoki using the current equations.

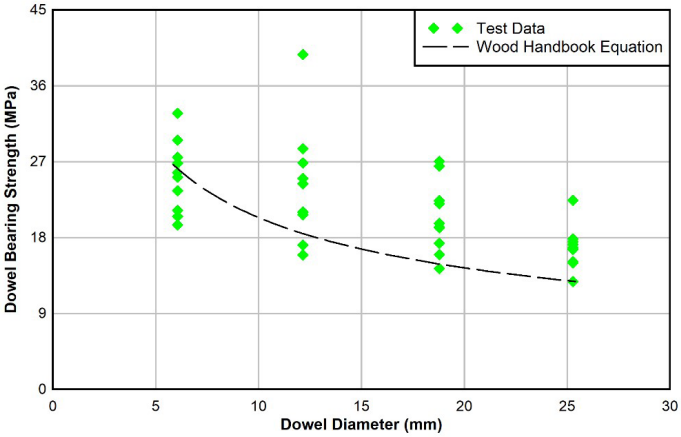

Figure 4. Variation in dowel bearing results of Hinoki perpendicular to grain with overlaid line of empirical Wood Handbook equation.

Dowel bearing (Sugi)

The dowel bearing tests were analyzed using the 5% offset method to determine the dowel bearing strength and are presented in Table 5. The dowel bearing strength showed a similar

Table 4. Hinoki dowel bearing strength experimental and Wood Handbook model data (FPL 2021).

Grain direction	Dowel diameter (mm)	Nominal diameter (mm)	Dowel bearing (MPa)	COV (%)	NDS equation (MPa)	Percent difference (%)
Parallel	3.5	3.5	27.21	12.2	25.27	7.68
Perpendicular	3.5	3.5	43.86	17.8	25.27	73.58
Both	All		35.54	15	25.27	40.63
Parallel	6.1	6.4	34.43	15.9	33.98	1.35
	12.2	12.7	34.23	37.7	33.98	0.74
	18.8	19.1	33.75	22.4	33.98	-0.67
	25.3	25.4	37.89	12.8	33.98	11.53
	All		35.08	23.3	33.98	3.24
Perpendicular	6.1	6.4	25.23	16.5	25.60	-3.68
	12.2	12.7	24.03	28.3	18.49	29.95
	18.8	19.1	20.37	20.5	14.87	36.94
	25.3	25.4	16.8	14.8	12.82	31.02

trend to the previous withdrawal results, with the Sugi typically exhibiting higher dowel bearing values than those suggested by equations from the NDS (AWC 2024). This is illustrated in Figure 5 for different dowel diameters tested.

The 3.5 mm dowel bearing tests revealed a distinct difference in strength between the parallel and perpendicular grain directions, despite the governing equation not accounting for grain orientation at this diameter. The average experimental values in both directions exceeded the predicted value. For dowel sizes between 6 mm and 25 mm loaded parallel to grain, experimental results closely matched the empirical equation, with only a 3% overall difference. However, in the perpendicular direction, agreement with the equation decreased as dowel diameter increased. Smaller dowels aligned well, but larger dowels diverged, as seen in Figure 7. This indicates that the current equations tend to underestimate bearing strength at larger diameters. While conservative, these results suggest that designers can safely use the existing equations for Sugi connections.

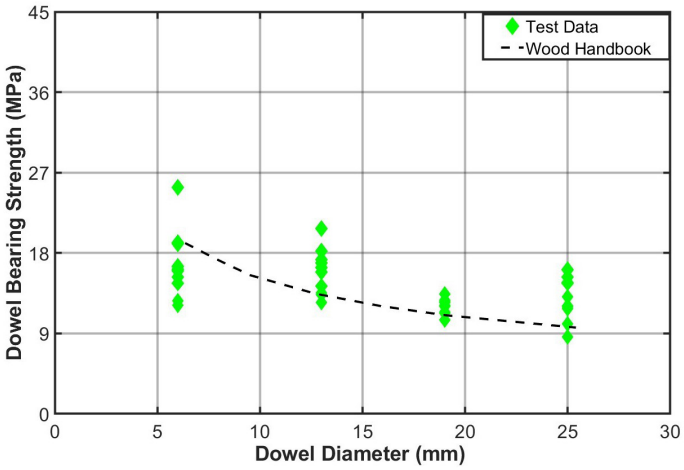

Figure 5. Variation in dowel bearing results of Sugi perpendicular to grain with overlaid line of empirical Wood Handbook equation

Lateral resistance

For both Hinoki and Sugi, the lateral resistance tests exhibited fairly consistent results, as summarized in Table 6. Yield strength and displacement at yield were determined using the 5% offset method, while stiffness was obtained from the initial linear portion of the load-displacement curves for Hinoki and Sugi, shown in Figure 6 and 7, respectively. The ultimate strength obtained from the load-displacement curve represents the maximum load that a connection can withstand prior to failure. However, the design of connections is based on the yield strength criterion (Sinha and Miyamoto 2014). The yield strength observed for Hinoki was higher than that

Table 5. Sugi dowel bearing strength experimental and Wood Handbook empiric model data (FPL 2021).

Grain direction	Dowel diameter (mm)	Nominal diameter (mm)	Dowel bearing (MPa)	COV (%)	NDS equation (MPa)	Percent difference (%)
Parallel	3.5	3.5	31.98	16.9	17.5	103.39
Perpendicular	3.5	3.5	18.22	20.7	17.5	15.90
Both	All		25.10	18.8	17.5	59.65
Parallel	6.2	6.4	29.14	21.4	27.8	11.00
	12.2	12.7	32.11	12.3	27.8	22.28
	18.7	19.1	32.11	16.2	27.8	22.28
	25.3	25.4	28.65	15.5	27.8	9.14
	All		30.50	16.35	27.8	16.18
Perpendicular	6.2	6.4	16.69	21.7	19.12	-6.52
	12.2	12.7	15.89	15.2	13.5	25.37
	18.7	19.1	12.26	6.5	11.0	19.63
	25.3	25.4	12.83	17.7	9.6	45.48

Table 6. Experimental lateral resistance results of Hinoki and Sugi with an 8d common nail and 12.5 mm plywood side member.

Species	Property	Yield strength (N)	Displacement at yield (mm)	Stiffness (N/mm)	Ultimate strength (N)	Displacement at ultimate (mm)
Hinoki	Mean	725.6	0.39	3159.5	2334.7	16.03
	COV (%)	17	22.1	58.4	7	17
Sugi	Mean	666	0.97	971.9	1165.7	12.0
	COV (%)	10.6	25.9	45.4	16.8	67.3

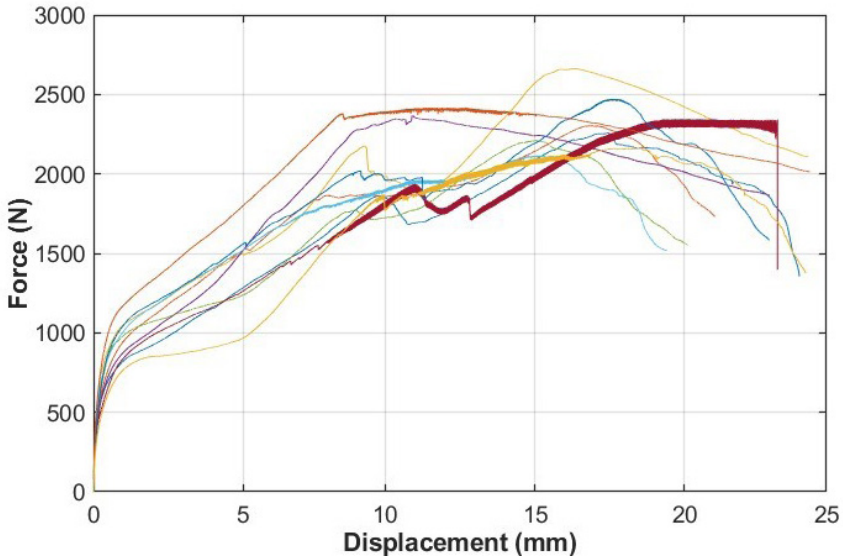

Figure 6. Load-displacement curve (Hinoki lateral test).

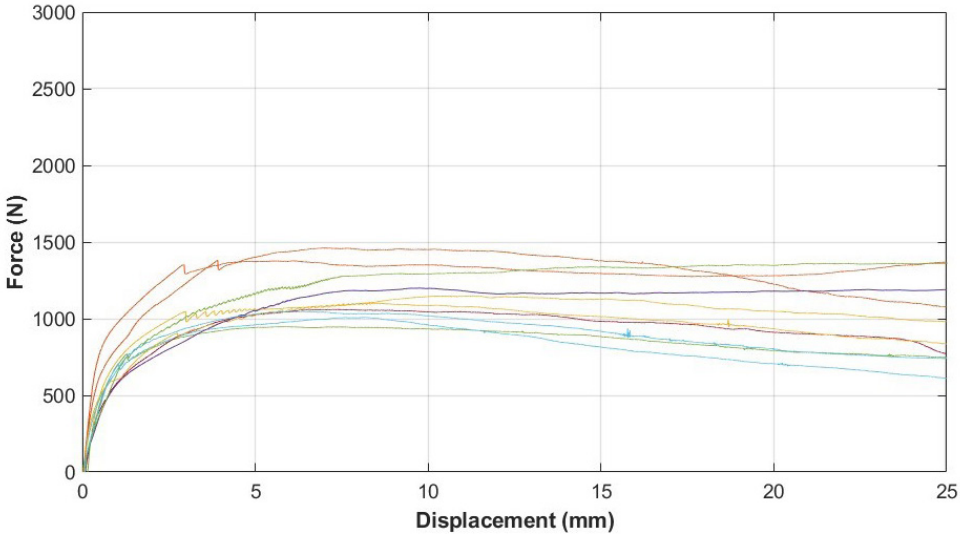

Figure 7. Load-displacement curves (Sugi lateral test).

of Sugi, which may be attributed to Hinoki's greater density and its influence on the embedment strength of the material surrounding the fastener (Huang et al. 2021). The coefficients of variation (COVs) observed in this study were relatively low for Hinoki (10.6%) and moderate for Sugi (17%). By comparison, similar level of variability has been reported in past studies, with COV in the range of 16% to 21% (Sinha et al. 2011; Sinha and Avila 2014) and values of 17% to 28% (Kent et al. 2004). Higher variability has also been documented, including COVs of 22% to 34% (Morris et al. (2018).

Design value predictions based on NDS

Table 7 presents the average experimental yield strengths, failure modes, and coefficient of variation for Hinoki and Sugi. This allowed meaningful comparison between the experimental results and the values predicted by the dowel bearing and NDS equations (AWC 2024). Observed yield strength was dictated by the 5% offset in testing. Both the dowel bearing and the NDS prediction are derived using the equation presented in Table 12.3.1A of the NDS Publication for Wood Construction, which as previously noted, is based on the European Yield

Table 7. Predictions using National Design Specification (AWC 2024) yield models for Hinoki and Sugi (N).

Yield strength predictions	Observed			Dowel bearing			NDS prediction		
Species	Yield strength	Yield mode	COV	Yield strength	Yield mode	Design index	Yield strength	Yield mode	Design index
Hinoki	726	IIIs, IV	17	727	IIIs	1.00	681	IIIs	1.07
Sugi	666	IIIs, IV	10	673	IIIs	0.99	613	IIIs	1.09

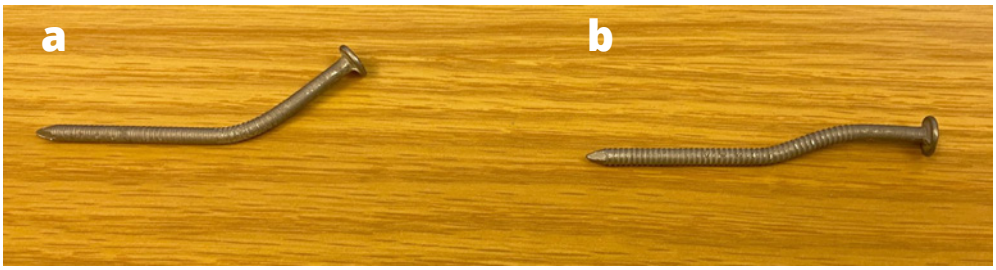

Figure 8. Yield modes observed. (a) Mode IIIs; (b) Mode IV.

Model (Johansen 1949). The values used are either the NDS-predicted values, corresponding to the dowel diameter, or the experimentally determined values from the dowel bearing tests.

To quantify the predictive accuracy, a design index, defined as the ratio of observed to predicted yield load, was employed. A design index greater than 1.0 indicates conservative or under-prediction, while values less than 1.0 suggest overestimation. For Hinoki, the design index was 1.00 for the dowel bearing model and 1.07 for the NDS model (Table 7), indicating that both approaches provided conservative estimates of connection strength. Similarly, Sugi exhibited design index of 0.99 and 1.09 for the dowel and NDS models, respectively, further confirming that both models yielded safe and conservative predictions

Previous studies by Sinha and Avila (2014) and Morris et al (2018) have reported strong agreement between NDS predictions and experimental results for various wood species, and the present findings align with these observations, demonstrating comparable agreement for Hinoki. This suggests that the NDS model offers a reasonable approximation of yield strength for common nail connections involving Hinoki and a typical sheathing material.

In addition to predicting the yield strength, the NDS yield model also identifies expected failure modes. For both Hinoki and Sugi, the predominant observed yield modes were IIIs and IV. According to NDS definitions (AWC 2024), mode IIIs corresponds to plastic hinging of the fastener within the main (framing) member, while mode IV involves bending of the fastener across both the framing and sheathing members, accompanied by the formation of plastic hinges at characteristic locations along the dowel (Figure 8).

The predicted and observed yield modes were consistent for both Hinoki and Sugi. Mode IIIs and IVs were the predominant failure modes observed experimentally, while the EYM predicted mode IIIs for both species. The occurrence of mode IV in some cases may be attributed to factors such as the presence of knots or manufacturing imperfections. Overall, the findings suggest that the model provides a reliable prediction of both yielding modes, and to a reasonable extent, the yield load for connections involving Hinoki and Sugi.

Conclusion

This study evaluated the performance of Hinoki and Sugi in dowel-type connections through withdrawal tests, dowel-bearing strength measurements, and laterally loaded connection tests with standard sheathing materials.

Experimental withdrawal tests characterized the behavior of both species, demonstrating generally higher resistance than predicted by NDS-based equations and confirming the practical reliability of these species at the single-fastener level. Dowel bearing tests revealed that parallel-to-grain loading aligned well with predictions, whereas perpendicular-to-grain loading showed higher strength for larger dowels, suggesting that current equations may underestimate bearing capacity in some cases.

Design indices confirmed that the models provided conservative and safe estimates of connection strength for both species. Predicted and observed yield modes were consistent, with experimental behavior reflecting expected failure mechanisms. Collectively, these experimentally validated results support the reliable use of Hinoki and Sugi in U.S. structural design practices and provide guidance for the design of wood connections using these species.

Acknowledgement

Financial support from JLIRA is greatly appreciated.

References

Annual Report on Forests and Forestry in Japan (2023). Annual Report Group. Policy Planning Division, Forest Policy Planning Department, Forestry Agency. Ministry of Agriculture, Forestry, and Fisheries (MAFF). 1-2-1 Kasumigaseki, Chiyoda-ku, Tokyo 100-8952, Japan. https://www.contactus.maff.go.jp/rinya/form/rinsei/inquiry_rinya_160801.html

ASTM International (2020) ASTM D1761-20: Standard Test Methods for Mechanical Fasteners in Wood and Wood-Based Materials. American Society for Testing and Materials, West Conshohocken, PA, USA. https://doi.org/10.1520/D1761-20

ASTM International (2024) ASTM D5764-24: Standard Test Method for Evaluating Dowel-Bearing Strength of Wood and Wood-Based Products. American Society for Testing and Materials, West Conshohocken, PA, USA. https://doi.org/10.1520/D5764-24

AWC-American Wood Council (2024) National Design Specification for Wood Construction. AWC. Leesburg, VA. https://awc.org/resources/2024-nds/

FPL-Forest Products Laboratory (2021) Wood Handbook—Wood as an engineering material. General Technical Report FPL-GTR-282. USDA Forest Service, Forest Products Laboratory, Madison, WI. https://research.fs.usda.gov/treesearch/62200

Harte AM (2009) Introduction to timber as an engineering material. In ICE Manual of Construction Materials, pp. 1–9. Institution of Civil Engineers, UK. DOI:10.1680/mocm.00000.0001 https://www.universityofgalway.ie/media/timberengineeringresearchgroup/Harte---2009---Introduction-to-timber-as-an-engineering-material.pdf

Huang R, Fujimoto N, Sakagami H, Feng S (2021) Sandwich compression of Sugi (*Cryptomeria japonica*) and Hinoki (*Chamaecyparis obtusa*) wood: Density distribution, surface hardness and their controllability. J Wood Sci 67(1):43. https://doi.org/10.1186/s10086-021-01970-y

Johansen KW (1949) "Theory of Timber Connections." International Association for Bridge and Structural Engineering, 9: 249–262.

Kent SM, Leichti RJ, Rosowsky DV, Morrell JJ (2004) Effect of wood decay by *Postia placenta* on the lateral capacity of nailed oriented strandboard sheathing and Douglas-fir framing members. Wood Fiber Sci 36(4):560–572.

McKeever DB (2009) Estimated annual timber products consumption in major end uses in the United States, 1950-2006 (FPL-GTR-181; p. FPL-GTR-181). USDA Forest Service, Forest Products Laboratory, Madison, WI. https://doi.org/10.2737/FPL-GTR-181

Miyamoto BT, Sinha A, Morrell, I (2020) Connection performance of mass plywood panels. For Prod J 70(1):88–99. https://doi.org/10.13073/FPJ-D-19-00056

Morris H, Sinha A, Miyamoto BT (2018) Technical note: Lateral connections and withdrawal capacity of western juniper. Wood Fib Sci 50(1):96–103. https://doi.org/10.22382/wfs-2018-010

OWIC (2011) Properties of hybrid poplar. Oregon Wood Innovation Center report, Corvallis, OR.

PLIB-Pacific Lumber Inspection Bureau (2024) Standard Grading Rules for West Coast and Imported Softwood Lumber. Publication no. 18. PLIB, Federal Way, WA. USA

Sinha A, Avila DG (2014) Lateral load-carrying connection properties and withdrawal capacity of hybrid poplar. Wood Fiber Sci 46(1):97–108. https://wfs.swst.org/index.php/wfs/article/view/835

Sinha A, Miyamoto BT (2014) Lateral load carrying capacity of laminated bamboo lumber and oriented strand board connections. J Mater Civ Eng 26(4):741–747. https://doi.org/10.1061/(ASCE)MT.1943-5533.0000848

Wang Y, Wen-ching S, Kasemsiri P, Hiziroglu S (2011) A comparison of the withdrawal resistance load of nails using experimental and interference approaches. Wood Mater Sci Eng 6(4):213–218. https://doi.org/10.1080/17480272.2011.619279

Zarnani P, Quenneville P (2014) Wood Load-Carrying Capacity of Timber Connections: An Extended Application for Nails and Screws. In S Aicher, H-W Reinhardt, H Garrecht (eds.), Materials and Joints in Timber Structures (RILEM Bookseries vol. 9, pp. 167–179). Springer, Dordrecht, Netherlands. https://doi.org/10.1007/978-94-007-7811-5_16

In situ biomineralization of metal phytates in wood for improved bio-durability and flame retardancy

Aynun Nishat Farhabi
Graduate Research Assistant
Warnell School of Forestry and Natural Resources
University of Georgia, Athens, GA
Email: af14314@uga.edu

Liang Liang
Graduate Research Assistant
Department of Forest, Rangeland and Fire Sciences
University of Idaho, Moscow, ID
Email: lliang@uidaho.edu

Lili Cai *†
Associate Professor of Forest Biomaterials
Warnell School of Forestry and Natural Resources
University of Georgia, Athens, GA
Email: lcai@uga.edu

(Received 17 December 2025)

Abstract: This study investigated the in-situ biomineralization of metal phytate in wood to improve the antifungal and flame-retardant properties. Pine and aspen wood were impregnated with phytic acid and metal chlorides (copper, aluminum, and iron) via two treatment pathways. Path-1 involved treating wood with metal chlorides followed by phytic acid, while Path-2 involved the reverse order. Mass gain and accelerated leaching tests were performed to assess the treatment retention, followed by soil-block decay testing against four wood-decaying fungi and fire-related assessments on aspen via thermogravimetric analysis (TGA) and mass loss calorimeter (MLC) test. Path-2 resulted in significantly higher initial mass gain than Path-1, but experienced more substantial mass loss during leaching, indicating weaker fixation of PA-derived components. Before leaching, most treated samples exhibited improved decay resistance, with mass loss values below 10%. However, decay resistance decreased after leaching, indicating the importance of fixation stability for long-term durability. TGA showed that treated samples before leaching exhibited earlier thermal degradation and higher residual char yield than controls, while MLC measurements revealed reduced peak heat release rate, total heat release, and fire growth index, as well as higher char residue. Importantly, these flame-retardant properties were largely retained even after leaching. Overall, these results indicate that in situ metal–phytate formation can provide measurable improvements in fire performance, while fungal protection remains dependent on treatment retention. Further optimization of fixation chemistry is recommended to achieve more durable, bio-based wood protection.

Keywords: Metal phytate; Mineralization; Fungal resistance; Flame retardancy; Biobased wood protection.

Introduction

Wood is a widely available, renewable, and biodegradable construction material with excellent structural performance, favorable strength-to-weight ratio, and low environmental footprint (Zhu et al. 2016; Berglund and Burgert 2018; Jia et al. 2019). However, its hygroscopic nature and abundance of nutrient-rich polysaccharides make it highly susceptible to biological degradation by fungi (Råberg et al. 2005). Additionally, wood's inherent flammability limits its safe use in modern infrastructure without proper protective treatments. Therefore, enhancing both the bio-durability and fire resistance of wood remains critical for broadening its safe and sustainable applications.

Halogen-based flame retardants (chlorinated and brominated formulations) have historically been effective at improving fire resistance through radical-quenching mechanisms (Liang et al. 2013; Zhang et al. 2017). However, their combustion can generate toxic gases and persistent pollutants, raising serious health and environmental concerns (Venier et al. 2015; Kovačević et al. 2021; Ilyas et al. 2021). This has accelerated the shift toward halogen-free and bio-derived flame-retardant systems (Costes et al. 2017; Liang et al. 2023).

* Corresponding author
† Society of Wood Science & Technology member

Phytic acid (PA), a natural myo-inositol hexakisphosphate abundant in seeds and grains, contains six phosphate groups and exhibits high phosphorus content (~28 wt%) (Lott1 et al. 2000; Viveros et al. 2000; Loewus 2001; Costes et al. 2017; Gänzle 2020). PA is recognized as a promising bio-based, halogen-free flame retardant due to its strong dehydration and char-forming capability (Guo et al. 2019). PA also has strong metal-chelating ability, enabling the formation of metal phytates, which are thermally stable salts capable of improving char structure and reducing flammable volatiles (Kremer et al. 2020; Zhang et al. 2022). Prior studies demonstrate that PA or metal phytates can improve fire performance and even inhibit fungal growth in some cases (Wang et al. 2022; Liang et al. 2024).

The fire performance of wood products was further improved, especially when synergized with chitosan (Zhao et al. 2020; Yang and Zhang 2022), protein (Li et al. 2021), urea (Antoun et al. 2022), uracil (Zhang et al. 2021), silica (Chen et al. 2021; Lin et al. 2023), polyelectrolyte complexes (Soula et al. 2021) and other chemical formulations reported in recent studies (Zhao et al. 2020; Tang and Fu 2020; Zhou and Fu 2020; Song et al. 2022; Tian et al. 2023). For example, Zhang et al. (2022) reported that metal-phytate-treated wood exhibited substantial smoke-suppression and flame-inhibition effects, achieving a 44.8% reduction in total heat release (THR) and a 92.0% reduction in total smoke production (TSP) compared with untreated wood. In another investigation, Zhang et al. (2023) found that a modest ~13.5% weight gain of copper phytate on the cell wall led to a 74.2% decrease in fire growth index, 85.4% lower smoke production, and a 33.3% decline in CO generation. Furthermore, Fan et al. (2024) demonstrated that applying phytic acid and zinc phytate to delignified wood via vacuum-pressure impregnation significantly enhanced the flame retardancy of Chinese fir, reducing THR from 55.66 MJ/m² to 5.90 MJ/m² and rapidly forming a compact, carbonized barrier. These improvements have been attributed to the synergistic dual-charring role of phosphorus and metal species, combined with the catalytic graphitization promoted by multivalent metal ions.

However, current research has primarily focused on fire performance, while the bio-durability of metal-phytate-treated wood, especially after leaching, remains insufficiently explored. This knowledge gap is crucial because water solubility and fixability strongly affect long-term performance in real-world environments. Additionally, in-situ biomineralization of metal phytates within the wood matrix is particularly advantageous, as it is hypothesized to facilitate mineral formation within cell walls and lumens, rather than solely on the surface. This internal precipitation is expected to enhance the fixation of phosphorus-metal species, minimize leaching, and produce a compact char layer during combustion, unlike surface-applied coatings or post-impregnation treatments. Furthermore, the sequence of chemical application may influence how phytates form and distribute within the wood structure, potentially altering fixation efficiency and overall protective behavior. Nevertheless, this has not been systematically investigated.

Inspired by recent phytate-based studies and existing knowledge gaps, this study uses three different metallic salts, namely, copper chloride, aluminum chloride, and ferric chloride, along with phytic acid, to generate metal phytates in-situ within samples of loblolly pine (*Pinus taeda* L.) and bigtooth aspen (*Populus grandidentata*) sapwood through a simple two-step impregnation process. Two different treatment pathways were designed to mimic different orders of phytate formation in wood. Path-1 involved treating wood with metal chlorides followed by phytic acid, while Path-2 involved the reverse order. The chloride salts of Cu^{2+}, Al^{3+}, and Fe^{3+} were selected for their high-water solubility, pronounced Lewis acidity, and facile dissociation, representing both divalent and trivalent systems. These characteristics allow a systematic assessment of how cation charge density and coordination behavior influence in-situ precipitation and localization of metal-phytate complexes within the wood structure. Additionally, due to differences in ion charge and stereochemistry, the sequence of addition may influence where solid metal-phytate deposits within wood, thereby affecting the distribution, depth of the deposit, and fixation efficiency.

Previous metal phytate/wood studies have demonstrated that several different metal species can be incorporated into wood to achieve excellent flame retardancy and smoke suppression, often within a single wood substrate and a fixed impregnation sequence. In contrast, the present study systematically compares three PA-based metal systems, two formation pathways (metal-PA vs. PA-metal), and two wood species (a softwood, loblolly pine, and a hardwood, bigtooth aspen) within one experimental matrix, while simultaneously assessing the leaching properties, fungal durability, and fire-retardant performance. These features allow us to examine how metal valence, solution acidity, and reagent sequence collectively influence in-situ formation and fixation of metal phytate complexes in wood, as reflected by mass gain, accelerated leaching test, decay resistance test, thermal stability, and mass loss calorimeter (MLC) test results.

Materials and method

Materials

PA solution (PA, $C_6H_{18}O_{24}P_6$, ca. 50% in water, ca. 1.1 mol/L, TCI, MW 660.03 g/mol), and three metal chlorides (denoted as M-Cl), including copper (II) chloride dihydrate ($CuCl_2 \cdot 2H_2O$, 99%, MW 170.48 g/mol), aluminum chloride hexahydrate ($AlCl_3 \cdot 6H_2O$, 99%, MW 241.43 g/mol), and iron (III) chloride anhydrous ($FeCl_3$, 98%, MW 162.21 g/mol) were purchased from Thermo Fisher Scientific Company, LLC (Waltham, MA, USA). These chemicals were diluted with deionized (DI) water into a PA solution of 0.0758 M and M-Cl solutions of 0.5 M at room conditions. The pH of all the treatment solutions is shown in Table 1.

Two brown-rot fungi, *Gloeophyllum trabeum* (Madison 617/ATCC 11539; *G.t.*), and *Rhodonia placenta* (Fr.) (ATCC#11538, *R.p.*), and two white-rot fungi, *Trametes versicolor* (*Linnaeus: Fries*) *Lloyd*, (ATCC#42462, *T.v.*), and *Irpex lacteus* (*Fr.*) Fr. (ATCC#11245, *I.l.*) were obtained from ATCC and used in the decay test.

Sapwood of the softwood, loblolly pine (525 ± 32 kg/m^3), and the hardwood, bigtooth aspen (509 ± 9 kg/m^3), were cut into wafers measuring 18 mm × 18 mm × 5 mm (R × T × L) for fungal decay tests according to American Wood Protection Association (AWPA) standard E22-22 (AWPA 2022). Aspen blocks with dimensions of 100 mm × 100 mm × 10 mm (L × T × R) were further prepared for the fire performance test. All wood samples were conditioned at 60°C for 48 h or until constant weight was reached before treatment.

Wood samples treatments

The wood samples were treated with two treatment solutions, M-Cl solution (0.5 M) and PA solution (0.0758 M), sequentially or in the reverse order, which were referred to as Path-1 when the M-Cl solution was first impregnated and Path-2 when the PA solution was first impregnated, as shown in Table 1. For example, the wood samples that underwent treatment Path-1 were labeled as Cu-PA, Al-PA, and Fe-PA, depending on the metal chloride used. Similarly, the wood samples treated in Path-2 schemes were denoted as PA-Cu, PA-Al, and PA-Fe. Wood samples vacuum-impregnated with only DI water served as the control group.

The wood samples used for the durability test were sequentially vacuum-impregnated with the treatment solutions (PA and M-Cl, depending on the treatment path) at 10 kPa for 1 h. For the fire performance test, the aspen wood samples were first vacuum-impregnated with one of the treatment solutions at a pressure of 10 kPa for 1 h, followed by a pressure impregnation (827 kPa) with the second treatment solution for 30 min. Upon completion of the first treatment, the treated wood samples were thoroughly washed under a continuous flow of DI water, then carefully wiped before being subjected to the subsequent treatment. After the second treatment, wood samples were washed following the same process and were then conditioned at 60°C for 48 h, until they reached a constant mass, and the masses of the wood samples both before and after each phase of the treatment procedure were documented, and the mass gain of the wood samples was calculated by employing Equation [1] below:

Table 1. Wood samples treatment paths.

Treatment path	1st step	2nd step	Label	Label after leaching
Path-1	M-Cl salts	PA	M-PA	M-PA-L
Path-2	PA	M-Cl salts	PA-M	PA-M-L

Note: PA = phytic acid solution (0.0758 M, pH 0.92 ± 0.03). M-Cl denotes metal chloride solutions (0.5 M) prepared from $FeCl_3$, $AlCl_3 \cdot 6H_2O$, and $CuCl_2 \cdot 2H_2O$, with pH values of 1.12 ± 0.02, 2.30 ± 0.02, and 2.76 ± 0.02, respectively.

$$Mass\ gain_{treat}\ (\%) = \frac{M_T - M_{UT}}{M_{UT}} \times 100\ \% \qquad [1]$$

where M_{UT} and M_T represent the masses of oven-conditioned wood samples before and after chemical treatment, respectively. The mass gain calculation included 12 replicates per treatment group. A detailed after-treatment mass gain plot for all treatment groups is shown in Figure S1 (Appendix).

Accelerated leaching test

An accelerated leaching test was performed on half of the wood samples in each treatment group, following the guidelines of the AWPA E11-16 standard (AWPA 2022) with some modifications. Six replicates from each treatment group intended for the durability test were immersed separately in 80 ml of deionized water (wood-to-water volume ratio 1:8) in individual beakers and vacuum-impregnated for 30 min. Likewise, three replicates from each treatment group designated for the fire performance test were immersed separately in 1200 ml of DI water (wood-to-water volume ratio 1:4) and vacuum-impregnated for 30 min. After impregnation, the leachate was discarded and replaced with an equal volume of fresh DI water. The beakers containing the wood samples were then agitated at 100 rpm for 4 h at room temperature, after which the leachates were again replaced with fresh DI water. This process was repeated until a total of

nine leachates had been replaced. The wet mass of the wood samples and their conditioned mass after oven-drying at 60°C for 48 h were recorded to determine the mass gain after leaching using Equation [2]. Wood samples subjected to leaching under Path-1 were labeled Cu-PA-L, Al-PA-L, and Fe-PA-L, while those under Path-2 were denoted PA-Cu-L, PA-Al-L, and PA-Fe-L (Table 1). The control group before and after leaching was designated control and control-L, respectively.

$$Mass\ gain_{leach}\ (\%) = \frac{M_L - M_{UT}}{M_{UT}} \times 100\% \quad [2]$$

Where M_{UT} and M_L represent the masses of oven-conditioned wood samples before chemical treatment and after leaching, respectively.

Fungal decay test

The fungal resistance of the in-situ biomineralized phytate wood samples (both before and after leaching) was evaluated following the AWPA E22-22 standard (AWPA 2022), with a minor adjustment to the sterilization procedure, as mentioned by Alorbu et al. (2023). Briefly, all wood samples were surface-sterilized by spraying with 70% ethanol and air-dried in a biosafety hood for 90 min. Each treatment group was subjected to a test fungus in soil culture bottles, with six replicates per group. The culture bottles were then incubated in the dark at 25°C and 75% relative humidity for 4 weeks. After the exposure period, the mycelia from the decayed wood were carefully removed by gentle brushing. The wet mass of the decayed samples was recorded, followed by oven-conditioning at 60°C for 48 h (or until a constant mass was achieved) to obtain the post-exposure dry mass. The moisture content (MC) and mass loss of decayed wood samples were determined using the following two equations:

$$Moisture\ content\ (\%) = \frac{(M_{wet} - M_{expo.})}{M_{expo.}} \times 100 \quad [3]$$

$$Mass\ loss\ (\%) = \frac{(M_{UT} - M_{expo.})}{M_{UT}} \times 100 \quad [4]$$

where M_{UT} refers to the dry mass of wood samples after conditioning (at 60°C for 48 h) before fungal exposure, whereas M_{expo} refers to the dry mass of wood samples after conditioning (at 60°C for 48 h) following fungal exposure. M_{wet} denotes the wet mass of the samples after undergoing decay. The detailed MC data of all the samples after the fungal decay test are provided in Table S1 (Appendix).

Thermogravimetric analysis

The thermal degradation properties of control and treated aspen wood samples (before and after leaching) were analyzed using thermogravimetric analysis (TGA) on a PerkinElmer TGA-7 instrument (Shelton, CT) under nitrogen (N_2) and air atmospheres. The samples (about 5–6 mg under each treatment group) were heated from room temperature to 800°C at a rate of 20°C/min under a gas flow of 30 mL/min. Thermogravimetric (TG) and derivative thermogravimetric (DTG) curves were recorded under both nitrogen and air atmospheres. The onset degradation temperature was determined as the intersection of tangents drawn at the baseline and the steepest part of the primary mass-loss region. The maximum degradation rate and its corresponding temperature (peak DTG) were identified from the extrema of the DTG curve. Residual mass at 800°C under N_2 and air was considered the final char/ash yield. All values listed in Table 2 represent the mean ± standard deviation of three replicates per treatment group.

Mass loss calorimeter test

The fire performance tests on the Path-1 and Path-2 treated wood blocks were conducted using the MLC (Fire Testing Technology, United Kingdom). The tests were carried out at an irradiation of 50 kW/m^2, in accordance with the ISO 13927 standard. The peak heat release rate (pHRR), the heat release rate (HRR), the total heat release (THR), and the amount of mass loss were recorded and examined. The wood samples treated with DI water alone were included as the control group and evaluated alongside the other treated wood samples for comparison.

Statistical analysis

The mass gain, mass loss, TGA, and MLC data were analyzed using one-way analysis of variance (ANOVA) in SAS 9.4 (SAS Institute Inc., Cary, NC) and R version 3.6.3. All statistical tests were conducted at a 95% confidence level ($\alpha = 0.05$). When significant differences were detected, post hoc comparisons were performed using Tukey's pairwise test or the Games-Howell test, depending on the homogeneity of variance.

Results and discussion

Mass gain

Mass gain of wood samples after treatment and leaching tests is shown in Figure 1. The control samples treated with (DI) water exhibited negative mass gains (pine: −0.88%; aspen: −0.45%), which were significantly lower ($p < 0.05$) than those of all other treatment groups. Overall, irrespective of treatment

Table 2. Onset temperature and residue of control and treated samples before and after leaching after the TGA test.

	N_2			Air			
Treatment	Onset (°C)	Degradation rate at peak T (%/min)	Residue (%)	1st Onset (°C)	2nd Onset (°C)	Degradation rate at peak T (%/min)	Residue (%)
Control	344 ± 1^{ab}	-24.66 ± 0.06^{ab}	11 ± 1^{ef}	341 ± 1^{a}	469 ± 2^{efg}	-51.92 ± 2.05^{bcd}	0 ± 0^{f}
Control-L	351 ± 4^{a}	-25.72 ± 0.3^{ab}	8.1 ± 1^{g}	336 ± 1^{ab}	480 ± 2^{cde}	-51.23 ± 1.30^{bc}	0 ± 0^{f}
Cu-PA	307 ± 2^{h}	-32.69 ± 1.04^{cd}	17 ± 1^{ab}	304 ± 5^{gh}	507 ± 6^{a}	-50.85 ± 0.63^{b}	0.4 ± 1^{def}
Cu-PA-L	340 ± 1^{bcd}	-35.50 ± 0.7^{d}	11 ± 1^{fg}	324 ± 2^{cd}	490 ± 5^{bc}	-52.43 ± 1.03^{bcd}	0 ± 0^{f}
Al-PA	322 ± 1^{fg}	-23.38 ± 4.27^{b}	14 ± 1^{cdef}	316 ± 7^{def}	462 ± 6^{fgh}	-74.84 ± 0.94^{f}	2.2 ± 1^{bc}
Al-PA-L	342 ± 1^{abc}	-30.68 ± 0.87^{c}	11 ± 2^{fg}	329 ± 3^{bc}	475 ± 4^{def}	-57.62 ± 3.39^{cde}	1.2 ± 1^{cde}
Fe-PA	336 ± 1^{bcd}	-25.44 ± 0.93^{ab}	15 ± 1^{bcd}	309 ± 1^{fg}	438 ± 5^{ij}	-35.29 ± 1.06^{a}	1.6 ± 1^{bcd}
Fe-PA-L	337 ± 2^{bcd}	-32.04 ± 1.93^{cd}	12 ± 1^{def}	315 ± 1^{def}	486 ± 2^{bcd}	-49.04 ± 0.76^{b}	2 ± 1^{bc}
PA-Cu	314 ± 1^{gh}	-32.42 ± 1.29^{cd}	18 ± 1^{a}	298 ± 2^{hi}	430 ± 6^{j}	-37.51 ± 0.78^{a}	2.8 ± 1^{ab}
PA-Cu-L	322 ± 4^{fg}	-35.38 ± 1.74^{d}	14 ± 1^{cdef}	315 ± 1^{def}	451 ± 1^{hi}	-47.28 ± 2.01^{b}	0.3 ± 1^{ef}
PA-Al	323 ± 2^{efg}	-21.95 ± 1.13^{ab}	17 ± 1^{abc}	305 ± 3^{gh}	459 ± 2^{gh}	-61.00 ± 0.58^{e}	2.2 ± 1^{bc}
PA-Al-L	330 ± 3^{def}	-24.31 ± 0.98^{a}	13 ± 2^{def}	321 ± 1^{cde}	495 ± 1^{ab}	-61.92 ± 0.88^{e}	2 ± 1^{bc}
PA-Fe	333 ± 3^{cde}	-25.18 ± 1.01^{ab}	15 ± 1^{bcde}	289 ± 5^{i}	381 ± 13^{k}	-52.37 ± 4.49^{bcd}	3.8 ± 1^{a}
PA-Fe-L	336 ± 4^{bcd}	-34.64 ± 1.50^{d}	13 ± 1^{def}	312 ± 1^{efg}	472 ± 1^{defg}	-58.21 ± 4.53^{de}	2.1 ± 1^{bc}

type or pathway, pine samples exhibited mass gains that were significantly higher ($p < 0.05$) than for aspen samples. The only exception was the Fe-PA groups, in which pine (3.67%) and aspen (3.78%) showed no statistically significant differences ($p > 0.05$). The greater mass gain observed in pine may be attributed to the anatomical differences between softwood and hardwood, as previously noted (Ding et al. 2008).

When comparing the two treatment pathways, Path-2 consistently resulted in significantly higher mass gains ($p < 0.05$) than Path-1 for both pine and aspen. Specifically, pine samples treated under Path-1 and Path-2 showed mass gains of approximately 3.6%–4.5% and 6%–11%, respectively, while aspen samples showed mass gains of about 1%–4% and 4%–6%. Among all groups, the Path-2 PA-Al treatment produced the

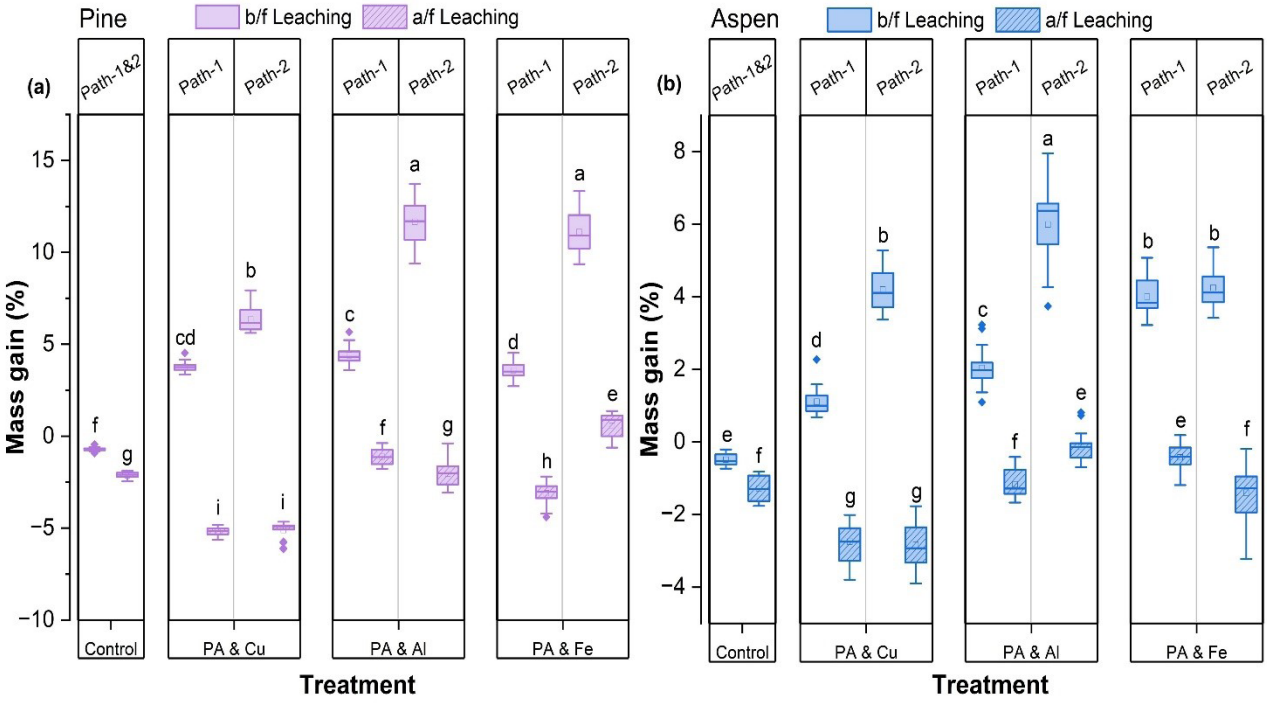

Figure 1. (a) Mass gain of pine samples before and after leaching test; (b) Mass gain of aspen samples before and after leaching test (n = 6).

highest mass gains, reaching 11.16% in pine and 6.12% in aspen (Figure 1).

However, after the accelerated leaching test, nearly all treatment groups (except PA-Fe-L in pine, 0.56%) showed significantly lower mass gains ($p < 0.05$) compared with their pre-leaching values (Figure 1a,b), regardless of wood species. Among the treatments, PA-Al and PA-Cu exhibited the greatest leaching losses, as indicated by the pronounced reductions in mass gain values. In contrast, the mass gains of Cu-PA-L and PA-Cu-L samples did not differ significantly after leaching ($p > 0.05$) for either pine or aspen. Overall, the leaching test revealed that Path-2 treatments were more prone to leaching than Path-1 treatments.

The possible reason could be that under Path-2, the introduction of metal ions into PA-saturated wood leads to rapid complexation and precipitation near the wood surface, forming surface-enriched metal-phytate deposits. This instantaneous reaction can partially block lumens and pits, physically retaining a larger amount of solids near the specimen surface and resulting in a higher apparent mass gain. In addition, incomplete conversion of PA during the second treatment step likely leaves a fraction of PA unreacted or weakly complexed, further contributing to mass gain. However, these surface-localized deposits and loosely bound PA species are more susceptible to removal upon water exposure, leading to greater leaching losses during the accelerated leaching test (Kremer et al. 2020; Marolt et al. 2020; Zhang et al. 2022). In contrast, under Path-1, metal cations are first able to diffuse into the wood structure and interact with negatively charged sites within the cell wall. Subsequent introduction of PA may promote in-situ precipitation at these pre-anchored locations, resulting in a more uniformly distributed and better-fixed metal-phytate network. Although this sequence may produce a lower initial mass gain, it likely enhances fixation efficiency and reduces leachability compared to Path-2 (Fan et al. 2024; Lebow 1996; Zhang et al. 2023).

Bio-durability test

Figure 2 shows the extent of mass loss in both control and treated wood samples (with and without leaching) after a 4-week exposure to the brown-rot (pine) and white-rot fungi (aspen). In general, control samples exposed to fungal attack showed an average mass loss ranging from 21%–34%. Similarly, the control-L group exhibited mass losses of 24%–38%, with no significant difference ($p > 0.05$) compared to the control. The substantial mass losses observed in the control groups can be attributed to the leaching of extractives throughout the decay exposure period (Sun et al. 2023).

In contrast, mycelial growth on treated samples was markedly inhibited, relative to the controls, regardless of leaching. Most treatment groups (both leached and unleached) exhibited mass losses below 10%, which were significantly lower than those of the controls ($p < 0.05$). However, exceptions were observed. The Al-PA group showed an average mass loss of 14% when exposed to *R.p.* ($p > 0.05$). In addition, Cu-PA-L, Al-PA-L, Fe-PA-L, PA-Cu-L, and PA-Al-L groups exposed to *R.p.*; the Al-PA-L and PA-Al-L groups exposed to *I.l.*; and the Al-PA-L group exposed to *T.v.* did not differ significantly from the control-L group. Moreover, PA-Al and PA-Cu treatment groups, which exhibited higher leachability and no significant difference in post-leaching mass gains, also showed relatively higher mass losses when exposed to *R.p*. Especially after leaching, Cu-PA-L, PA-Cu-L, and PA-Al-L groups recorded the highest mass losses under *R.p.* attack (Figure 2). These findings indicate that *R.p.* was the most aggressive fungus against the metal phytate treatments, while *G.t.* was the least aggressive among the four test fungi. In addition to mass loss, the moisture content of all samples after the 4-week exposure was determined to verify that conditions were suitable for fungal activity. The average MC of the control and control-L samples ranged from 28%–69% (Table S1, Appendix), which falls within or above the range generally considered favorable for brown-rot and white-rot decay (typically 30%–40% and often 40%–80%) (Lebow and Lebow 2018). Treated samples showed the average MC ranging from 27%–122% (Table S1, Appendix), which remained comparable or well above the minimum threshold for fungal growth, indicating that the lower mass loss in treated samples can be attributed to the efficacy of the metal-phytate treatment, rather than insufficient moisture.

Previous studies have also reported that inorganic metals, such as $FeCl_3$ and Al_2O_3, when fixed in treated wood, can enhance resistance against decay fungi (Acosta et al. 2022; Sun et al. 2023). Moreover, phytic acid has been reported to inhibit the growth of both brown-rot and white-rot fungi by limiting enzymatic activity (Li et al. 2023; Liang et al. 2024). The protective effect is further supported by the acidic nature of the phytate complexes (Table 1) that might have compromised the structural integrity of the fungal cell wall and diminished the activity of essential enzymes necessary for wood decay fungi. Collectively, these findings suggest that phytic acid-metal treatments confer substantial decay resistance, although susceptibility varies depending on both the fungal species and the leaching stability of the respective treatments.

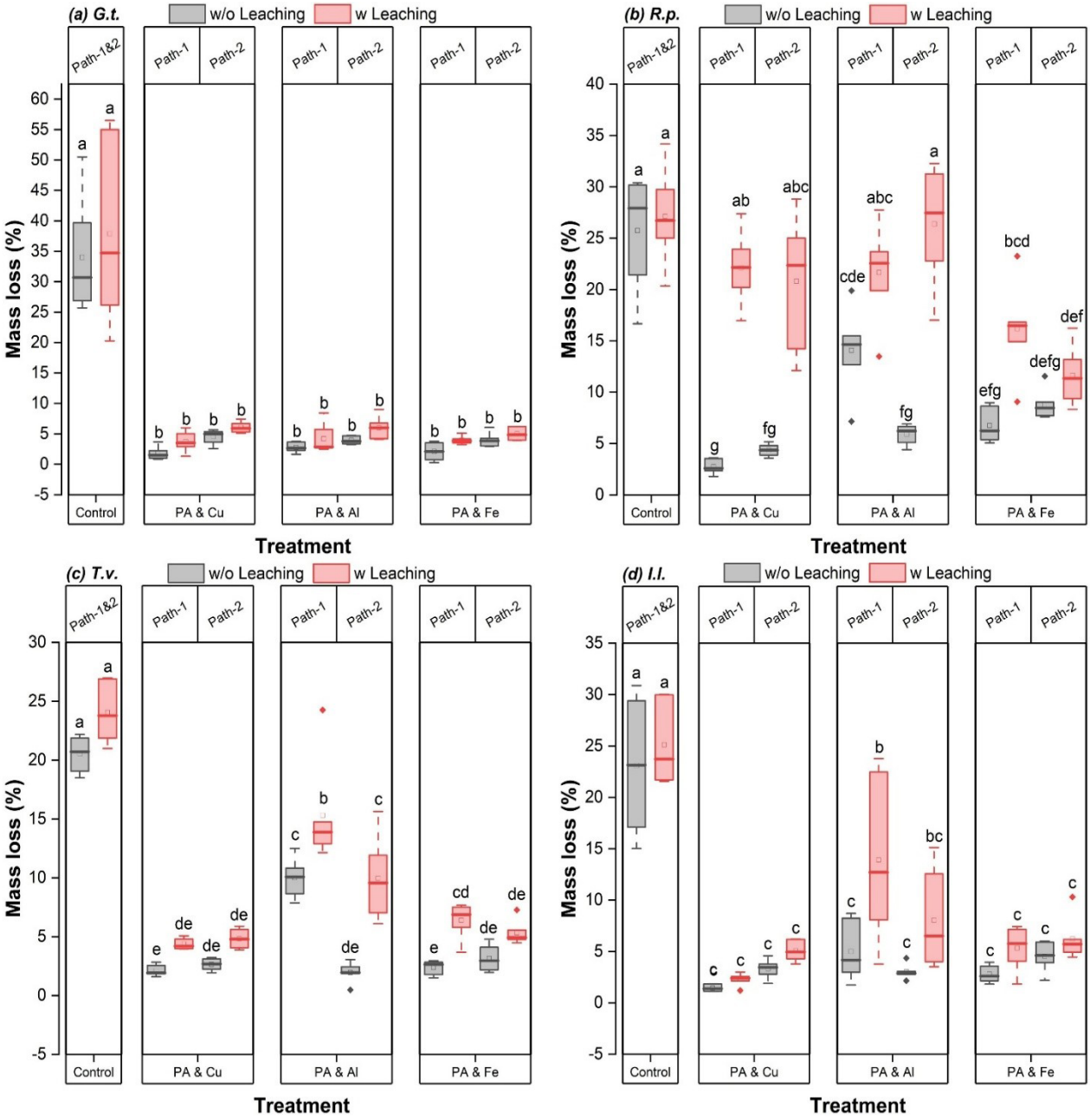

Figure 2. Mass loss of control and treated samples with and without leaching after exposure to each fungus: (a) *G.t.*; (b) *R.p.*; (c) *T.v.*; and (d) *I.l.* (n = 6).

Thermal stability

The thermal stability of the control and treated aspen wood samples was evaluated using thermogravimetric (TG) and derivative thermogravimetric (DTG) analyses under nitrogen (N_2) and air atmospheres (Figures 3 and 4), and the key parameters are summarized in Table 2.

Under N_2, the thermal decomposition of all samples followed three distinct stages, with a similar first stage but distinct temperature ranges for the second and third stages. Specifically, the first stage (30°C–160°C) involved the evaporation of moisture and light volatiles, corresponding to a minor mass loss (< 5%). For control and control-L samples, the mass of the samples remained relatively stable until reaching its second stage, from approximately 235°C to 550°C. This stage (a major weight loss of 80–85%) was mainly associated with the degradation of hemicellulose, cellulose, and lignin, with onset decomposition temperatures of 344°C for the control and 351°C for the control-L samples.

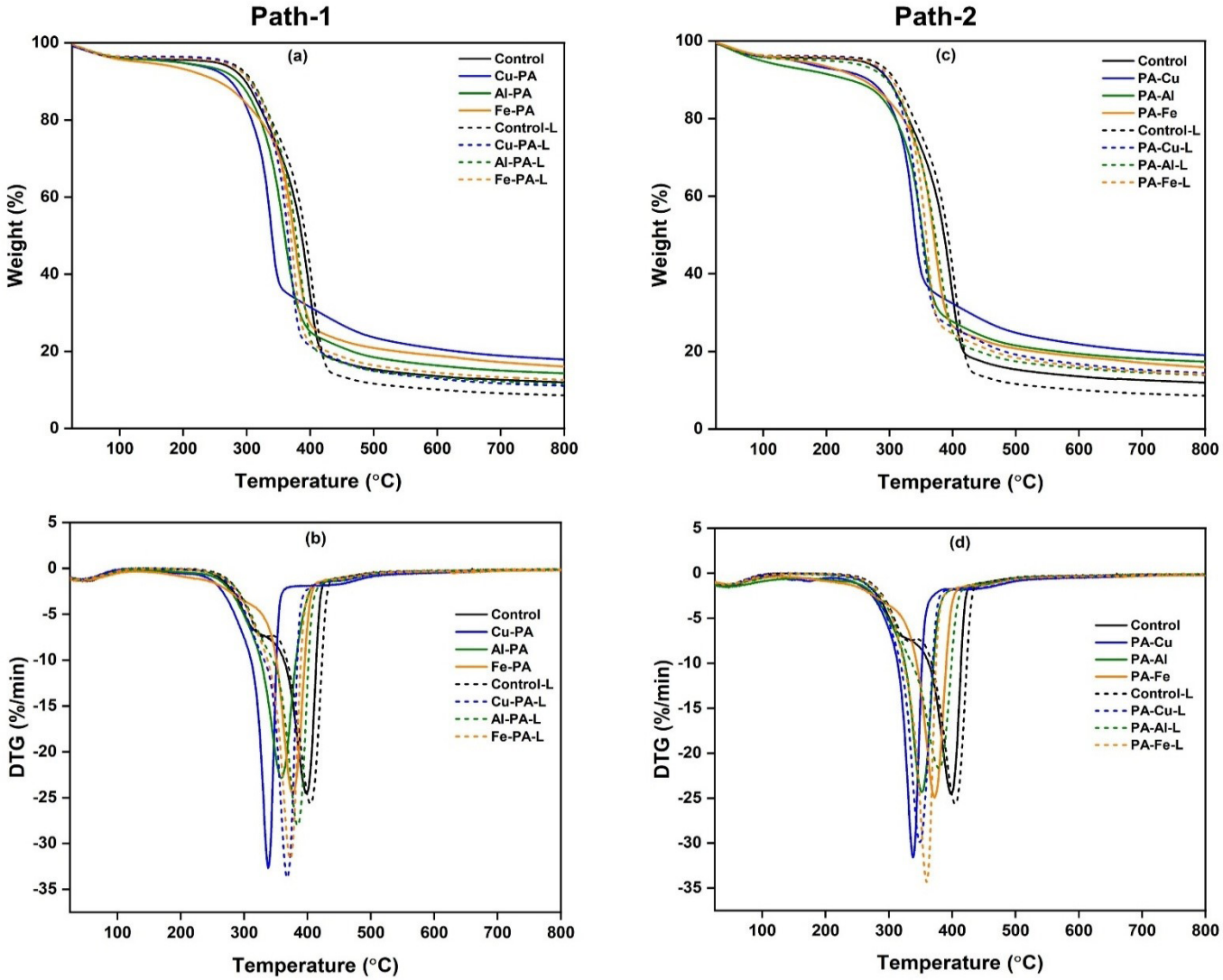

Figure 3. TG/DTG thermograms of control and treated samples before and after leaching (a, b) for Path-1; and (c, d) for Path-2 under N_2 (n = 3).

For the phytate-treated samples, the main decomposition shifted to lower temperatures of 180°C–450°C before leaching and 220°C–500°C after leaching, with onset temperatures of ~307°C–336°C and ~322°C–340°C, respectively. The corresponding mass losses were 64%–74% before leaching and 78%–82% after leaching. As shown in the DTG curves (Figure 3b,d), the peak decomposition temperatures of treated samples were 20°C–50°C lower than those of the controls (above 400°C), with the primary degradation peak appearing in the range of 300°C–400°C, indicating enhanced dehydration and char-promoting effects. This shift in the peak temperature of maximum degradation is attributed to the catalytic effect of the early decomposition of metal phytates, which accelerates char formation through phosphoric acid-induced dehydration reactions (Liu et al. 2022; Zhang et al. 2022). The third decomposition stage (450°C–800°C) corresponded to carbonization and aromatic char formation. All treated samples showed similar final-stage behavior, with total mass losses below 3%. The residual char yields of treated samples were significantly higher (14%–18% before leaching and 11%–14% after leaching) compared to the control (11%) and control-L (8%) samples, confirming improved thermal stability and non-volatile char retention.

The decomposition pattern under air followed a similar three-stage trend but included oxidative reactions in the later phase (Figure 4). During the first two stages, all samples exhibited comparable mass loss behavior up to ~315°C–365°C. However, control and control-L samples displayed an additional shoulder peak at 215°C–310°C, attributed to hemicellulose oxidation (Gao et al. 2004). This peak was absent in the phytate-treated

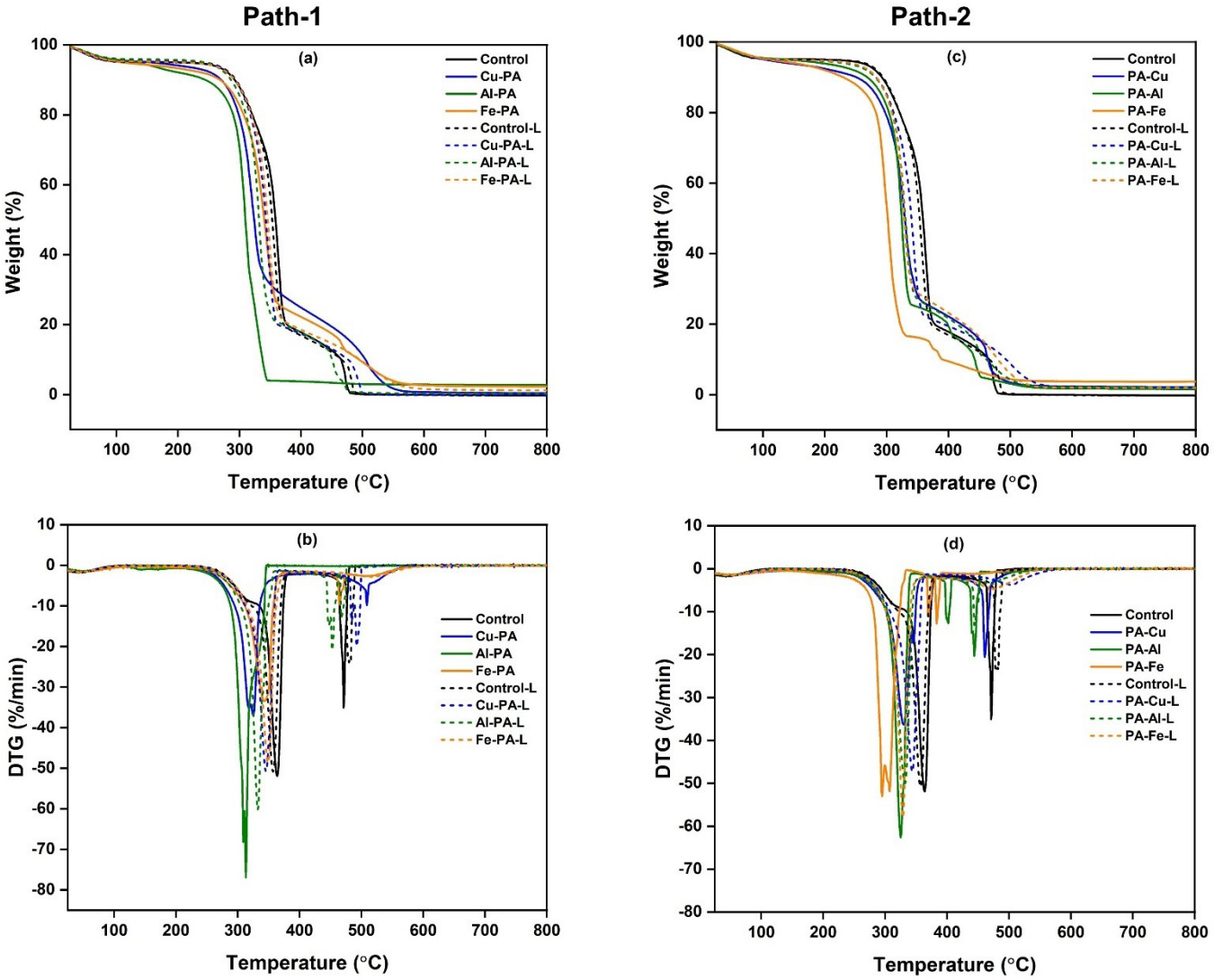

Figure 4. TG/DTG thermograms of control and treated samples before and after leaching (a, b) for Path-1; and (c, d) for Path-2 under Air (n = 3).

samples, indicating suppressed oxidative degradation due to the protective phosphorus-metal complex layer. In the third stage (> 400°C), the treated samples exhibited a narrower, delayed DTG peak (below 440°C) compared to controls, reflecting slower combustion of the carbonaceous char (Figure 4b,d). The primary degradation peak for all the treated samples (before and after leaching) appeared in the range of 300°C–350°C, whereas for the control samples, that degradation peak was observed above 380°C. Thus, the peak temperature at the peak thermal degradation rate of the treated samples was shifted towards a lower temperature range than the control and control-L, while their residual ash contents increased from 0% (control) to 0.4%–3.8% (treated), corresponding to the presence of thermally stable metal-phytate residues. These results demonstrate that metal-phytate formation effectively promotes early dehydration and crosslinking, while suppressing oxidative degradation at higher temperatures. The enhanced residue yield and reduced mass-loss rate confirm that the treated samples undergo a more controlled pyrolysis pathway, resulting in improved thermal stability and char integrity under both inert and oxidative environments.

Fire performance test

The MLC test was performed to assess the flame-retardant properties of the treated aspen wood samples. Figure 5 presents the heat release rate (HRR), total heat release (THR), and mass loss curves for control and treated wood samples before and after leaching, while Table 3 summarizes the key fire-performance parameters. Photographs of wood sample residues after combustion are shown in Figure 6.

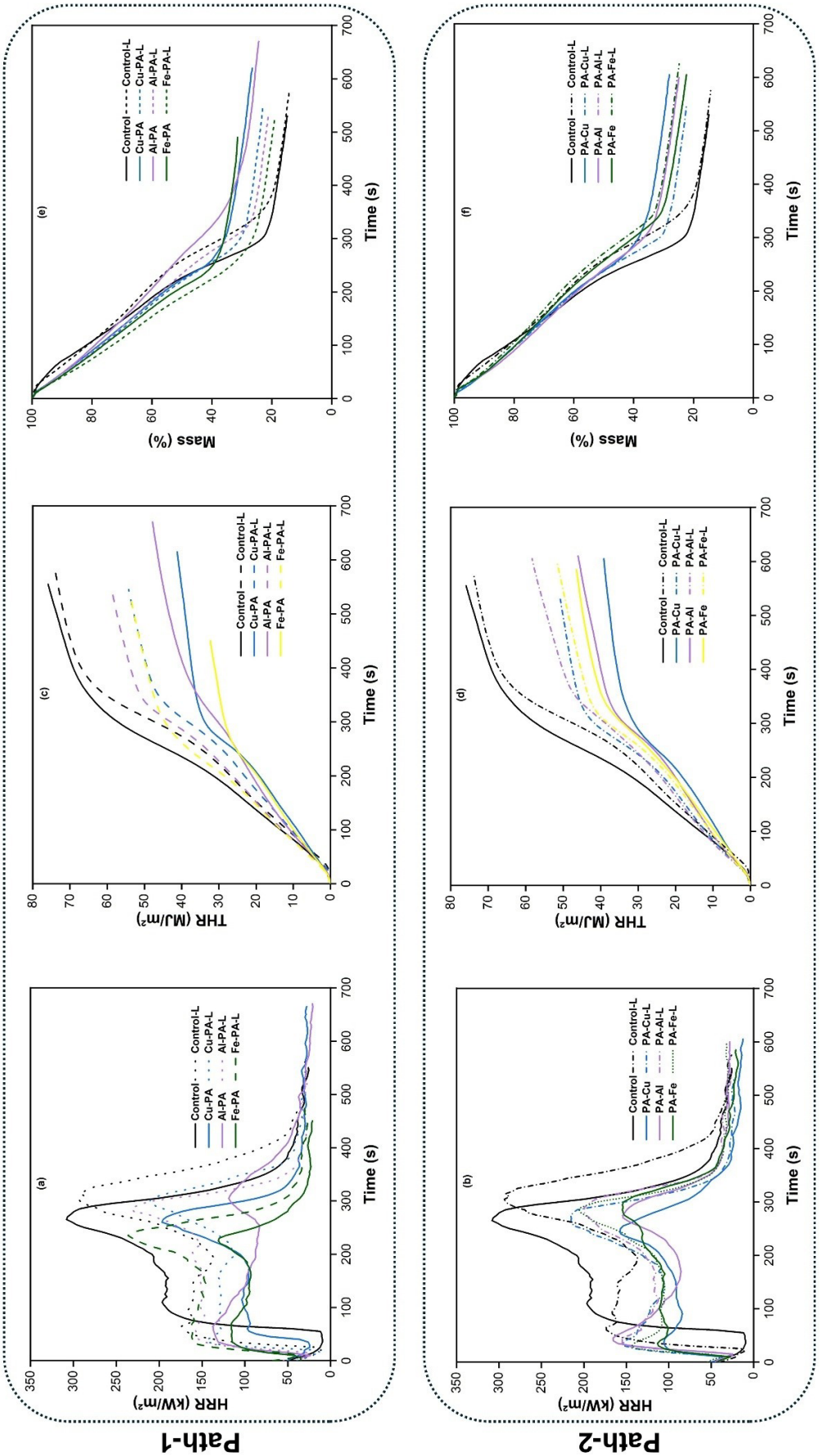

Figure 5. (a, b) Heat release rate (HRR); (c, d) total heat release (THR); and (e, f) mass loss curves of control and Path-1 and Path-2 treated samples before and after leaching following the mass loss calorimeter (MLC) test (n = 3).

Table 3. Mass loss calorimeter test data of all tested samples before and after the leaching test.

	Treatment	TTI (s)	TTF (s)	$pHRR_1$ ($k \cdot W/m^2$)	T_1 (s)	$pHRR_2$ ($k \cdot W/m^2$)	T_2 (s)	FGI ($k \cdot W/m^2.s^{-1}$)	THR ($M \cdot J/m^2$)	Residue (%)	Mass gain (%)
Path-1	Control	26±1^{a}	444±75^{abcd}	179±7^{a}	100±17^{a}	303±8^{a}	262±8^{bcd}	1.15±0.04^{a}	63±9^{ab}	15±2^{d}	-0.46±0.05^{f}
	Control-L	25±2^{a}	400±51^{bcd}	176±3^{ab}	73±11^{b}	284±14^{a}	298±11^{abc}	0.96±0.03^{bc}	65±4^{a}	14±1^{d}	-1.06±0.31^{f}
	Cu-PA	12±2^{bcd}	498±39^{ab}	104±7^{e}	50±13^{bc}	198±3^{bcd}	255±8^{cd}	0.78±0.04^{cd}	41±2de	26±0.70^{b}	11±0.20^{a}
	Cu-PA-L	14±3^{bc}	425±3^{abcd}	142±5^{bcd}	34±3^{c}	199±11^{bcd}	284±17^{abc}	0.70±0.02^{de}	46±3^{cd}	24±0.83^{bc}	0.02±0.99^{f}
	Al-PA	12±1^{bcd}	516±38^{a}	125±7de	55±5^{bc}	143±6^{e}	315±13^{a}	0.45±0.01^{f}	46±1^{cd}	24±1^{bc}	8.5±0.5^{b}
	Al-PA-L	14±2^{bcd}	406±4^{abcd}	162±3^{abc}	54±2^{bc}	225±8^{b}	288±10^{abc}	0.78±0.05^{cd}	53±1^{bc}	21±0.27^{c}	-0.85±0.42^{f}
	Fe-PA	12±1^{bcd}	347±22^{d}	98±18^{e}	53±11^{bc}	145±15^{e}	225±1^{d}	0.65±0.09^{de}	30±1^{e}	31±1^{a}	6.08±0.34^{cd}
	Fe-PA-L	13±1^{bcd}	376±24^{cd}	160±2^{abc}	44±3^{c}	217±19^{b}	230±10^{d}	0.96±0.05^{b}	49±4^{cd}	21±2^{bc}	-5.99±2^{h}
Path-2	PA-Cu	9±1^{d}	468±30^{abcd}	127±18de	34±3^{c}	164±13de	257±16^{cd}	0.64±0.07^{de}	40±3de	26±2^{bc}	8.04±0.50^{bc}
	PA-Cu-L	9±3^{d}	432±26^{abcd}	145±9^{bcd}	34±3^{c}	205±9^{bc}	275±10^{abc}	0.75±0.04^{de}	46±1^{cd}	23±1^{bc}	-3.66±0.56^{gh}
	PA-Al	12±2^{bcd}	485±5^{abc}	148±3^{abcd}	40±5^{c}	172±6^{cde}	282±3^{abc}	0.61±0.02^{ef}	44±3^{cd}	24±1^{bc}	5.05±0.33^{de}
	PA-Al-L	15±2^{b}	481±26^{abc}	152±7^{abcd}	42±3^{c}	185±13^{cd}	282±18^{abc}	0.66±0.06^{de}	52±2^{c}	24±2^{bc}	-1.76±0.19^{fg}
	PA-Fe	10±1^{cd}	490±56^{abc}	138±22^{cd}	38±17^{c}	175±21^{cde}	275±20^{abc}	0.64±0.10^{de}	46±3^{cd}	23±4^{bc}	3.67±1^{e}
	PA-Fe-L	13±1^{bcd}	482±19^{abcd}	143±6^{bcd}	35±5^{c}	200±9^{bcd}	302±17^{ab}	0.68±0.05^{de}	47±1^{cd}	26±0.84^{bc}	-1.47±0.53^{fg}

Note: pHRR refers to the highest HRR (Heat Release Rate) value; THR (Total heat Release) refers to the heat release calculated from the start of the test to 2 minutes after the flame out; Fire growth index, defined as the ratio of $pHRR_2$/ T_2.

Figure 6. Photographs of all tested samples before and after the mass loss calorimeter (MLC) test.

As shown in Figure 5a and 5b and in Table 3, the control and control-L samples exhibited rapid combustion, with HRR rising steeply and reaching early peak values ($pHRR_1$) of 179 kW/m² and 176 kW/m² at 100 s and 73 s, respectively. Prior to 250 s, intense pyrolysis and volatilization caused the surface layer of control samples to ignite quickly and transition into vigorous flaming, after which the surface began to char and form a carbonized layer (Guo et al. 2019). However, this char fractured as the burning duration increased, exposing deeper layers and leading to a second rise in HRR. This resulted in a secondary peak ($pHRR_2$) of 303 kW/m² and 279 kW/m² at 262 s and 298 s, respectively.

All treated samples, whether before or after leaching, exhibited markedly improved heat-release behavior. Although the time to $pHRR_1$ was advanced to 45–66 s (before leaching) and 19–39 s (after leaching) relative to the controls, the $pHRR_1$ values were reduced by 18%–45% before leaching and by 8%–29% after leaching. Similar improvements were observed for $pHRR_2$, with treated samples exhibiting reductions of 35%–53% before leaching and 19%–48% after leaching. Among all formulations, the Fe-PA treatment yielded the highest decrease in both peaks.

Figure 5c and 5d and Table 3 show that all treated samples released significantly less heat than the controls. The total heat released by treated samples was 27%–52% lower before leaching and 19%–29% lower after leaching than the control (63 MJ/m² for control, 65 MJ/m² for control-L). This reduction can be attributed to the formation of high-yield, thermally stable char layers derived from metal-phytate networks, which acted as physical barriers to heat and mass transfer. Similarly, the fire growth index (FGI)—the ratio of $pHRR_2$ to the time to peak—was consistently lower for treated samples than for controls, further indicating enhanced flame-retardant behavior. The Fe-PA sample again showed the strongest overall effect among the treatment groups.

As shown in Figure 5e and 5f and Table 3, irrespective of treatment pathways, the residual mass of all treated samples before and after leaching was significantly higher than the residual mass of the control (~15%) and control-L (~14%) samples. The residual mass values were recorded to be 54%–107% higher (for before-leaching samples) and 47%–80% higher (for after-leaching samples) compared to control and control-L samples, respectively. These findings are comparable to the existing literature, which reported that phosphorus-metal interactions promote dehydration, cross-linking, and graphitized carbon formation during combustion, resulting in more cohesive and thermally resistant char layers (Zhang et al. 2022, 2023). The time to ignition (TTI) of treated wood samples was 9–14 s, substantially lower than that of the control (~26 s) and control-L (~25 s). Similar reductions were reported for PA-treated wood by Liang et al. (2024), who attributed the shortened TTI to the acidic nature of PA. The acid promotes early dehydration and accelerates char formation, rather than allowing volatile, flammable gases to accumulate. Although the TTI was shorter, the overall heat release, peak intensity, and fire growth behavior were significantly reduced due to the protective char barrier.

After the MLC test (Figure 6), the control samples displayed fractured, brown-grey char. In contrast, all treated samples formed dense, cohesive, and continuous char layers that effectively shielded the underlying wood. Distinct coloration was also observed depending on the metal species. Under Path-1, Cu-PA samples produced bluish-black char, and Fe-PA samples yielded reddish-black char—corresponding to the known colors of $CuCl_2$ and $FeCl_3$ residues. Al-PA samples formed a whitish-black, highly stable char layer. These distinctive colors were less pronounced under Path-2, consistent with the shallower penetration and less uniform deposition of metal phytates.

Overall, the results indicate that metal-phytate complexes decompose at lower temperatures than wood polymers, releasing non-combustible products and promoting early char formation. The phosphorus-metal synergy facilitates dehydration, induces aromatic cross-linking, and enhances the graphitization of the carbonaceous residue (Zhang et al. 2022). This dual action restricts heat transfer and oxygen access, suppresses both primary and secondary combustion, and results in lower $pHRR_2$, THR, and FGI values, while increasing the final char yield. Even after leaching, the treated samples retained notable flame-retardant performance due to the persistent presence of phosphorus and metal species within the wood matrix.

Conclusions

This study examined the bio-durability and flame-retardant performance of wood treated through two sequential metal-phytate formation pathways. Overall, Path-2 resulted in higher initial mass gains, whereas Path-1 produced lower mass gains but generally better fixation and reduced leaching. After leaching, all treated samples exhibited lower retained mass, with Path-2 showing more pronounced loss, indicating limited long-term stability of loosely bound phytate species. The antifungal results demonstrated that most treated samples achieved improved decay resistance relative to the controls, although leached samples were less effective, and *R. placenta* remained the most aggressive fungus. Thermal and combus-

tion analyses indicated consistent enhancements in char formation and reduced heat-release behavior for all treatments. Thermogravimetric analysis showed an earlier onset of dehydration and higher char residue, while MLC testing confirmed reductions in $pHRR_2$ and THR and increases in residual mass, even after leaching. These results support that metal-phytate formation can promote catalytic charring and mitigate combustion intensity, although the magnitude of improvement varied among metals and pathways. Future work should focus on improving fixation chemistry, optimizing pH and reaction conditions, exploring crosslinking or buffering strategies, or incorporating co-treatments to stabilize PA-metal complexes.

Acknowledgements

This project was supported by the USDA NIFA Award #2022-67022-37607. Any opinions, findings, conclusions, or recommendations expressed in this publication are solely those of the authors and do not necessarily reflect the views of the U.S. Department of Agriculture. The authors would also like to thank Dr. Armando McDonald from the University of Idaho for access to FTIR and TGA.

References

Acosta AP, Gallio E, Cruz N, Aramburu AB, Lunkes N, Missio AL, Delucis R de A, Gatto DA (2022) Alumina as an antifungal agent for *Pinus elliottii* wood. J Fungi 8(12):1299. https://doi.org/10.3390/JOF8121299

Alorbu C, Carey J, McDonald AG, Cai L (2023) Antifungal properties of lauric arginate (LAE) treated wood. Holzforschung 77(8):640–647. https://doi.org/10.1515/HF-2023-0013/DOWNLOADASSET/SUPPL/J_HF-2023-0013_SUPPL_001.DOCX

Antoun K, Ayadi M, El Hage R, Nakhl M, Sonnier R, Gardiennet C, Le Moigne N, Besserer A, Brosse N (2022) Renewable phosphorous-based flame retardant for lignocellulosic fibers. Ind Crops Prod 186. https://doi.org/10.1016/j.indcrop.2022.115265

AWPA-American Wood Protection Association (2022) E22-22: Laboratory Method for Rapidly Evaluating the Decay Resistance of Wood-Based Materials Against Pure Basidiomycete Cultures Using Compression Strength: Soil/Wafer Test. AWPA Book of Standards, American Wood Protection Association, Birmingham, AL. 8 p. https://standards.globalspec.com/std/14519046/e22

AWPA-American Wood Protection Association (2022) E11-16 (2016, Reaffirmed 2022): Standard Method for Accelerated Evaluation of Preservative Leaching. AWPA Book of Standards, American Wood Protection Association, Birmingham, AL. 3 p. https://standards.globalspec.com/std/10030239/awpa-e11

Berglund LA, Burgert I (2018) Bioinspired wood nanotechnology for functional materials. Adv Mater 30(19):1704285. https://doi.org/10.1002/ADMA.201704285

Chen Z, Zhang S, Ding M, Wang M, Xu X (2021) Construction of a phytic acid-silica system in wood for highly efficient flame retardancy and smoke suppression. Materials 14(15):4164. https://doi.org/10.3390/MA14154164/S1

Costes L, Laoutid F, Brohez S, Dubois P (2017) Bio-based flame retardants: When nature meets fire protection. Materi Sci Eng R Rep 117:1–25. https://doi.org/10.1016/J.MSER.2017.04.001

Ding WD, Koubaa A, Chaala A, Belem T, Krause C (2008) Relationship between wood porosity, wood density and methyl methacrylate impregnation rate. Wood Mater Sci Eng 3(1–2):62–70. https://doi.org/10.1080/17480270802607947

Fan S, Gao X, Yang X, Li X (2024) Infusing phytate-based biomass flame retardants into the cellulose lumens of Chinese fir wood attains superior flame retardant efficacy. Int J Biol Macromol 258:128975. https://doi.org/10.1016/J.IJBIOMAC.2023.128975

Gänzle MG (2020) Food fermentations for improved digestibility of plant foods – an essential ex situ digestion step in agricultural societies? Curr Opin Food Sci 32:124–132. https://doi.org/10.1016/J.COFS.2020.04.002

Gao M, Shuying LI, Sun C (2004) Thermal degradation of wood in air and nitrogen treated with basic nitrogen compounds and phosphoric acid. Combust Sci Technol 176(12):2057–2070. https://doi.org/10.1080/00102200490514840

Guo H, Luković M, Mendoza M, Schlepütz CM, Griffa M, Xu B, Gaan S, Herrmann H, Burgert I (2019) Bioinspired struvite mineralization for fire-resistant wood. ACS Appl Mater Interfaces 11(5):5427–5434. https://doi.org/10.1021/ACSAMI.8B19967/ASSET/IMAGES/MEDIUM/AM-2018-199674_M002.GIF

Ilyas RA, Sapuan SM, Asyraf MRM, Dayana DAZN, Amelia JJN, Rani MSA, Norrrahim MNF, Nurazzi NM, Aisyah HA, Sharma S, Ishak MR, Rafidah M, Razman MR, Ilyas RA, Sapuan SM, Asyraf MRM, Dayana DAZN, Amelia JJN, Rani MSA, Norrrahim MNF, Nurazzi NM, Aisyah HA, Sharma S, Ishak MR, Rafidah M, Razman MR (2021) Polymer composites filled with metal derivatives: A review of flame retardants. Polymers 13(11):1701. https://doi.org/10.3390/POLYM13111701

Jia C, Chen C, Mi R, Li T, Dai J, Yang Z, Pei Y, He S, Bian H, Jang SH, Zhu JY, Yang B, Hu L (2019) Clear wood toward high-performance building materials. ACS Nano 13(9):9993–10001. https://doi.org/10.1021/acsnano.9b00089

Kovačević Z, Grgac SF, Bischof S, Kovačević Z, Grgac SF, Bischof S (2021) Progress in biodegradable flame retardant nano-biocomposites. Polymers 13(5):1–30. https://doi.org/10.3390/polym13050741

Kremer C, Torres J, Bianchi A, Savastano M, Bazzicalupi C (2020) Myo-inositol hexakisphosphate: Coordinative versatility of a natural product. Coord Chem Rev 419:213403. https://doi.org/10.1016/J.CCR.2020.213403

Lebow S (1996) Leaching of wood preservative components and their mobility in the environment—Summary of pertinent literature. Gen Tech Rep FPL-GTR-93. USDA Forest Service, Forest Products Laboratory, Madison, WI. 36 p. https://doi.org/10.2737/FPL-GTR-93

Lebow ST, Lebow PK (2018) Internal moisture content and temperature of standardized aboveground wood durability test specimens. Research Paper FPL-RP-694. USDA Forest Service, Forest Products Laboratory, Madison, WI. 14 p. https://doi.org/10.2737/FPL-RP-694

Li L, Chen Z, Lu J, Wei M, Huang Y, Jiang P (2021) Combustion behavior and thermal degradation properties of wood impregnated with intumescent biomass flame retardants: phytic acid, hydrolyzed collagen, and glycerol. ACS Omega 6(5):3921–3930. https://doi.org/10.1021/acsomega.0c05778

Li N, Wu YX, Zhang Y Di, Wang SR, Zhang GC, Yang J (2023) Phytic acid is a new substitutable plant-derived antifungal agent for the seedling blight of *Pinus sylvestris* var. *mongolica* caused by *Fusarium oxysporum*. Pestic Biochem Physiol 191:105341. https://doi.org/10.1016/J.PESTBP.2023.105341

Liang L, Alorbu C, McDonald A, Cai L (2024) Phytic acid for dual wood protection against fungi and fire. Wood Fiber Sci 56(2):72–82. https://doi.org/10.22382/wfs-2024-07

Liang S, Neisius NM, Gaan S (2013) Recent developments in flame retardant polymeric coatings. Prog Org Coat 76(11):1642–1665. https://doi.org/10.1016/J.PORGCOAT.2013.07.014

Liang Y, Jian H, Deng C, Xu J, Liu Y, Park H, Wen M, Sun Y (2023) Research and application of biomass-based wood flame retardants: A review. Polymers 15(4):950. https://doi.org/10.3390/polym15040950

Lin CF, Zhang C, Karlsson O, Martinka J, Mantanis GI, Rantuch P, Jones D, Sandberg D (2023) Phytic acid-silica system for imparting fire retar-

dancy in wood composites. Forests 14(5):1021. https://doi.org/10.3390/f14051021

Liu L, Zhu M, Ma Z, Xu X, Mohesen Seraji S, Yu B, Sun Z, Wang H, Song P (2022) A reactive copper-organophosphate-MXene heterostructure enabled antibacterial, self-extinguishing and mechanically robust polymer nanocomposites. Chem Eng J 430:132712. https://doi.org/10.1016/J.CEJ.2021.132712

Loewus FA (2001) Biosynthesis of phytate in food grains and seeds. Pp 53–62 in Reddy NR, Sathe SK, eds. Food Phytates. CRC Press, Boca Raton, FL. https://doi.org/10.1201/9781420014419.CH4

Lott1 JNA, Ockenden I, Raboy V, Batten GD (2000) Phytic acid and phosphorus in crop seeds and fruits: a global estimate. Seed Sci Res 10(1):11–33. https://doi.org/10.1017/S0960258500000039

Marolt G, Gričar E, Pihlar B, Kolar M (2020) Complex formation of phytic acid with selected monovalent and divalent metals. Front Chem 8:582746. https://doi.org/10.3389/FCHEM.2020.582746

Råberg U, Edlund ML, Terziev N, Land CJ (2005) Testing and evaluation of natural durability of wood in above ground conditions in Europe - An overview. J Wood Sci 51(5):429–440. https://doi.org/10.1007/S10086-005-0717-8

Song F, Liu T, Fan Q, Li D, Ou R, Liu Z, Wang Q (2022) Sustainable, high-performance, flame-retardant waterborne wood coatings via phytic acid based green curing agent for melamine-urea-formaldehyde resin. Prog Org Coat 162:106597. https://doi.org/10.1016/j.porgcoat.2021.106597

Soula M, Samyn F, Duquesne S, Landry V (2021) Innovative polyelectrolyte treatment to flame-retard wood. Polymers (Basel) 13(17):2884. https://doi.org/10.3390/polym13172884

Sun M, Zhao C, Alorbu C, Cai L, Yu Y, Sun M, Zhao C, Alorbu C, Cai L, Yu Y (2023) Antique wood preparation by inorganic salts treatment and its performance. Maderas ciencia y tecnología 25. https://doi.org/10.4067/S0718-221X2023000100423

Tang T, Fu Y (2020) Formation of chitosan/sodium phytate/nano-Fe_3O_4 magnetic coatings on wood surfaces via layer-by-layer self-assembly. Coatings 10(1):51. https://doi.org/10.3390/coatings10010051

Tian Y, Wang C, Ai Y, Tang L, Cao K (2023) Phytate-based transparent and waterproof intumescent flame-retardant coating for protection of wood. Mater Chem Phys 294:127000. https://doi.org/10.1016/j.matchemphys.2022.127000

Venier M, Salamova A, Hites RA (2015) Halogenated flame retardants in the Great Lakes environment. Acc Chem Res 48(7):1853–1861. https://doi.org/10.1021/ACS.ACCOUNTS.5B00180

Viveros A, Centeno C, Brenes A, Canales R, Lozano A (2000) Phytase and acid phosphatase activities in plant feedstuffs. J Agric Food Chem 48(9):4009–4013. https://doi.org/10.1021/jf991126m

Wang K, Meng D, Wang S, Sun J, Li H, Gu X, Zhang S (2022) Impregnation of phytic acid into the delignified wood to realize excellent flame retardant. Ind Crops Prod 176:114364. https://doi.org/10.1016/j.indcrop.2021.114364

Yang G, Zhang Q (2022) In situ polymerization and flame retardant mechanism of bio-based nitrogen and phosphorus macromolecular flame retardant in plywood. Macromol Rapid Commun 43(8):2200018. https://doi.org/10.1002/MARC.202200018

Zhang J, Wu Q, Li G, Li MC, Sun X, Ring D (2017) Synergistic influence of halogenated flame retardants and nanoclay on flame performance of high density polyethylene and wood flour composites. RSC Adv 7(40):24895–24902. https://doi.org/10.1039/C7RA03327C

Zhang L, Yi D, Hao J, Gao M (2021) One-step treated wood by using natural source phytic acid and uracil for enhanced mechanical properties and flame retardancy. Polym Adv Technol 32(3):1176–1186. https://doi.org/10.1002/pat.5165

Zhang S, Wang X, Ding M, Huang Y, Li L, Wang M (2022) In-situ incorporation of metal phytates for green and highly efficient flame-retardant wood with excellent smoke-suppression property. Ind Crops Prod 187:115287. https://doi.org/10.1016/j.indcrop.2022.115287

Zhang S, Zhao X, Peng Y, Yang T, Huang Y, Li L, Wang M (2023) In-situ synthesis of copper phytate-hierarchically porous MOF-199 hybrid in wood towards multifunctional flame-retardant wood composite. Ind Crops Prod 204:117233. https://doi.org/10.1016/J.INDCROP.2023.117233

Zhao F, Tang T, Hou S, Fu Y (2020) Preparation and synergistic effect of chitosan/sodium Phytate/MgO nanoparticle fire-retardant coatings on wood substrate through layer-by-layer self-assembly. Coatings 10(9):848. https://doi.org/10.3390/coatings10090848

Zhou L, Fu Y (2020) Flame-Retardant wood composites based on immobilizing with chitosan/sodium phytate/Nano-TiO2-ZnO coatings via layer-by-layer self-assembly. Coatings 10(3):296. https://doi.org/10.3390/coatings10030296

Zhu M, Song J, Li T, Gong A, Wang Y, Dai J, Yao Y, Luo W, Henderson D, Hu L, Zhu M, Song J, Li T, Gong A, Wang Y, Dai J, Yao Y, Luo W, Henderson D, Hu L (2016) Highly anisotropic, highly transparent wood composites. Adv Mater 28(26):5181–5187. https://doi.org/10.1002/ADMA.201600427

Appendix

Table S1. Average moisture content of the samples after decay (n = 6).

	Average moisture content (%) after decay			
Treatment	*G.t*	*R.p*	*T.v*	*I.l*
Control	45.77 ± 22.48	34.15 ± 4.48	58.82 ± 15.78	28.60 ± 6.49
Control-L	69.02 ± 31.66	41.02 ± 4.44	53.90 ± 7.78	31.47 ± 5.52
Cu-PA	69.02 ± 6.81	74.01 ± 17.47	46.42 ± 9.81	40.57 ± 10.43
Cu-PA-L	29.34 ± 6.27	37.44 ± 4.25	31.83 ± 3.59	28.10 ± 1.84
Al-PA	39.70 ± 11.75	33.57 ± 6.61	31.13 ± 9.05	35.26 ± 9.16
Al-PA-L	32.20 ± 11.92	37.67 ± 4.48	47.92 ± 14.60	34.19 ± 7.71
Fe-PA	49.50 ± 19.38	78.51 ± 16.64	43.99 ± 8.92	48.23 ± 12.18
Fe-PA-L	28.00 ± 2.67	68.09 ± 43.85	38.97 ± 3.80	40.61 ± 3.44
PA-Cu	88.27 ± 11.30	122.17 ± 10.85	97.63 ± 22.00	71.34 ± 2.02
PA-Cu-L	35.73 ± 11.56	41.72 ± 8.10	31.52 ± 3.58	33.32 ± 2.60
PA-Al	73.37 ± 11.91	97.67 ± 21.69	62.70 ± 4.20	88.47 ± 13.80
PA-Al-L	36.04 ± 12.10	43.01 ± 4.60	41.71 ± 8.15	43.97 ± 7.91
PA-Fe	60.71 ± 8.71	76.84 ± 14.14	57.45 ± 15.86	54.15 ± 15.70
PA-Fe-L	27.09 ± 2.74	36.49 ± 3.91	40.68 ± 9.47	47.49 ± 2.47

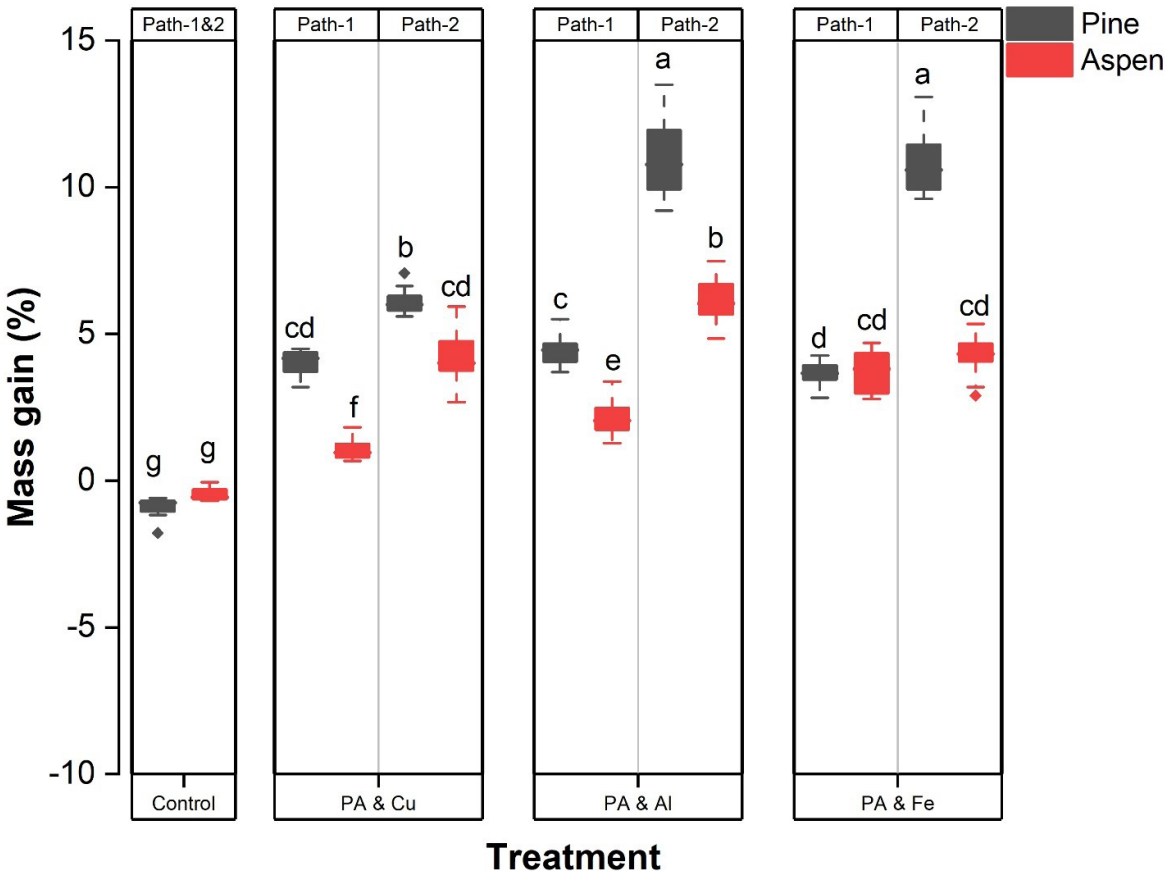

Figure S1. Mass gain of samples after treatment (n = 12).

[This page is intentionally left blank.]